RAPID PYROLYSIS OF SWEET GUM WOOD AND MILLED WOOD LIGNIN

by

Theodore Robert Nunn

B.S., Chemical Engineering
University of California (1980)

Submitted in Partial Fulfillment
of the Requirements for the
Degree of

Master of Science in
Chemical Engineering
at the
Massachusetts Institute of Technology
October 1981

Signature of Author _____
Department of Chemical Engineering
October, 1981

Certified by _____
Jack B. Howard, Thesis Supervisor

_____
John P. Longwell, Thesis Supervisor

_____
William A. Peters, Thesis Supervisor

Accepted by _____
Glenn C. Williams, Chairman
Departmental Graduate Committee

RAPID PYROLYSIS OF SWEET GUM WOOOD AND MILLED WOOD LIGNIN

by

Theodore Robert Nunn

Submitted to the Department of Chemical Engineering in October, 1981 in partial fulfillment of the requirements for the degree of Master of Science in Chemical Engineering.

ABSTRACT

Data were obtained on the yields, compositions, and rates of evolution of major products from the fast pyrolysis of sweet gum hardwood and sweet gum milled wood lignin in a capitve sample apparatus.

The wood and lignin samples were heated at rates of 1000 K/s to peak temperatures of between 600 and 1400K in a 5 psig helium atmosphere. Samples were cooled at an average nominal rate of 200K/s after zero residence time at the maximum temperature. Gaseous and light liquid products were analyzed by gas chromatography. Tar (heavy liquid) and char yields were determined gravimetrically and characterized by elemental analysis.

High ultimate yields of volatile material were obtained from both the wood and lignin pyrolyses. The overall weight loss achieved from wood pyrolysis was 93 wt. % while the yield of volatiles from lignin pyrolysis was 86 wt. %. The major constituent of the volatile material was a heavy liquid product (tar), which reached a maximum yield of 55 percent by weight of original material from wood pyrolysis and 53 percent by weight from lignin pyrolysis. Secondary cracking of this heavy liquid material contributed significantly to the total gas yield at temperatures above 950K.

On a weight basis, carbon monoxide was the dominant gaseous product above 850K, reaching ultimate yields of 17 wt. % and 19 wt. %, respectively, from wood and lignin pyrolysis. On an energy basis, ultimate CH_4 yields approached those of CO (75-95%), despite much smaller methane yields (2-3 wt. %). Carbon dioxide and chemical water were the other major products from both materials, having ultimate yields of 4-6 wt. % for CO_2 and 4-5 wt. % for water. Total hydrocarbons (CH_4, C_2H_4, C_2H_6, C_3H_6) amounted to 4-5 wt. % of the pyrolysis material and light oxygenated liquids, such as formaldehyde, methanol, and acetaldehyde, accounted for 9 wt. % from wood pyrolysis and 5 wt. % from lignin pyrolysis.

A single-step, first-order reaction model was used to obtain kinetic parameters for the formation of the individual pyrolysis products, with good results.

The weight loss behavior of sweet gum wood was well simulated from the corresponding weight loss of milled wood lignin and filter paper cellulose (from a previous study) weighted, respectively, by the fraction of lignin and of holocellulose (cellulose + hemicellulose) in the whole wood. Yields of individual products, however, could not be predicted by this approach.

Thesis supervisors: Jack B. Howard, Professor of Chemical Engineering
John P. Longwell, Professor of Chemical Engineering
William A. Peters, Principal Research Engineer, Energy Laboratory.

MASSACHUSETTS INSTITUTE OF TECHNOLOGY

DEPARTMENT OF CHEMICAL ENGINEERING

Room number: 66-059 Cambridge, Massachusetts 02139 Telephone: (617) 253-6535

October, 1981

Professor Jack P. Ruina
Secretary of the Faculty
Massachusetts Institute of Technology

Dear Professor Ruina:

In accordance with the regulations of the faculty, I submit herewith a thesis entitled "Rapid Pyrolysis of Sweet Gum Wood and Milled Wood Lignin," in partial fulfillment of the requirements for the degree of Master of Science in Chemical Engineering at the Massachusetts Institute of Technology.

Respectfully submitted,

Theodore R. Nunn

Acknowledgements

First and foremost, I would like to thank my thesis supervisors, Professor John P. Longwell, Professor Jack B. Howard, and especially Dr. William A. Peters for their enthusiastic support and guidance throughout my stay at M.I.T.

I would also like to thank my fellow pyrolyzers, Michael A. Serio and Richard G. Cosway, for their valuable discussions and assistance in the laboratory. Dr. Howard D. Franklin was most generous with his time and introduced me to the kinetic analysis computer programs and for this I am grateful.

Thanks are due to Professor Hou-min Chang and his associates at North Carolina State University for the careful preparation of the biomass samples used in this study.

Thanks for the typing of this manuscript are due to Rebecca Sharp.

My educational experience at M.I.T. involved the interaction with many persons of different cultures and backgrounds, some of whom became very close friends and associates. In particular, I shall always cherish the friendships of Mark A. Philip (South Africa), Pablo G. Debenedetti (Argentina), Vince I. Paul (England), Patrick J. Van-de-Wijr (Belgium), Michael J. Snow (Los Angeles - there's always one in the crowd), and Thomas M. Bartos (somewhere in Michigan).

The author gratefully acknowledges the financial support for this project from the United States Department of Energy under Grant No. DE-FG02-79ET00084 and from the Edith C. Blum Foundation of New York.

To my parents I owe an enormous debt of gratitude for their continuous support and understanding throughout my years of schooling and especially for their encouragement over this past year.

Finally, I would like to express my deepest thanks to my special friend, Marti. She helped me maintain a reasonable degree of insanity while at M.I.T. and for this I shall never forget her.

TABLE OF CONTENTS

LIST OF FIGURES

LIST OF TABLES

1.0 Introduction

The years since the 1973 Arab oil embargo have witnessed a rapid increase in United States research and development on alternative fuels to take the place of petroleum and natural gas. It is hoped that liquid and gaseous fuels and feedstocks from domestic sources of coal, oil shale, tar sands, and biomass will greatly contribute to our national goal of energy self-sufficiency.

Unlike coal and oil shale, biomass offers the particularly attractive advantage of being a renewable energy resource and the potential to therefore provide high quality fuels and chemical feedstocks long after the world's fossil fuel reserves have been depleted to economically unrecoverable levels.

Of the many different materials defined as biomass, wood is of particular national interest as a nonfossil fuel resource because of the already existing and substantial U.S. forest industry. Although this industry exists primarily for the production of paper and building materials, there has been increasing interest in expanding the use of raw forestry materials for the production of valuable fuels and chemicals.

The use of wood as a fuel and chemical feedstock is not a new concept. Prehistoric cavemen burned wood to heat their caves and cook their food. Ancient Chinese and Egyptians heated wood in limited amounts of air to supply charcoal for metallurgical purposes as well as liquids for use as embalming fluids. The process of hardwood distillation was developed during the eighteenth century for the production of charcoal and the valuable by-products methanol, acetone, formaldehyde, and

acetic acid.

More recent technologies have been aimed at converting the solid biomass into higher quality liquid and gaseous products. Some conversion processes utilize biological pathways such as fermentation, which can reduce solid biomass materials to liquids such as ethanol via enzymatic digestion. Other processes involve the application of heat to the biomass in order to decompose the solid structure into the desired liquid and gaseous materials. The thermal processes have the advantage of being able to convert larger quantities of material per unit time for a given reactor volume.

One thermal conversion process which has received concentrated attention is pyrolysis. Pyrolysis, (from the Greek "pyro," meaning fire, and "lysis," meaning cleavage), is the thermal degradation of a material in an inert or oxygen deficient atmosphere. The pyrolysis process is known to precede or accompany other thermal processes such as combustion and gasification and, as such, a detailed knowledge of the pyrolysis mechanism is a necessary first step in the understanding of any biomass thermal conversion reaction.

Many investigators have studied the pyrolysis of cellulose, the main constituent of wood, while relatively few have examined the pyrolysis of wood and the other wood constituents, lignin and hemicellulose. Even fewer investigations are reported where the individual wood components have been pyrolyzed in order to gain a better understanding of and possibly simulate the pyrolysis behavior of the parent wood substrate. It has been qualitatively observed that wood thermal behavior can be

approximated by the sum of the individual constituents' thermal responses, although this postulate has yet to be reinforced by a rigid quantitative analysis (Shafizadeh and Chin, 1977).

Hajaligol (1980) has systematically examined the effects of various operating conditions on the rates and extents of conversion of cellulose pyrolysis to specific products. The present work examined the pyrolysis behavior of wood and lignin with the objective of obtaining an increased understanding of how the individual wood constituents influence the behavior of the wood during thermal processing.

2.0 Background

2.1 Wood Chemistry

Wood is made up of three principal chemical materials: cellulose, hemicellulose, and lignin. Wood also contains extraneous substances known as "extractives," which include turpenes, fatty acids, aromatics, resins, and essential oils. Typical distributions of these four constituents in softwoods and hardwoods are given in Table 2.1-1. Detailed discussions of the chemistry of wood and wood constituents are available in the literature (Wenzl, 1970; Pearl, 1967; Kollman and Cote, 1968; Sarkanen and Ludwig, 1971; Brauns, 1952).

Of the three major wood constituents, cellulose has by far been the most extensively studied due to its importance in the forest product industries and because it is the chief component of wood. Cellulose is a linear macromolecule of anhydro-β-glucopyranose units combined by ether-type linkages, known as glycosidic bonds, as shown in Figure 2.1-1. It is this important linear cellulosic structure which contributes high tensile strength to the parent wood.

Hemicellulose is a more complex cross-linked polymer composed of several monomer units, which is what helps to distinguish it from cellulose. Hemicelluloses are built up of D-xylose, D-mannose, D-glucose, D-galactose, L-arabinose, 4-O-methyl-D-glucuronic acid and, to a lesser extent, D-galacturonic acid and D-glucuronic acid as shown in Figure 2.1-2. Hemicelluloses have relatively few sugar units (50 to 200) as compared to native cellulose (7000 to 10,000), and exhibit a more branched molecular structure.

Table 2.1-1 Average Chemical Composition of Softwoods and Hardwoods (wt. %)*

Constituent	Softwoods	Hardwoods
Cellulose	42 ± 2	45 ± 2
Hemicellulose	27 ± 2	30 ± 5
Lignin	28 ± 3	20 ± 4
Extractives	3 ± 2	5 ± 3

*Taken from Thomas (1977)

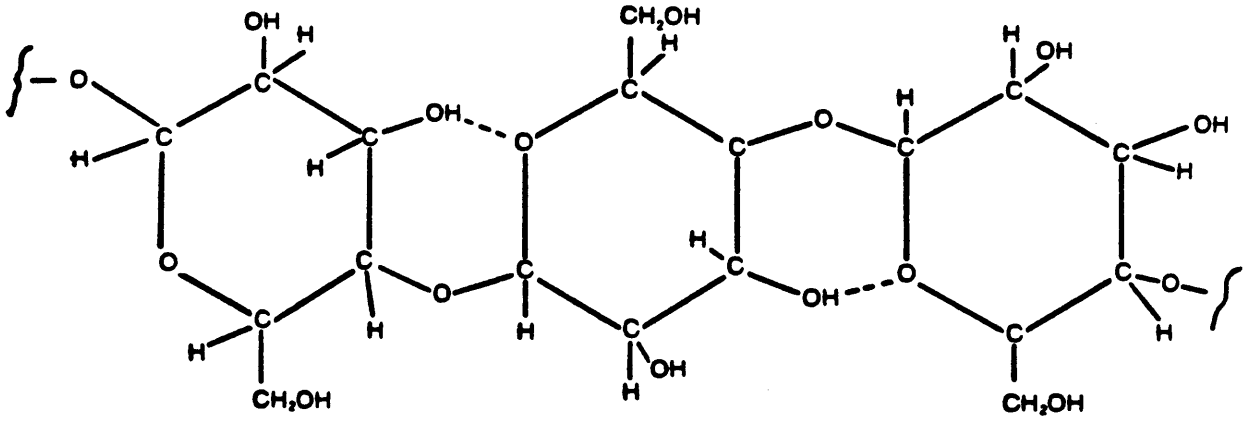

Figure 2.1-1 The Cellulose Molecule (SERI,1979).

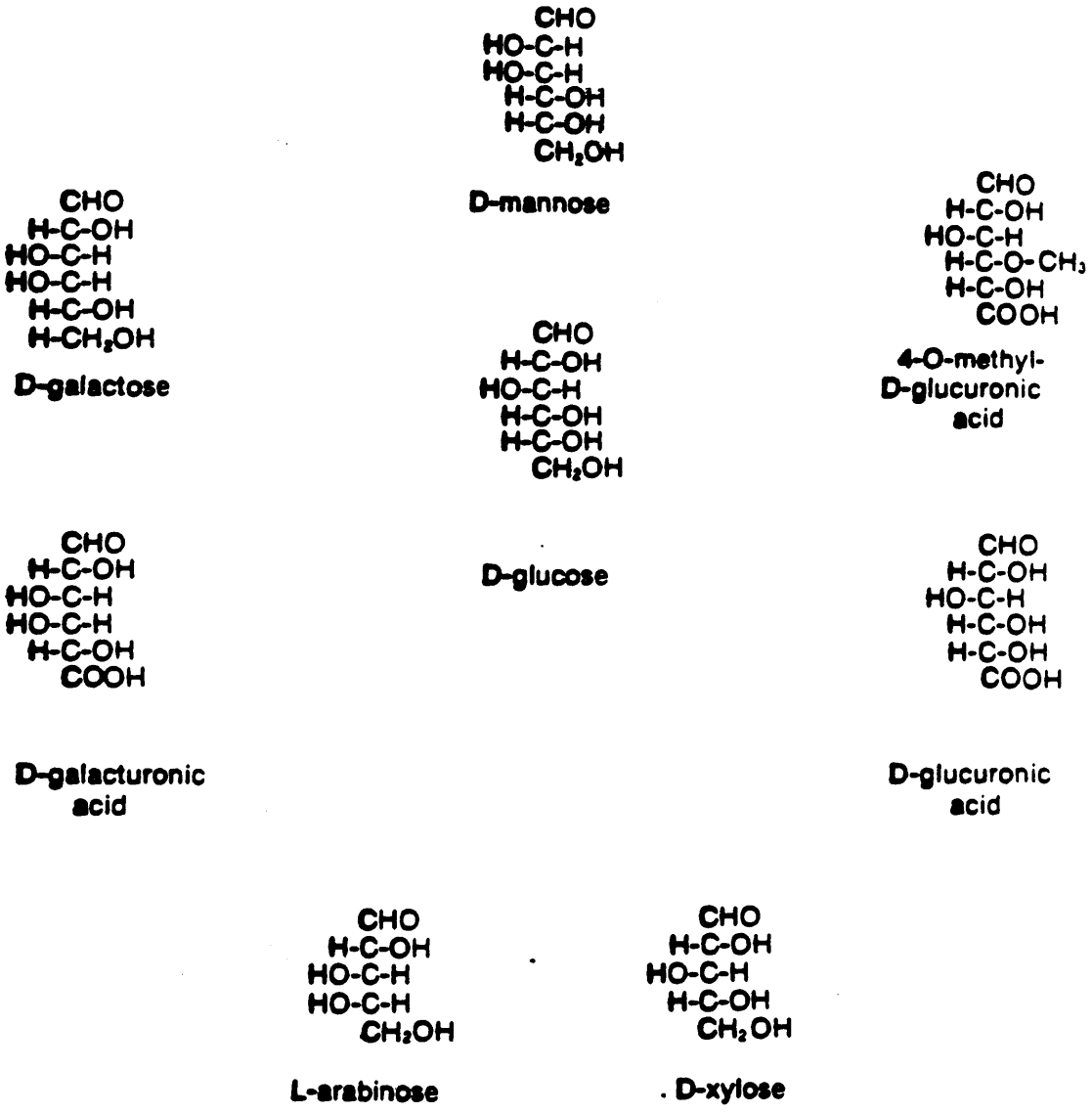

Figure 2.1-2 Sugar Units Commonly Found as Hemicellulose Components (SERI,1979).

Hardwoods contain two principal types of hemicellulose: O-Acetyl-4-O-methylglucurono-xylan and Glucomannan. Xylan is the predominant hemicellulose of all hardwoods, accounting for 25 to 35 wt. % with glucomannan forming 5 to 6 wt. % of the wood. Xylan is a polymer of the pentose sugar, D-xylose, and can contain some carboxylic acid and methyl-ether groups. Glucomannan is made up of randomly distributed D-mannose and D-glucose residues in a ratio of roughly 2:1.

Lignin is a three-dimensional polymer of phenylpropane units and acts as a cementing agent for the cellulose and hemicellulose fibers in wood. The complex chemical structure of lignin has been the subject of many investigations, and the classical structural representation determined by Freudenberg (1968) is shown in Figure 2.1-3.

2.2 Previous Work on Pyrolysis

Many investigations into the pyrolysis (also known as "thermal degradation" or "destructive distillation") of biomass materials are described in the literature, with the emphasis being on the study of cellulose pyrolysis. Among the most recent literature reviews are works by Molton (1977), Peters (1978), SERI (1979), Hajaligol (1980), and Klein (1981). Other classical discussions are presented by Wenzl (1970) on wood pyrolysis and by Allan and Mattila (1971) on the high energy degradation of lignin. Roberts (1970) presents an excellent review of the literature on the kinetics of biomass pyrolysis.

In an early review of the biomass pyrolysis, Brauns (1952) compared the products obtained by different investigators and

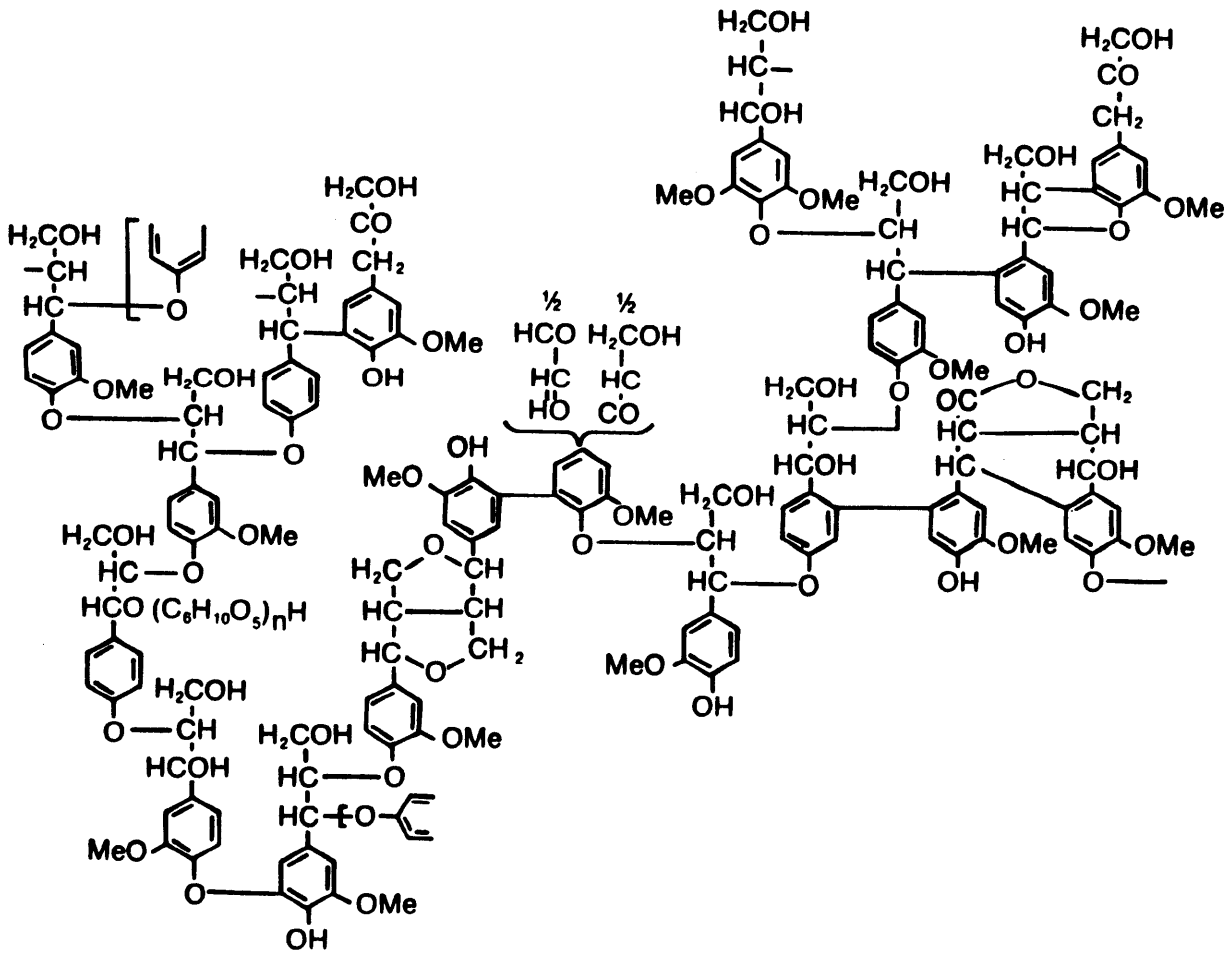

Figure 2.1-3 Lignin Structural Model (SERI,1979)

compiled the data shown in Table 2.2-1. The dry distillation of biomass is seen to produce char as the major product. Lignin produces higher ultimate yields of char (44-50 wt. %) than either wood (29-38 wt. %) or cellulose (28-35 wt. %) and also produced much less methanol than their corresponding woods, in spite of the higher methoxyl content of the lignin. The lower yield of methanol from lignin was thought to be caused by a change in the lignin during its isolation from the parent wood. The variations in the spruce lignin data are attributed to differing conditions of pyrolysis (Brauns, 1952).

The literature results reported for various biomass pyrolysis investigations are subject to differences arising from variations in experimental operating conditions. The operating conditions in different works are often poorly documented, which makes comparisons even more difficult. It is well known that slight variations in operating conditions can greatly affect the pyrolysis product distribution (Probstein and Hicks, 1981). Also, lignin pyrolysis results from different studies sometimes exhibit extremely large variations in product distributions which may be the result of the use of different types of lignin, a specification which is often omitted from the technical description. For example, Kraft lignin, obtained as a by-product of the Kraft pulping process, undergoes much more chemical modification during preparation than does milled wood (Björkman) lignin. The latter is extracted from the parent wood in an essentially unaltered chemical state (Pearl, 1967; Kollmann and Cote, 1968).

Iatridis and Gavalas (1979) investigated the pyrolysis of

Table 2.2-1 Products of the Dry Distillation of Wood, Cellulose, and Lignin*(%)

	Wood		Cellulose		Hydrochloric Acid Lignin		
Product	Spruce	Aspen	Spruce	Aspen	Spruce	Spruce	Aspen
Char	37.81	29.45	34.86	28.08	50.64	45.0	44.30
Tar	8.08	9.83	6.28	4.27	13.00	9.6	14.25
Methanol	0.96	1.48	0.07	0.00	0.90	0.7	0.87
Acetone	0.20	0.79	0.13	0.20	0.19	0.1	0.22
Acetic Acid	3.19	7.37	2.79	2.66	1.09	0.6	1.28
Carbon Dioxide	50.50	--	62.90	--	9.60	--	--
Carbon Monoxide	32.55	--	32.42	--	50.90	--	--
Methane	9.23	--	3.12	--	37.50	--	--
Ethane	1.72	--	1.56	--	2.00	--	--

*Data are from Brauns (1952).

Kraft lignin under constant temperature conditions for different solids residence times in a captive sample reactor similar to the one used in the present study. They report an ultimate char yield of less than 35 weight percent at 750 deg. C, which is somewhat less than the 44-50 wt. % char yield reported by Brauns (1952) for hydrochloric acid lignin. Different reactor configurations and operating conditions as well as different types of lignin were used in the separate studies, and this may account for the variations in char yields.

A recent investigation of Kraft lignin pyrolysis in a helium plasma was carried out by Graef et al. (1981). These investigators achieved high heating rates (actual values not reported) and obtained the narrow distribution of pyrolysis products shown in Table 2.2-2. The char yield of 33 wt. % reported by Graef et al. compares favorably to the yield of 35 wt. % presented by Iatridis and Gavalas (1979). The microwave plasma pyrolysis apparatus used by Graef et al. caused very severe degradation of the lignin sample, as is evidenced by the high yields of hydrogen, carbon monoxide, and acetylene (Table 2.2-2).

Shafizadeh and Chin (1977) examined the thermal decomposition of wood and its constituents using thermal gravimetric techniques and concluded that the pyrolysis behavior of whole wood reflects the sum of the thermal responses of its three major components. They also discuss the chemical reactions that take place during biomass pyrolyses and used electron spin resonance (ESR) to study the temperature dependence of free radical formation from wood and its components. Their ESR data showed that the free radical formation in wood is

Table 2.2-2 Overall Product Distribution in the Microwave Plasma Pyrolysis of Kraft Lignin*

Product	Yield (wt.%)
Char	33
Volatile Fraction**	10
Gases	54
Individual Gases(Vol.%)	
Carbon Monoxide	44
Carbon Dioxide	2
Hydrogen	43
Methane	2
Ethane	Trace
Acetylene	14
Higher Hydrocarbons	Trace

*From Graef et al.(1981)

**Includes water, methanol, acetone, acetic acid, and phenolic compounds.

roughly the summation of that for its three principal constituents.

Wenzl (1970) presents a detailed review of the pyrolysis behavior of wood constituents as well as a discussion of the product distributions from the pyrolysis of different wood species. Very little was mentioned about the relative thermal reactivity of the individual wood constituents, although it was made clear that hemicellulose is the most reactive component of wood, while lignin is more thermally stable.

The overall rate and kinetics of the thermal decomposition of wood have been investigated in several works. A good review on wood pyrolysis kinetics is that of Roberts (1970) which covers a wide variety of experimental investigations.

Most investigators have correlated the overall pyrolysis rates using a single step, first-order expression with an Arrenhius rate constant equation, as in equation 2.2-1.

$$\frac{dV}{dt} = k(V^* - V) \qquad (2.2\text{-}1)$$

where $k = k_o \exp(-E/RT)$ = Arrenhius rate constant

V = fractional weight loss for the overall reaction

V^* = ultimate value of V (i.e., at long times)

k_o = Arrenhius frequency factor

E = apparent Arrenhius activation energy

R = gas constant

T = absolute temperature.

Equation 2.2-1 can be integrated and fitted to laboratory data to provide best fit values for the empirical parameters k_o, E, and V^*.

Stamm (1956) reports values for E and k_o of 29.8 kcal/mole and 2.8 x 10^7 sec^{-1}, respectively, for the pyrolysis of Sitka spruce veneer under molten metal over a temperature range of 167-300°C and residence times of 1 min. to 60 days. Roberts and Clough (1963) found that values of 15 kcal/mole for E and 1.5 x 10^3 sec^{-1} for k_o fit their weight loss data for the pyrolysis of beech wood dowels over a temperature range of 350-435°C.

Roberts (1970) concluded that values of 30 kcal/mole and 7 x 10^7 sec^{-1} for E and k_o, respectively, well represented the literature data for the pyrolysis of small wood samples over a temperature range of 230-400°C. In the most recent kinetic investigation of wood pyrolysis, Thurner and Mann (1981) found an activation energy of 25.5 kcal/mole and a frequency factor of 7.4 x 10^5 sec^{-1} to describe the kinetics of their wood pyrolysis over a temperature range of 300-400°C.

An Arrenhius plot of the above literature values for the single step, first-order reaction model for overall wood pyrolysis weight loss is shown in Figure 2.2-1. This plot of the reaction rate constant, k in equation 2.2-1, versus reciprocal absolute temperature shows how the reaction rates can vary between the different investigations.

Much less is known about the kinetics of lignin pyrolysis. Domburg and Sergeeva (1969) analyzed the thermal behavior of sulphuric acid lignins using a derivatographic technique to obtain activation energies for lignin pyrolysis weight loss in the range of 17-38 kcal/mole over temperatures of 200-400°C for lignin samples from different wood species. Wenzl (1970) reports

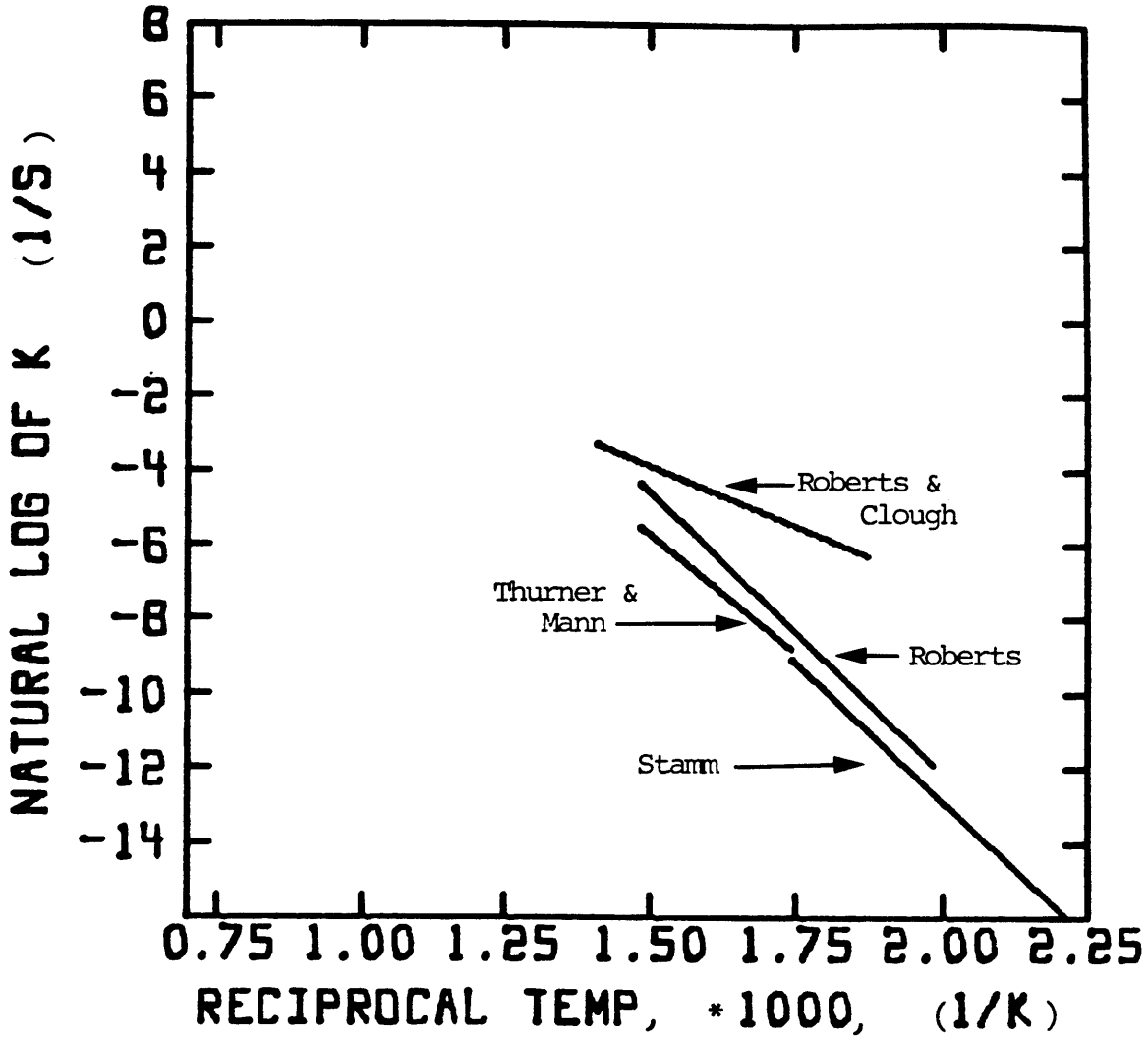

Figure 2.2-1 Rate Constant for Wood Pyrolysis Measured by Various Investigators.

an overall activation energy of 23.4 kcal/mole for lignin pyrolysis and Tang (1967) obtained Arrenhius parameters of 9 kcal/mole for activation energy and 0.93 sec^{-1} for frequency factor.

The kinetic investigations discussed above provide a good basis for further investigations of biomass pyrolysis kinetics. Much more work is needed in the area of modelling the pyrolysis reactions, especially in the area of lignin pyrolysis, where very little kinetic information is available.

3.0 Apparatus and Procedure

3.1 Sample Preparation

The sweet gum hardwood and milled wood lignin samples used in this work were supplied by Professor H.-M. Chang at the Department of Wood and Paper Science at North Carolina State University. The chemical composition of the wood is shown in Table 3.1-1 and the elemental compositions of both the wood and lignin are included in Table 3.1-2.

The wood powder was sieved to a size range of 45-88 micron particles. The lower limit was restricted by the captive sample screen size and the upper limit was chosen to eliminate heat and mass transfer effects (see Appendix A-1). Great care was taken to assure that particles below 45 micron were not collected, because such particles would fall through openings in the captive sample screen. This material was then dried over silica gel dessicant for at least one month prior to use.

The milled wood lignin preparation posed a more difficult problem, in that only a small quantity of feedstock (approximately 40 gm) was available. Attempts were made to sieve this feedstock to obtain a 45-88 micron size fraction, as in the analysis for wood. The lignin adhered to the sides of the sieves and appeared to be clogging the sieve openings. This was totally unacceptable because a major portion of the expensive lignin powder would be rendered unavailable for experimental runs.

The next idea was to try to approach Hajaligol's (1980) technique of using strip forms of cellulose. A small, hand operated catalyst pelletizing press was acquired along with

Table 3.1-1 Chemical Composition of Sweet Gum Hardwood* (wt. % of extractive free wood)**

Cellulose	43.2
Hemicellulose (Xylan + Glucomannan)	31.1
Lignin (Kraft analysis)	27.3

*From Chang(1981)
**The components total slightly more than 100 percent because the analytical methods used somewhat over-determine the individual percentages (Andrews,1980).

Table 3.1-2 Elemental Compositions of Sweet Gum Hardwood and Milled Wood Lignin* (wt. % of dry material)

	Carbon	Hydrogen	Oxygen
Sweet Gum Hardwood	49.46	6.13	44.64
Milled Wood Lignin	59.11	6.01	32.02

*Analysis performed by Huffman Laboratories, Inc., Wheat Ridge, Colorado.

two 1 x 6 inch parallel plates for use in preparing flakes from the powdered lignin. Approximately 20 mg of lignin was placed between the plates, pressure was applied, and the powdered lignin emerged in the form of small, thin flakes (less than 0.1 mm thick). The lignin flakes adhered to the parallel plates and had to be chipped off with a microspatula. During this chipping process, most of the 10 mm diameter flakes broke up into even smaller fragments; these fragments being unacceptable for pyrolysis experiments. Thus, several lignin pressings were needed before enough good-size flakes were obtained to carry out a 100 mg pyrolysis run. The lignin flakes, in spite of the problems mentioned, allowed more efficient utilization of the sample than the sieving approach, and were thus chosen as the sample configuration for the lignin pyrolysis experiments. These flakes were dried over dessicant prior to use.

Although the lignin flakes gave reasonable pyrolysis data, and were not believed to cause mass and heat transfer limitations, this situation is far from optimal in terms of reproducibility of sample distribution on the screen and further work is needed in this area.

3.2 Apparatus Description

The pyrolysis apparatus used in this work was a scaled-up version of the captive sample reactor first built by Anthony (1974) for coal pyrolysis studies. A glass version of the original reactor design was used by Lewellen et al. (1977) to investigate cellulose pyrolysis and was later modified by

Suuberg (1977) to permit the determination of product distributions in coal pyrolysis and hydropyrolysis studies. This apparatus has also been used by Franklin (1980) and Cosway (1981) for coal pyrolysis experiments. These investigations showed that good kinetic data could be obtained for the total weight loss and yields of individual products from coal and cellulose pyrolysis.

The captive sample apparatus allows for the independent control of such reaction conditions as heating rate, peak temperature, holding time at peak temperature, and reactor pressure over the range of operations shown in Table 3.2-1.

This reactor has the additional advantage of allowing good thermal contact between the sample and the heating medium, accurate measurement of the sample time-temperature history, and near zero volatiles residence time at high temperatures and rapid quenching of volatile products. This reactor design thus minimizes, (but does not totally eliminate) the effects of secondary reactions of volatile compounds and hence allows the primary decompositions of organic materials to be more reliably studied.

A disadvantage of Anthony's system was that it could accomodate only a very small quantity of pyrolysis material (on the order of 15 mg), which resulted in even smaller amounts of products available for analysis. This problem was circumvented for biomass studies by the design and construction of a large-scale reactor (Caron, 1979) which could handle a sample size 10 times larger than that for the previous investigations. This larger reactor was used by Hajaligol (1980) for the pyrolysis of cellulose.

Table 3.2-1 Variability of Pyrolysis Reaction Conditions

Operating Parameter	Range of Control
Heating Rate	50 to 100,000 K/s
Peak Temperature	400 to 1500 K
Holding Time at the Peak Temperature	0 to infinity sec
Pressure	0.0001 to 4.0 atm*

*A separate reactor is available for experiments at up to 100 atm pressure.

A schematic of the reactor system is shown in Figure 3.2-1. The reactor is a nine inch by nine inch Corning Pyrex cylindrical pipe sealed on each end by stainless steel plate flanges. Inside the reactor are two large brass electrodes between which a 325-mesh (45 micron) stainless steel screen containing the sample is placed. A chromel-alumel thermocouple (0.001 inch diameter wire, 0.003 inch diameter bead) is placed between the folds of the screen and connected to a fast response Hewlett-Packard 680M strip chart recorder.

The screen is heated by the circuit shown in Figure 3.2-2. In the present study, this circuit is set to heat the screen at a rate of 1000K/s to a desired peak temperature (up to 1500K) and immediately cooling begins. The average cooling rate is 200K/s by natural convection and radiation.

The pyrolysis products (except hydrogen) are collected follows. Char remains on the screen and its yield is determined gravimetrically. Tar is collected on an aluminum foil on the bottom of the reactor, on a filter paper secured at the reactor exit, and on the various exposed surfaces of the reactor. The reactor surfaces are washed with preweighed tissues soaked in a 2:1 (v:v) methanol: acetone solvent.

Some of the more volatile tar leaves the reactor with the product gases and is condensed in the first gas trap. This trap is a 14-inch long 3/8-inch U-shaped stainless steel tube packed with glasswool and immersed in a bath of dry ice and methanol at 195K. The gaseous products are recovered from the trap by heating it to 373K and the light tars are subsequently recovered by extraction of the glasswool with the methanol:

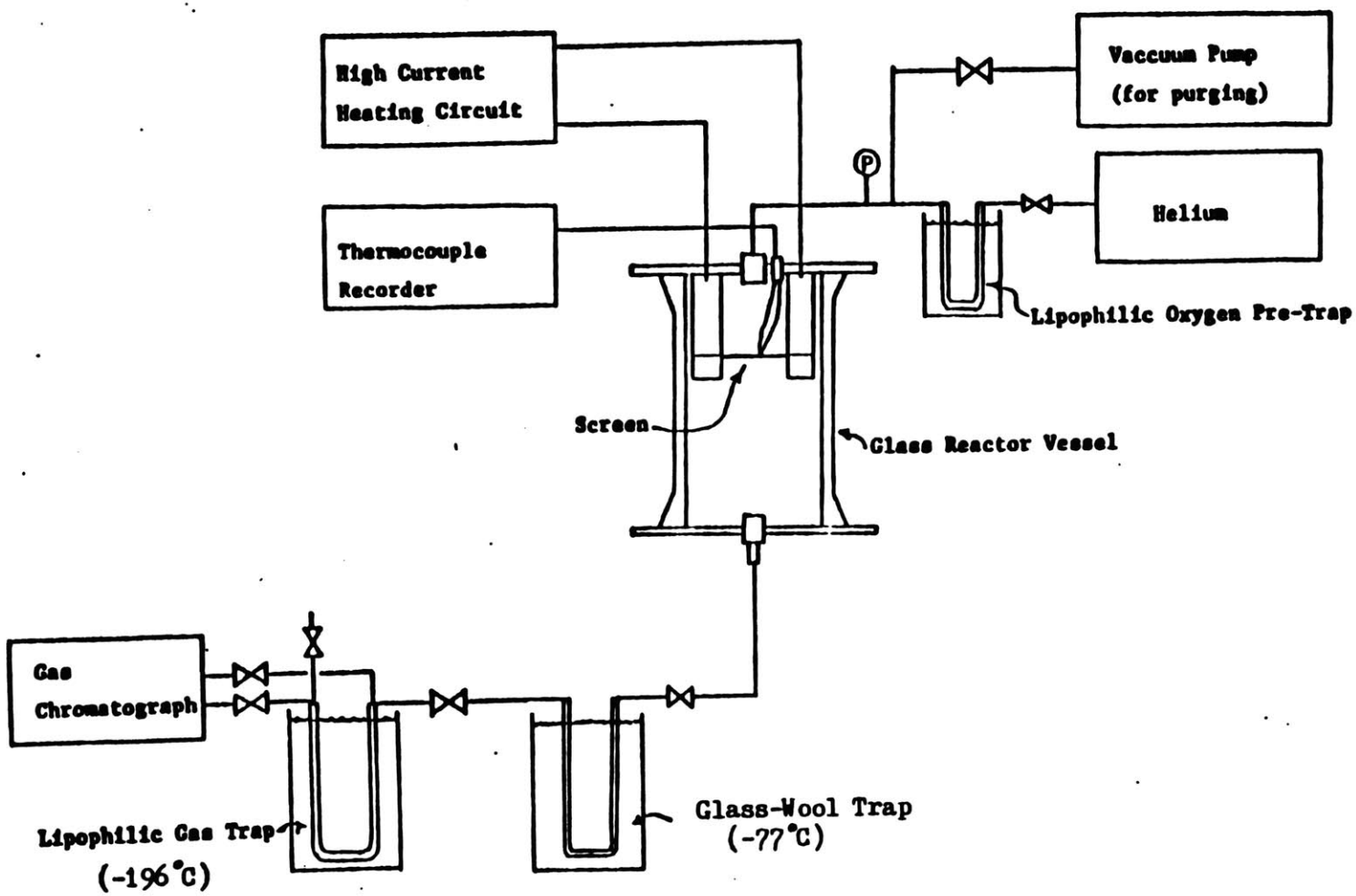

Figure 3.2-1 Schematic of Captive Sample Apparatus (Hajaligol,1980)

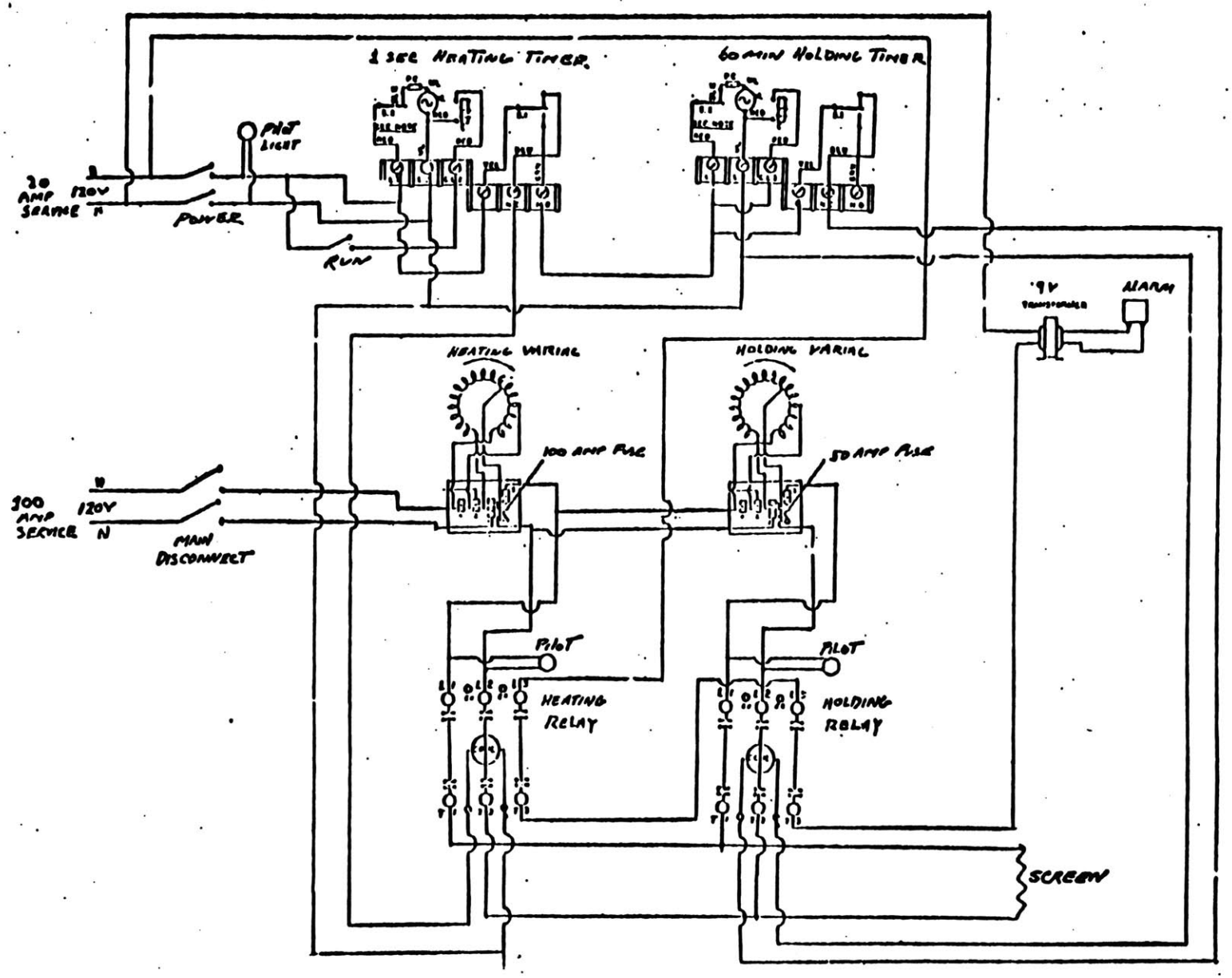

Figure 3.2-2 Captive Sample Reactor Wiring Diagram (Caron, 1979).

acetone solvent.

A second downstream trap is identical in dimensions to the glasswool trap except that it is packed with 50/80 mesh Porapak QS and is immersed in a liquid nitrogen bath at 75K. This lipophilic trap collects the lighter gases (except hydrogen) and any liquid material not captured by the glasswool trap.

The gases are analyzed on a Perkin Elmer Model 3920B gas chromatograph with dual flame ionization/thermal conductivity detectors. The trap contents were analyzed on a 12 foot by 1/4 inch, 50/80 mesh Porapak QS column temperature programmed from 195 to 513K at a rate of 16K/min with an initial holding time of 2 minutes. Response factors and retention times for these conditions and a helium carrier gas flow rate of 60 cc/min are reported in Appendix A-2.

A few runs were made to analyze the effect of peak temperature on yields of hydrogen. Because hydrogen and helium have very similar thermal conductivities, nitrogen gas had to be used in the reactor and as the GC carrier gas in order to detect a hydrogen signal. The other run procedures were followed as described previously except that, instead of purging the gaseous products from the reactor, gas samples were removed through a septum at the top of the reactor with a precision syringe. These samples were injected directly into the GC, operating isothermally at 303K with a Spherocarb 80/100 mesh, 10 foot by 1/8 inch column and a nitrogen carrier gas flow rate of 60 cc/min. The nitrogen carrier gas gave a much noisier GC baseline than did helium, and it was thus difficult

to quantify the small amounts of hydrogen produced.

3.3 Run Procedure

The 325-mesh stainless steel screens were cut into 14 x 15 cm rectangular strips and folded over twice. The result (after trimming) was a 4.5 x 14 cm screen with three layers of stainless steel mesh. Each screen was prefired in a helium atmosphere at 1300K for a few seconds to clean off any residual cutting oil.

Approximately 100 mg of sample (45-88 micron particles for wood runs and 5-10 mm flakes for lignin runs) were spread evenly on the bottom layer of a preweighed screen and stored overnight in a petri dish full of silica gel dessicant. The screen was then weighed several times until an equilibrium weight was reached. This degree of care was also taken with the aluminum foil and the reactor exit filter and nut. Satisfactory equilibrium weight was achieved when successive weighings differed by less than 0.1 mg.

The aluminum foil, filter and nut were secured on the bottom of the reactor and the screen was carefully clamped between the two electrodes by tightening the wing nuts which forced the two electrode pieces together. The thermocouple was carefully placed between the top two layers of the screen and the reactor vessel was bolted shut. The reactor was then evacuated to 0.1 mm Hg and flushed 4 or 5 times with helium gas. The helium was prepurified by passing it through a lipophilic trap at 75K. The reactor pressure was then brought to 5 psig, the temperature recorder was turned on, and the screen

was heated to the desired peak temperature and immediately allowed to begin cooling.

The reactor atmosphere was allowed to become stagnant for up to 10 minutes after the reaction so that most of the tar produced would settle on the aluminum foil. After this settling period, the reactor was gently pressurized to its maximum allowable pressure of 15 psig and the gases were purged from the reactor through the traps at a flow rate of 15 cc/min for at least one hour. Running the purge cycle at 15 psig inhibited air leakage into the system, which could create problems in the GC analysis if not controlled.

The screen, foil, and filter paper were weighed to get the char yield and some of the tar weight. Additional tar was obtained by wiping the reactor surfaces with two preweighed, predried Kimwipe tissues soaked in a 2:1 (v:v) methanol:acetone solvent. The tissues were predried in small petri dish dessicators in order to limit the effects of atmospheric moisture and two tissues were used because it was found that not all of the wood and lignin pyrolysis tars were collected with just one tissue. These tissues were placed in a fume hood for one hour to evaporate the solvent and were then placed back in the petri dish dessicators until an equilibrium weight was reached.

A control tissue was used with the run tissues to monitor the effectiveness of the tissue weighing procedure. The tissue weights rarely changed by more than ±0.5 percent by weight of tissue (±2 mg). However, it is important that the dessicant be changed every 2-3 days for effective moisture control.

The contents of the two traps were analyzed by gas chromatography. The glasswool trap was also extracted with about 10 ml of methanol:acetone solvent to collect light tars that may have condensed there and not been injected into the GC.

Samples of lignin, wood, and selected tars and chars were sent to Huffman Laboratories, Inc., Wheat Ridge, Colorado for C, H, and O elemental analysis. Some elemental analysis was also performed in-house by Rau (1981).

3.4 Experimental Error Analysis

Each weighing had associated with it a maximum probable uncertainty of 0.1 mg. According to Shoemaker et al. (1974), the limit of error in the difference between two weighings is equal to $\sqrt{2}$ times the limit of the error in a single weighing. Thus, the error in the weight of a wood or lignin sample is approximately ±0.14 mg. This error is propagated to the char analysis, giving an uncertainty in char yield of ±0.14 percent by weight of wood or lignin when 100 mg samples are pyrolyzed.

Assuming an error of 0.1 mg in each weighing for tar analysis and a 2 mg uncertainty in weight for each tissue weighing due to moisture effects, a random error analysis (see Appendix A-3) leads to an error in tar yield of ±3 to 5 percent by weight of wood or lignin. While the present tar data showed reasonable precision, it is obvious that there is still room for improvement in the tar collection procedure. This error is believed to account for some of the low material balances in the wood runs.

The products that are analyzed by gas chromatography are subject to calibration uncertainties of 1 to 3 percent by weight of component being measured. In addition, tailing of the water peak is thought to yield errors of up to 30% by weight of each component which is analyzed after water. However, the collective weight of these components is so small that the error in percent by weight of wood or lignin is less than 4%.

Some amount of air leaks into the system and thus creates an uncertainty in the carbon monoxide GC analysis due to the fact that oxygen and CO have similar retention times on the Porapak QS GC column. This interference was minimized by increasing the system pressure during purging to reduce the amount of air leakage and by slightly altering the GC analysis temperature program to allow better resolution between oxygen and carbon monoxide peaks. The amounts of oxygen corresponding to typical air leaks would cause an error of approximately 3 percent by weight of carbon monoxide or about 0.5 wt. % of wood or lignin.

The uncertainty of the thermocouple readings was found by Hajaligol (1980) to be ±15K in the range of interest of this work.

4.0 Results and Discussion

4.1 Sweet Gum Hardwood

The data reported in this section are for the pyrolysis of 45-88 micron-sized particles of sweet gum wood. Data on the yields and compositions of the products of sweet gum wood pyrolysis were obtained under the reaction conditions specified in Table 4.1-1. These data are presented in Figures 4.1-1 and 4.1-3 through 4.1-16 with all yields being expressed as a percent by weight of dry wood. The curves in Figures 4.1-1 through 4.1-16 were drawn by hand in order to illustrate the trends in the data.

Figure 4.1-1 presents the results for the yields of char, tar, and gas (including water). Under the conditions of Table 4.1-1, decomposition of the wood is first observed at about 600K and increases with temperature until 93 percent of the wood is converted to volatile material at 950K. Above this temperature, the char yield remains constant at 7 wt. %. It is apparent that most of the sample weight loss occurs between 700 and 900K.

Tar and gas products are formed at the same initial rate starting at 600K but the production of tar becomes much greater as the peak temperature is increased above 700K. The tar yield goes through a maximum of about 55 wt. % at 850-950K and approaches an asymptotic yield of 46 wt. % as temperature increases. The decrease in tar yield at temperatures above 950K is believed to arise from secondary cracking reactions of the tar to yield light volatiles.

The secondary cracking of biomass tars to form light vola-

Table 4.1-1 Reaction Conditions for Sweet Gum Hardwood Pyrolysis

Heating Rate	1000 K/s
Peak Temperature	600 - 1520 K
Holding Time at the Peak Temperature	0 s
Reactor Pressure	5 psig
Reactor Environment	Helium

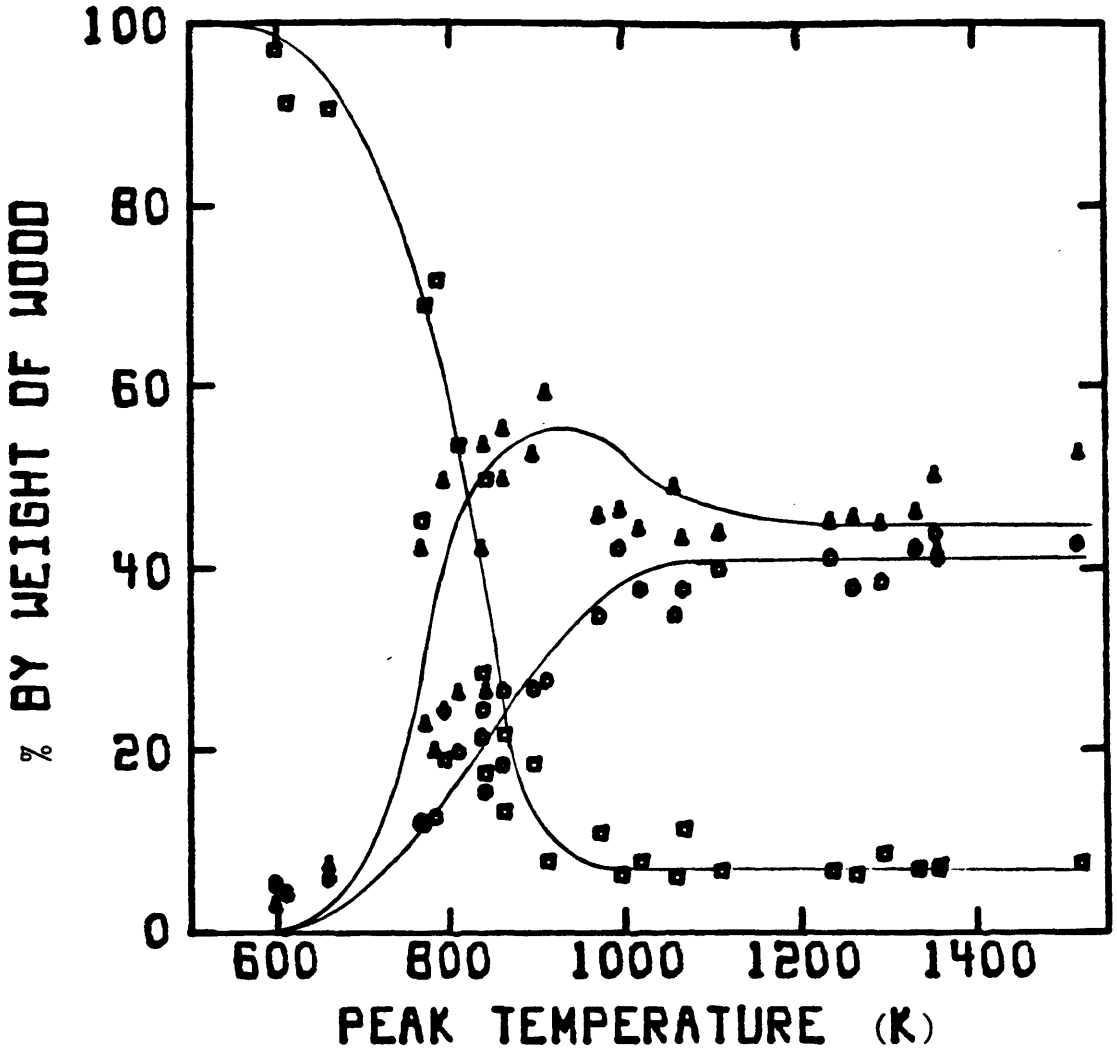

Figure 4.1-1 Char (□), Tar (△), and Gas (○) Yields From Sweet Gum Wood Pyrolysis.

tiles was also observed in Hajaligol's cellulose pyrolysis studies (Hajaligol, 1980). Figure 4.1-2 includes Hajaligol's results for the pyrolysis of cellulose filter paper strips under conditions similar to those of this work.

The reason for the termination of the tar secondary cracking reactions above 1200K is not altogether clear. It is possible that biomass pyrolyses produce two distinct kinds of tar, one that is reactive and one that is unreactive. As temperature increases above 950K, the reactive tar cracks to yield light volatiles while the unreactive tar remains intact. Most of the reactive tar is converted to either light volatiles or unreactive tar by 1200K. This phenomenon of the formation of two different kinds of tars has been seen in other biomass pyrolysis studies (Hajaligol, 1980; Wenzl, 1970; Stamm and Harris, 1953).

Tars produced from biomass pyrolyses are known to be highly aromatic in nature, and it is possible that the tars formed below 900K are highly substituted aromatic compounds that undergo cleavage reactions at higher temperatures. Once all of the available side chains have been removed by 1200K, the tars will not undergo further reactions. The validity of this explanation for the tar yield behavior will be borne out in future work on the qualitative and quantitative understanding of biomass pyrolysis tar chemistry.

The effects of peak temperature on the yields of individual gaseous products from wood pyrolysis are shown in Figures 4.1-3 through 4.1-16. These data are presented in the order in which the corresponding compounds elute from the gas

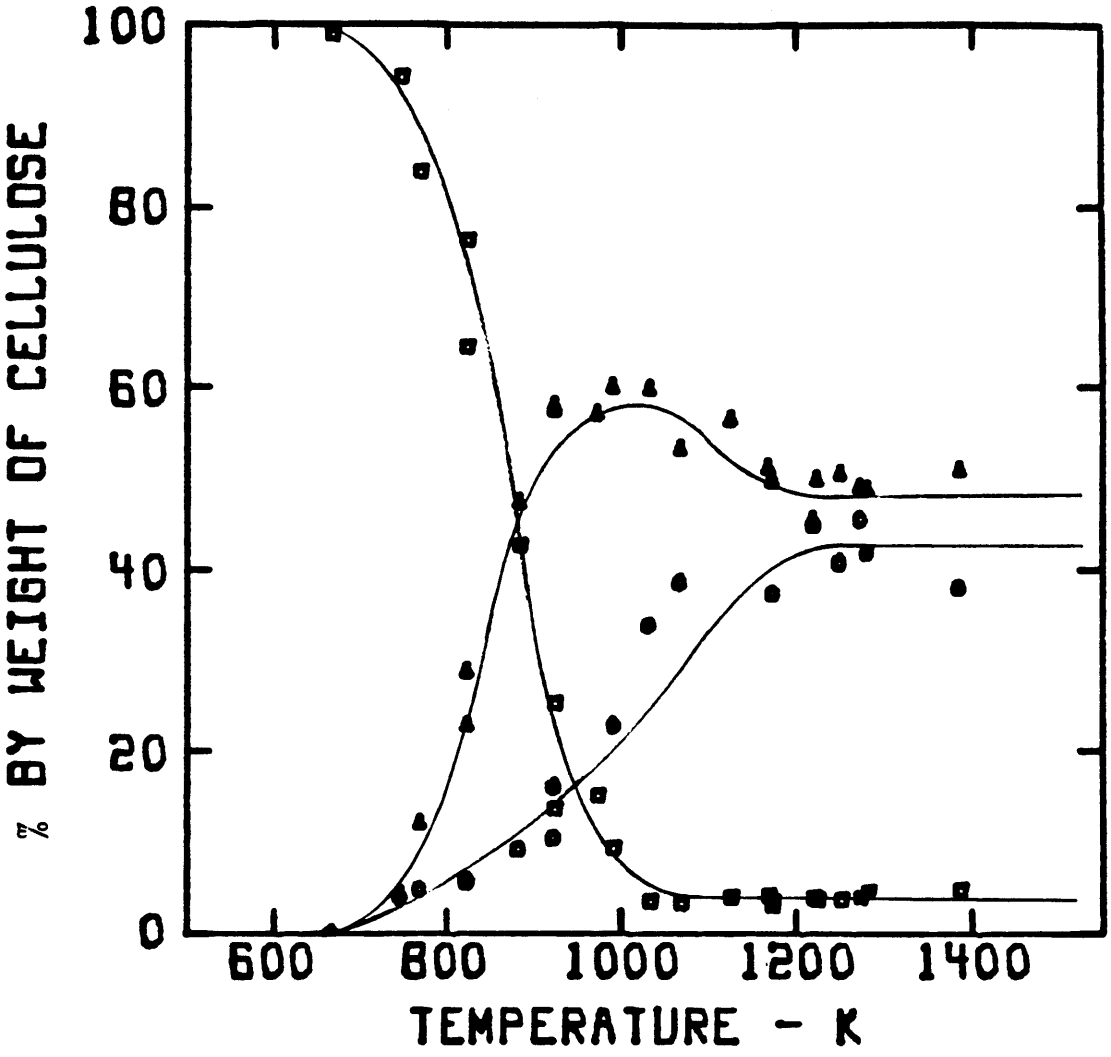

Figure 4.1-2 Char (□), Tar (Δ), and Gas (○) Yields From Filter Paper Cellulose Pyrolysis. (Data from Hajaligol, 1980)

chromatograph. The ultimate yields of these products and the corresponding peak temperatures at which these yields occur are summarized in Table 4.1-2.

Figure 4.1-3 shows the yield of carbon monoxide as a function of peak temperature. Carbon monoxide first appears at about 800K and reaches its asymptotic value of 17 wt. % near 1200K. Since significant additional amounts of CO are produced at temperatures above 950K (the temperature at which the char weight becomes constant), it is concluded that carbon monoxide is a major product of the secondary cracking reactions of the tar. The amount of CO produced above 950K (about 8 wt. %) accounts for a good deal of the 9 wt. % decrease in tar yield beyond 950K. At temperatures greater than 900K, CO is by far the most abundant gaseous product from sweet gum hardwood pyrolysis under the present conditions.

The effect of peak temperature on the yield of methane is shown in Figure 4.1-4. As with CO, methane production starts at 800K and increases rapidly with temperature. Methane yield also continues to increase at temperatures above 950K, indicating that it is a product of secondary tar cracking, and accounts for another 1 wt. % of the tar consumed above 950K. However, unlike CO, methane yield continues to increase with increasing temperature even above 1200K. The maximum measured yield of methane was 2.3 wt. % at 1520K.

The stainless steel screen used to contain the pyrolysis sample limits the maximum peak temperature to not more than 1550K. Above this temperature, the screen begins to degrade. It would be useful to obtain higher peak pyrolysis temperatures

Table 4.1-2 Yields of Individual Gaseous Products From Sweet Gum Hardwood Pyrolysis

Product	Estimated Ultimate Yield (wt.% of dry wood)	Approximate Peak Temperature (K)†
Carbon Monoxide	17.0	1200
Methane	2.3*	1520*
Carbon Dioxide	6.1	950
Ethylene	1.3*	1520*
Ethane	0.17	950
Water	5.1	900
Formaldehyde	2.0	900
Propylene	0.42	950
Methanol	1.0-2.0	**
Acetaldehyde	1.4	900
Butene + Ethanol	0.4-0.8	**
Acetone + Furan	0.7-1.1	**
Acetic Acid	1.0-2.0	**
Misc. Oxygenates	0.5-0.9	**
Hydrogen	< 1.0	**

† Approximate temperature at which the product yield becomes constant.

* Yield still increasing as temperature increases.

** Insufficient data to determine.

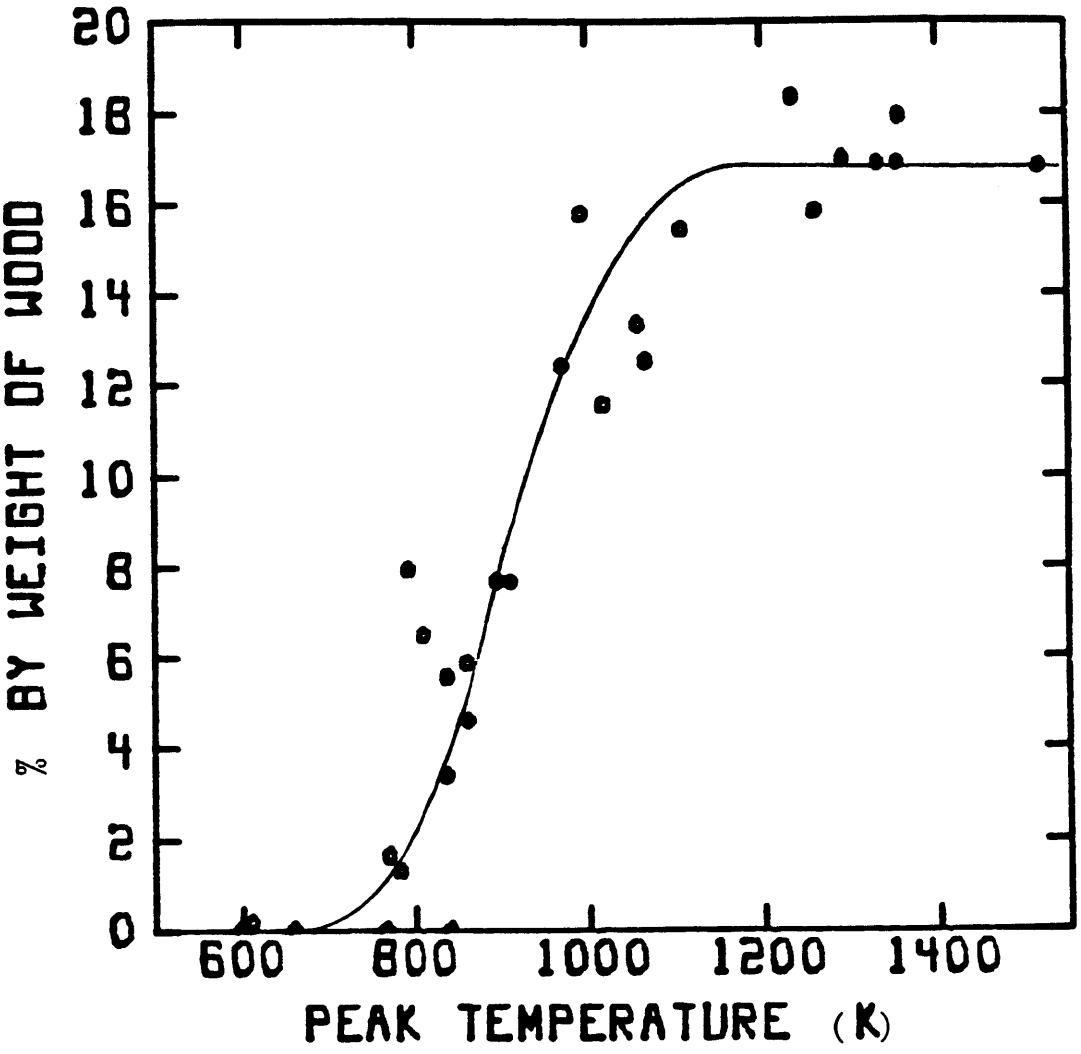

Figure 4.1-3 Carbon Monoxide Yield From Sweet Gum Wood Pyrolysis.

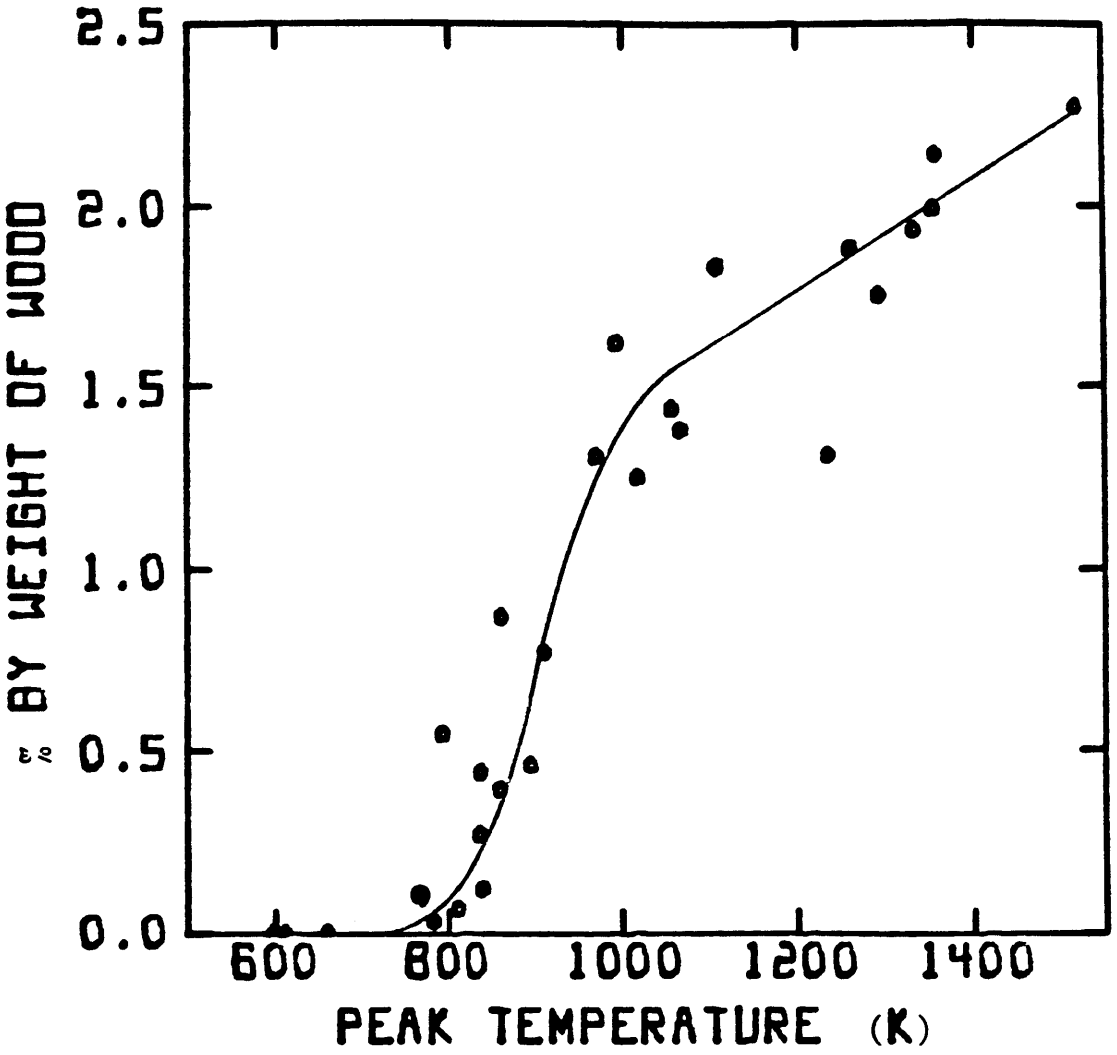

Figure 4.1-4 Methane Yield From Sweet Gum Wood Pyrolysis.

in order to establish whether or not the yield of methane reaches a plateau. This may be made possible by using higher melting point metals (such as tungsten or molybdenum) as the screen material in future studies.

Figure 4.1-5 illustrates the yield of carbon dioxide. Measurable quantities of carbon dioxide are found at temperatures as low as 600K. The carbon dioxide yield levels off at 6 wt. % near 950K, suggesting that it is probably produced mainly from the direct degradation of the wood particles and that the secondary cracking reactions contributing to CO and methane yields do not furnish much of the produced carbon dioxide.

Figure 4.1-6 shows the yield of ethylene as a function of peak temperature. Its behavior is very similar to methane. Ethylene is produced starting at 800K and increases steadily with temperature. At 950K there is an abrupt change in the slope of the ethylene curve, and its yield increases more slowly with further temperature increases. The maximum yield measured for ethylene was 1.4 wt. % at 1520K, but this does not appear to be an asymptotic value. This behavior indicates that the reactions that produce increasing amounts of methane above 950K may also be responsible for the increasing yields of ethylene.

The production of ethane is illustrated in Figure 4.1-7. Measurable ethane yield is seen at 800K, and a plateau of 0.17 wt. % is reached at 950K. Although ethane is not evolved until 800K, its behavior is similar to that of carbon dioxide in that the yield has just about levelled off at the temperature where the asymptotic char yield is first attained (950K).

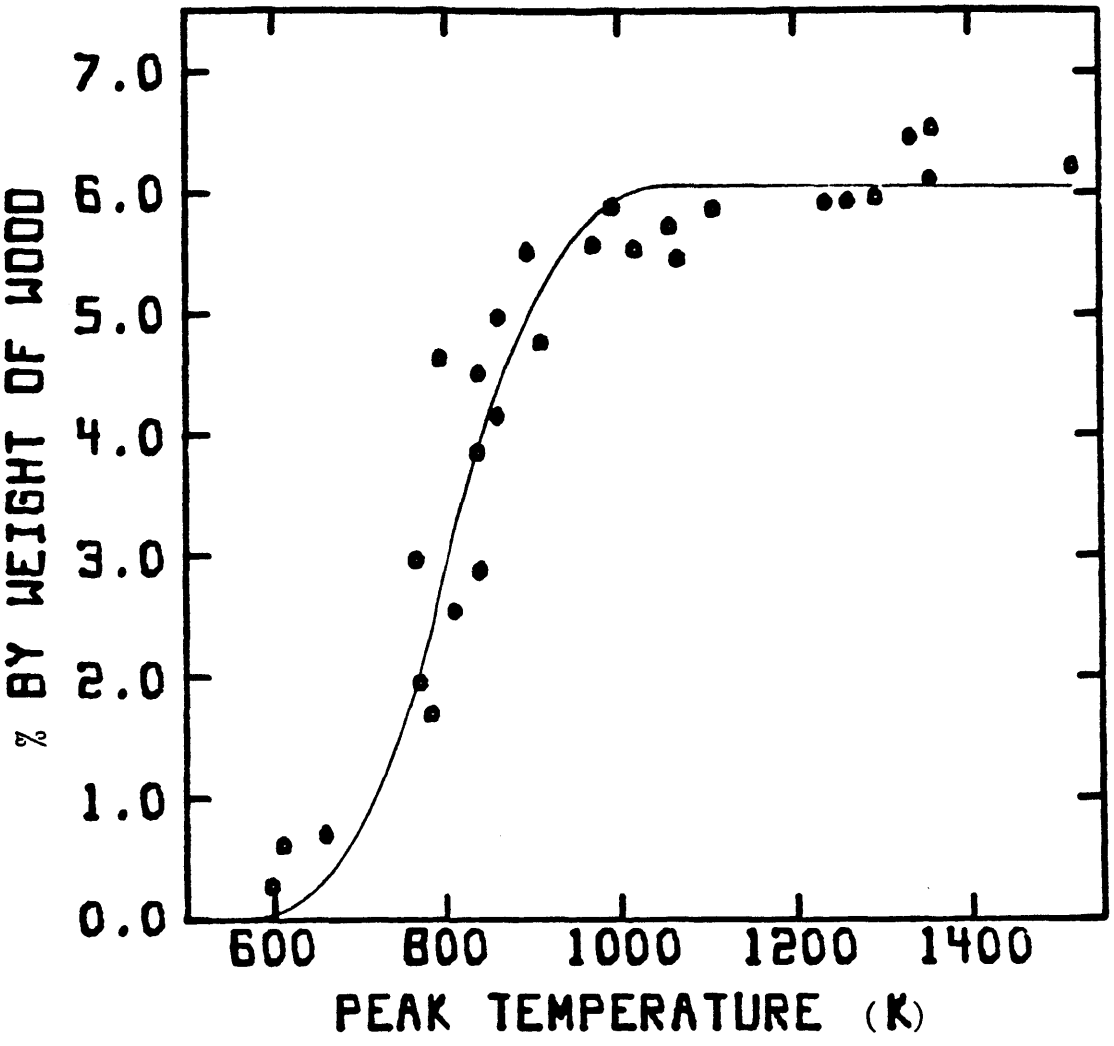

Figure 4.1-5 Carbon Dioxide Yield From Sweet Gum Wood Pyrolysis.

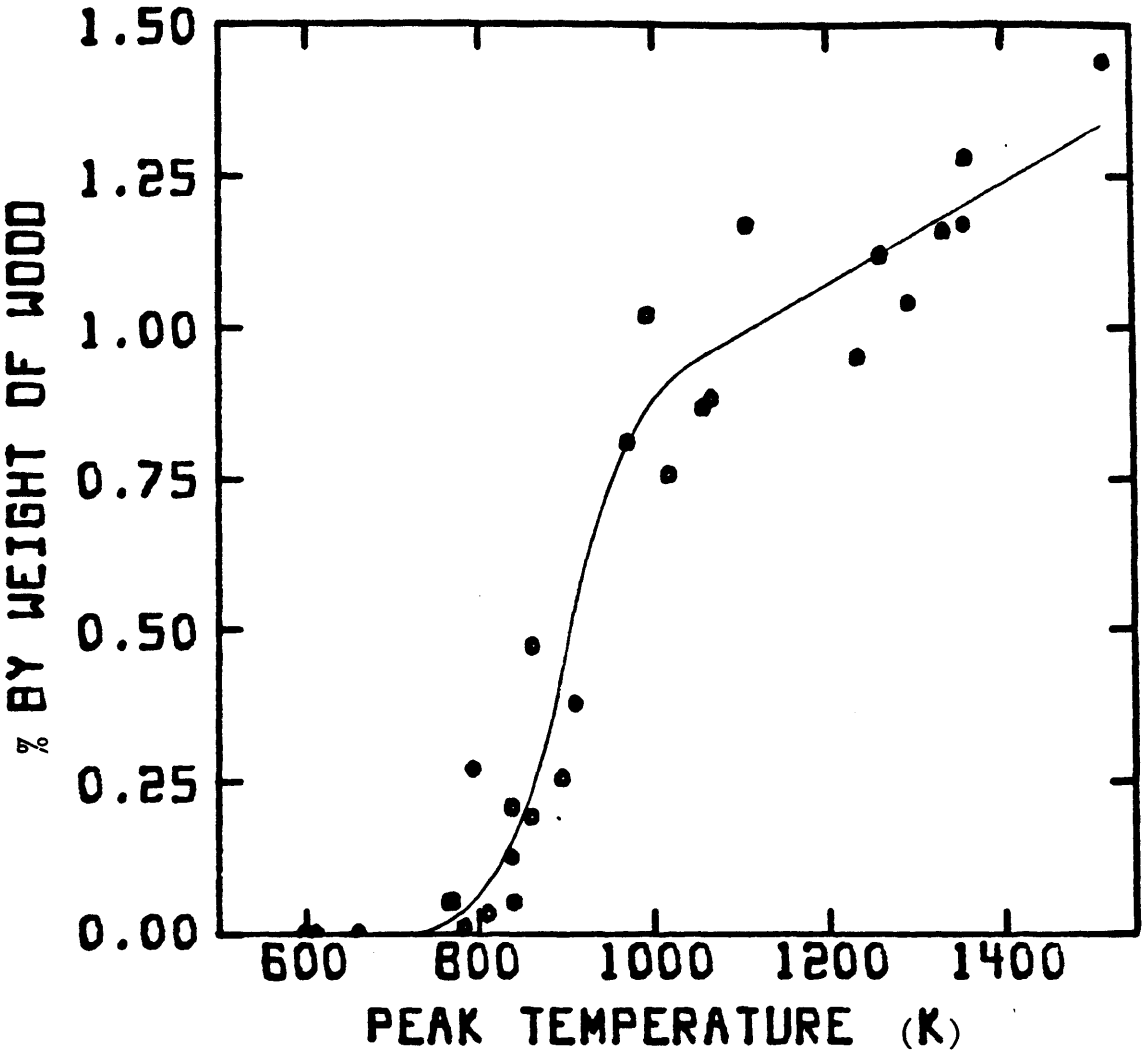

Figure 4.1-6 Ethylene Yield From Sweet Gum Wood Pyrolysis.

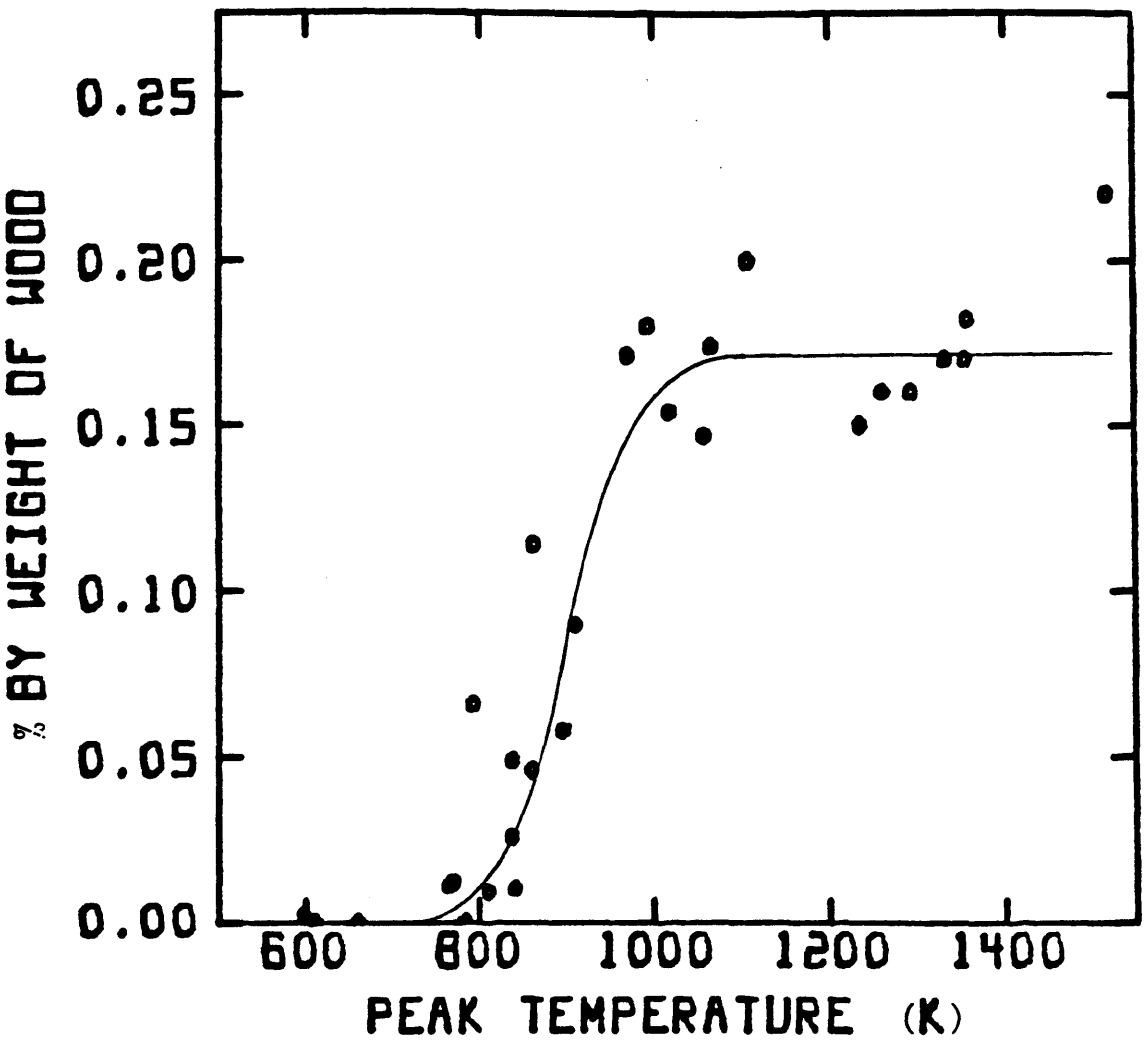

Figure 4.1-7 Ethane Yield From Sweet Gum Wood Pyrolysis.

This suggests that ethane is also formed primarily by the pyrolysis of wood, although it may be evolved via different chemical pathways than the carbon dioxide.

The yields of chemical (non-moisture) water are shown in Figure 4.1-8. The water data exhibit somewhat more scatter than the previous components, and this has been attributed by Cosway (1981) to the fact that the water peak exhibits severe tailing during the GC analysis. Even with this scatter the trend of the data is fairly certain. Water is evolved immediately after decomposition starts. This observation supports the postulate that the major pathways for water formation are dehydration and depolymerization reactions, which can occur at low temperatures (Hajaligol, 1980). The water yield plateau of 5.0 wt. % is reached at 900K. This behavior is similar to that of carbon dioxide which is also believed to be a primary product.

Figure 4.1-9 displays the formaldehyde data. The data scatter for this and other light oxygenated compounds is more pronounced because these products elute from the GC detector in the tail of the water peak. The HCHO data level off at a yield of 2 wt. % near 900K and are very similar to the water data.

Propylene is evolved in a manner that closely parallels the yield behavior of ethane. Figure 4.1-10 shows that propylene production begins at a peak temperature near 800K, rises extremely rapidly between 850 and 900K, and levels off at its ultimate yield of 0.42 wt. % near 950K. The propylene data exhibit some scatter, which is probably the consequence

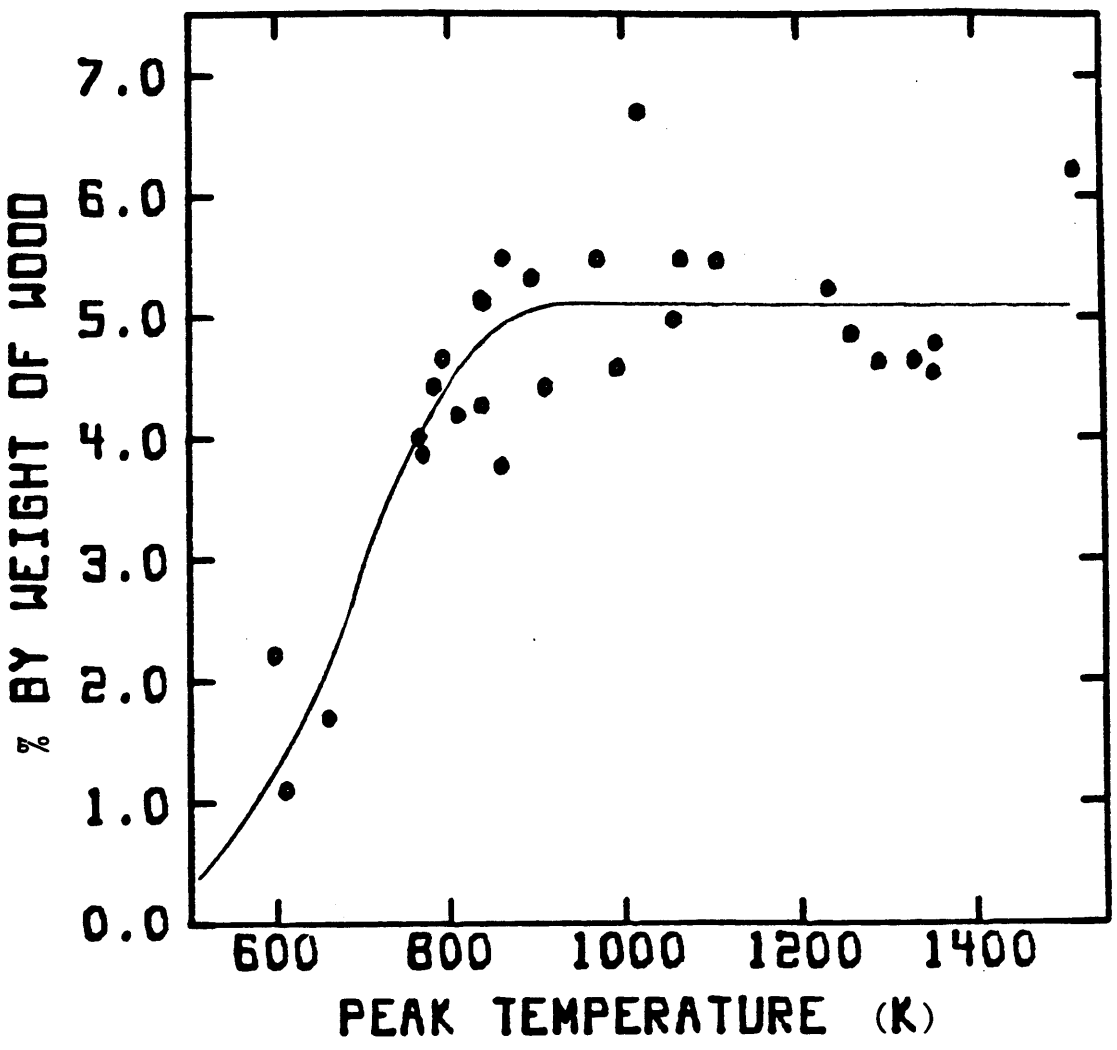

Figure 4.1-8 Water Yield From Sweet Gum Wood Pyrolysis.

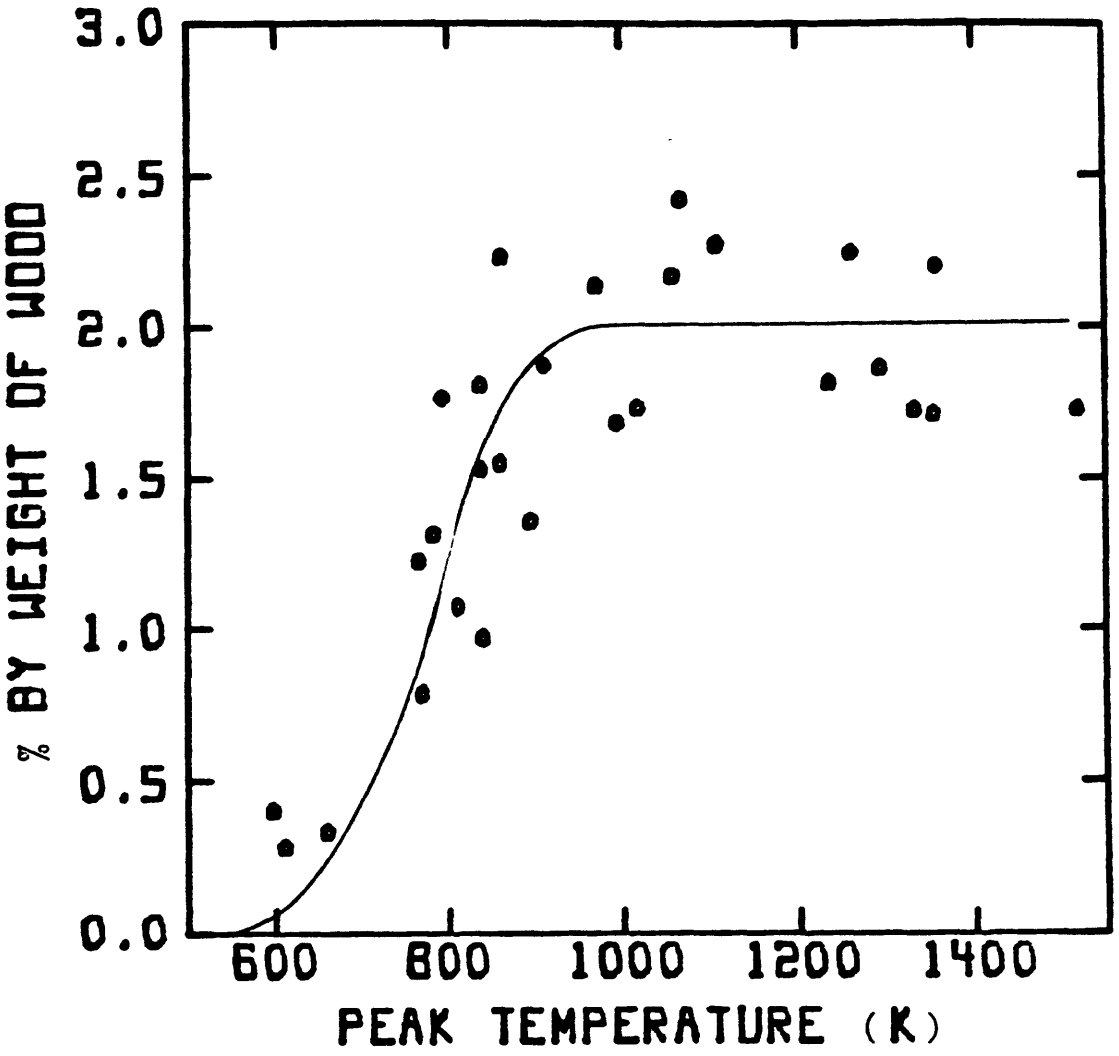

Figure 4.1-9 Formaldehyde Yield From Sweet Gum Wood Pyrolysis.

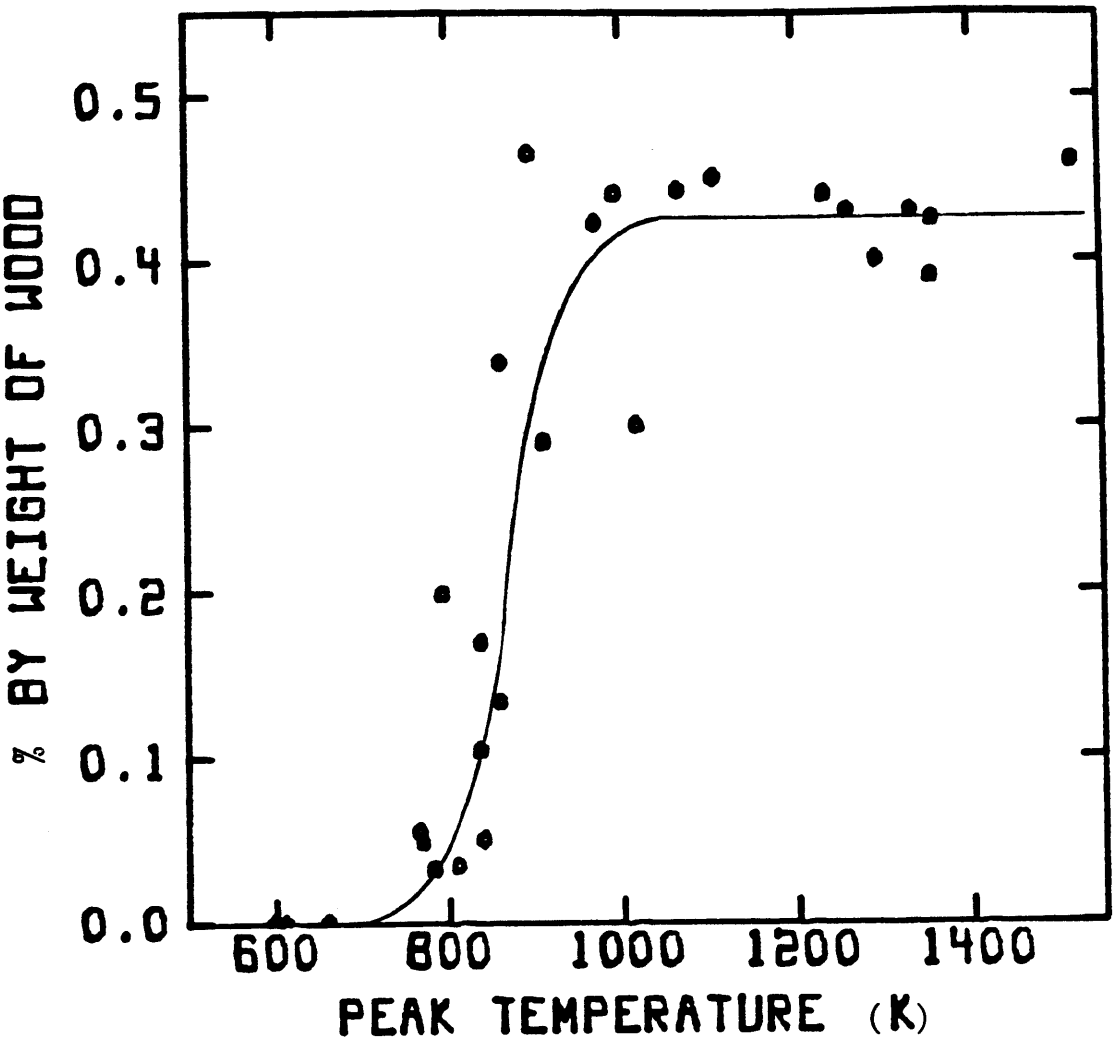

Figure 4.1-10 Propylene Yield From Sweet Gum Wood Pyrolysis.

of occasional water interference on the GC. However, the overall precision in these data is generally quite good and may be attributed to the fact that propylene is collected and analyzed in the downstream lipophilic trap, while most of the water is collected in the upstream glasswool/dry ice/methanol trap and is analyzed separately.

Figures 4.1-11 through 4.1-16 (with the exception of Figure 4.1-12) have such a high degree of data scatter that it is difficult to ascertain what trends, if any, are followed. In addition to the uncertainty created by the tailing of the water peak in the GC analysis, minute amounts of residual methanol/acetone solvent in the system can cause extremely large errors in the measured yields of methanol and acetone/furan. A residual quantity of acetone on the order of 0.001 ml would create an uncertainty of 100%. These data for methanol (Figure 4.1-11), butene and ethanol (Figure 4.1-13), acetone and furan (Figure 4.1-14), acetic acid (Figure 4.1-15), and miscellaneous oxygenated compounds (Figure 4.1-16) are included for the sake of completeness and to show the degree of uncertainty with these compounds. Some of the high temperature runs have a higher degree of reliability than others, which allows the ultimate yields to be estimated. These estimates are included in Table 4.1-2.

The acetaldehyde data of Figure 4.1-12, while fluctuating about the average by about 30 percent by weight of acetaldehyde at higher temperatures, still exhibit a discernible trend. Evolution begins at 700K and levels off to a yield of

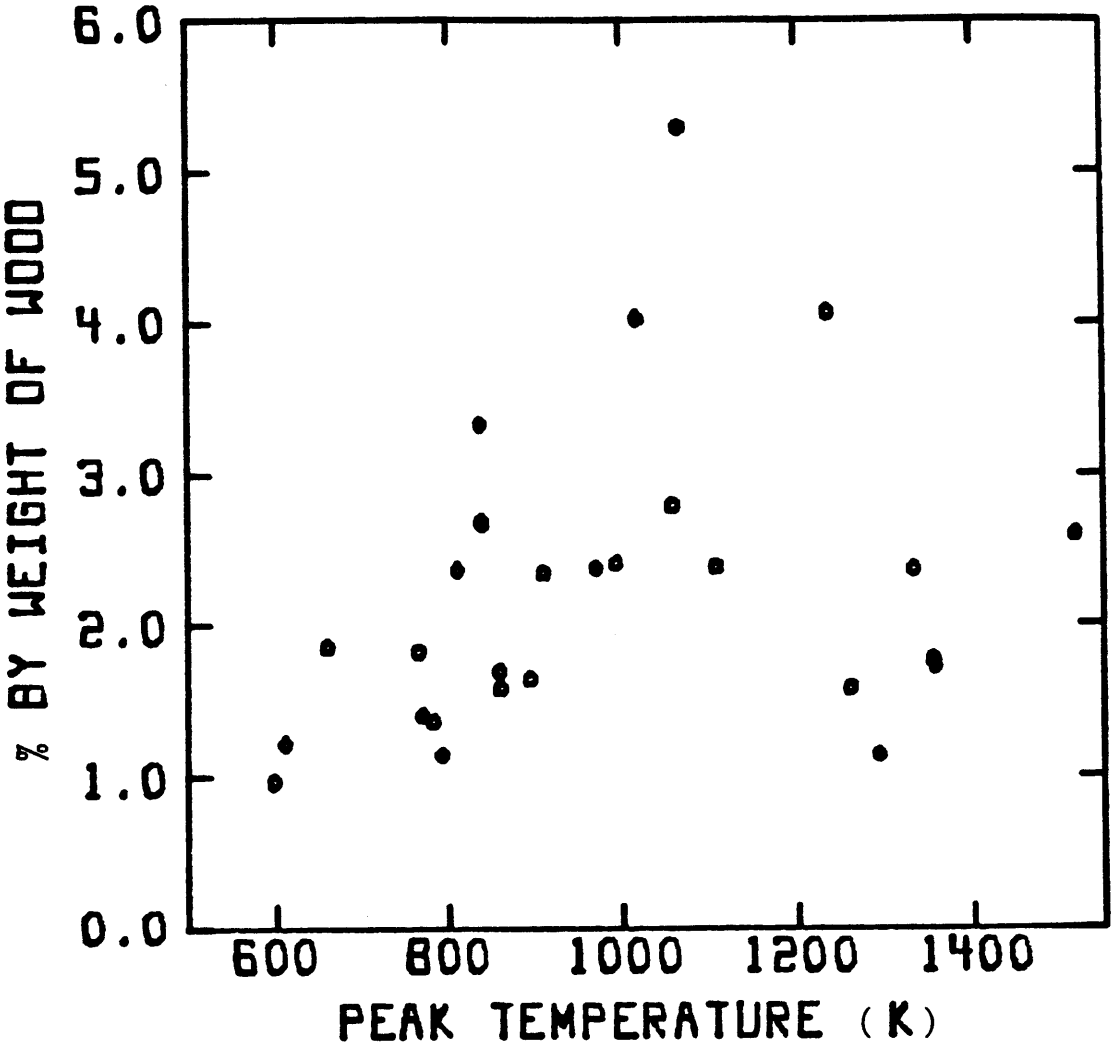

Figure 4.1-11 Methanol Yield From Sweet Gum Wood Pyrolysis.

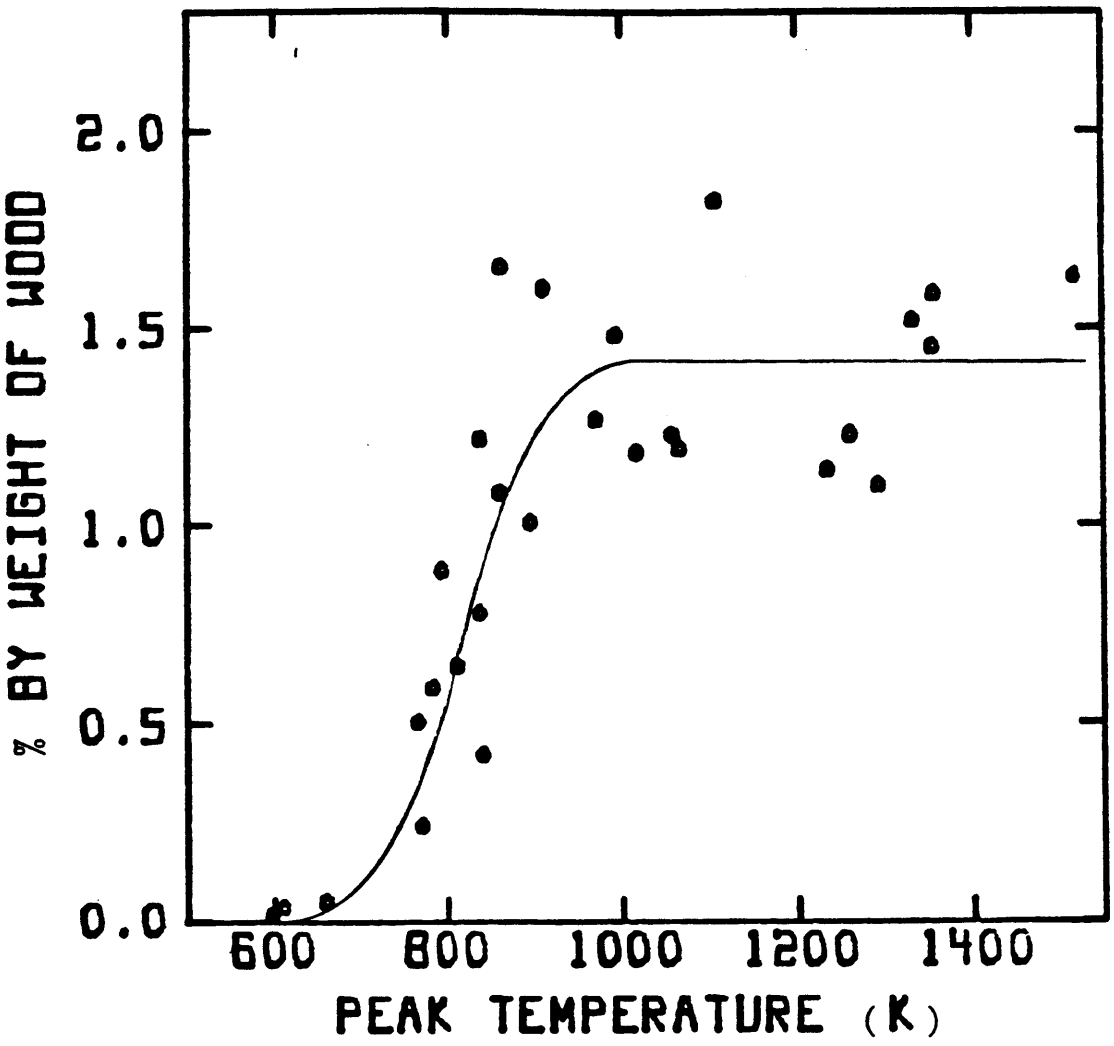

Figure 4.1-12 Acetaldehyde Yield From Sweet Gum Wood Pyrolysis.

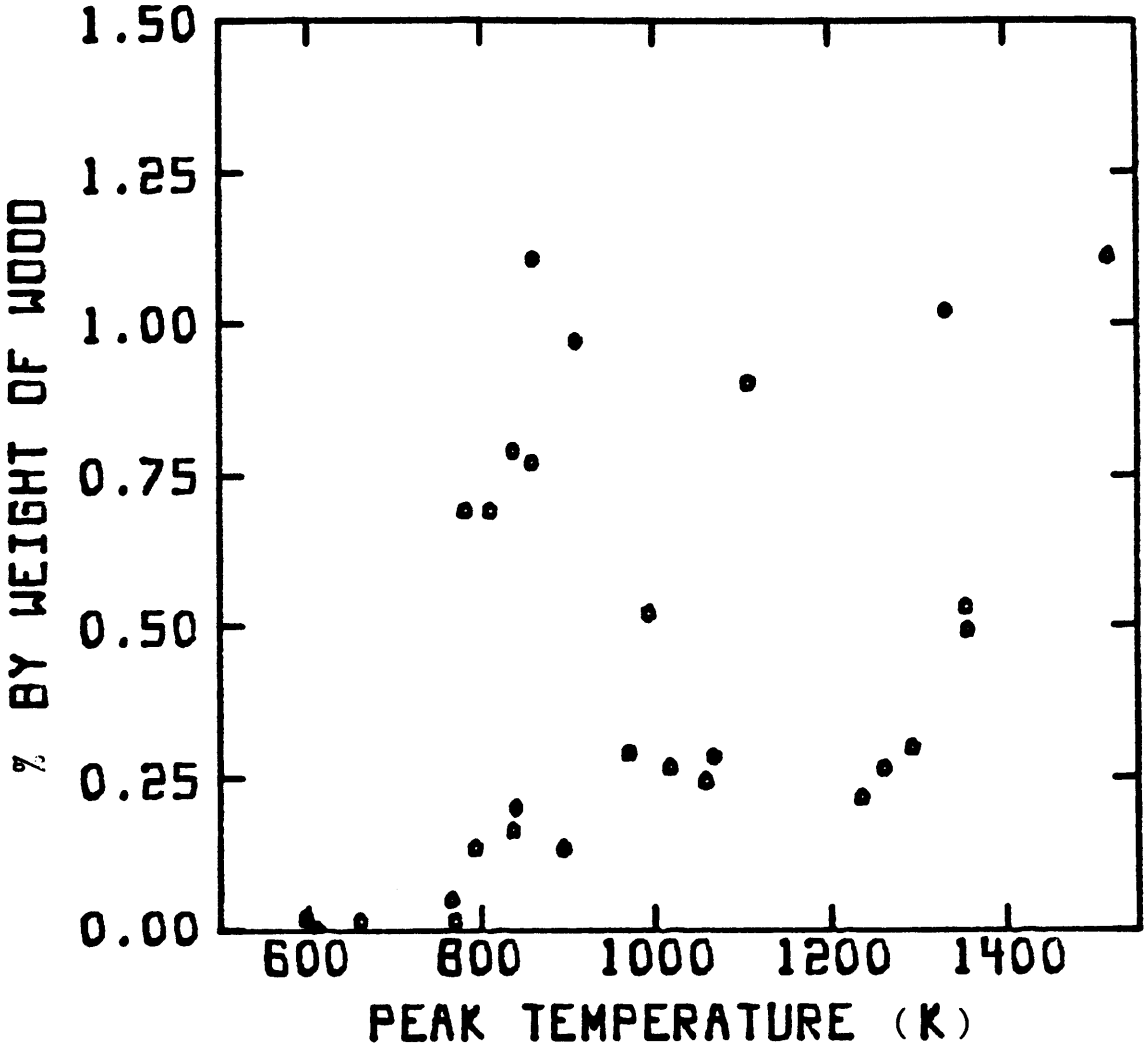

Figure 4.1-13 Butene + Ethanol Yield From Sweet Gum Wood Pyrolysis.

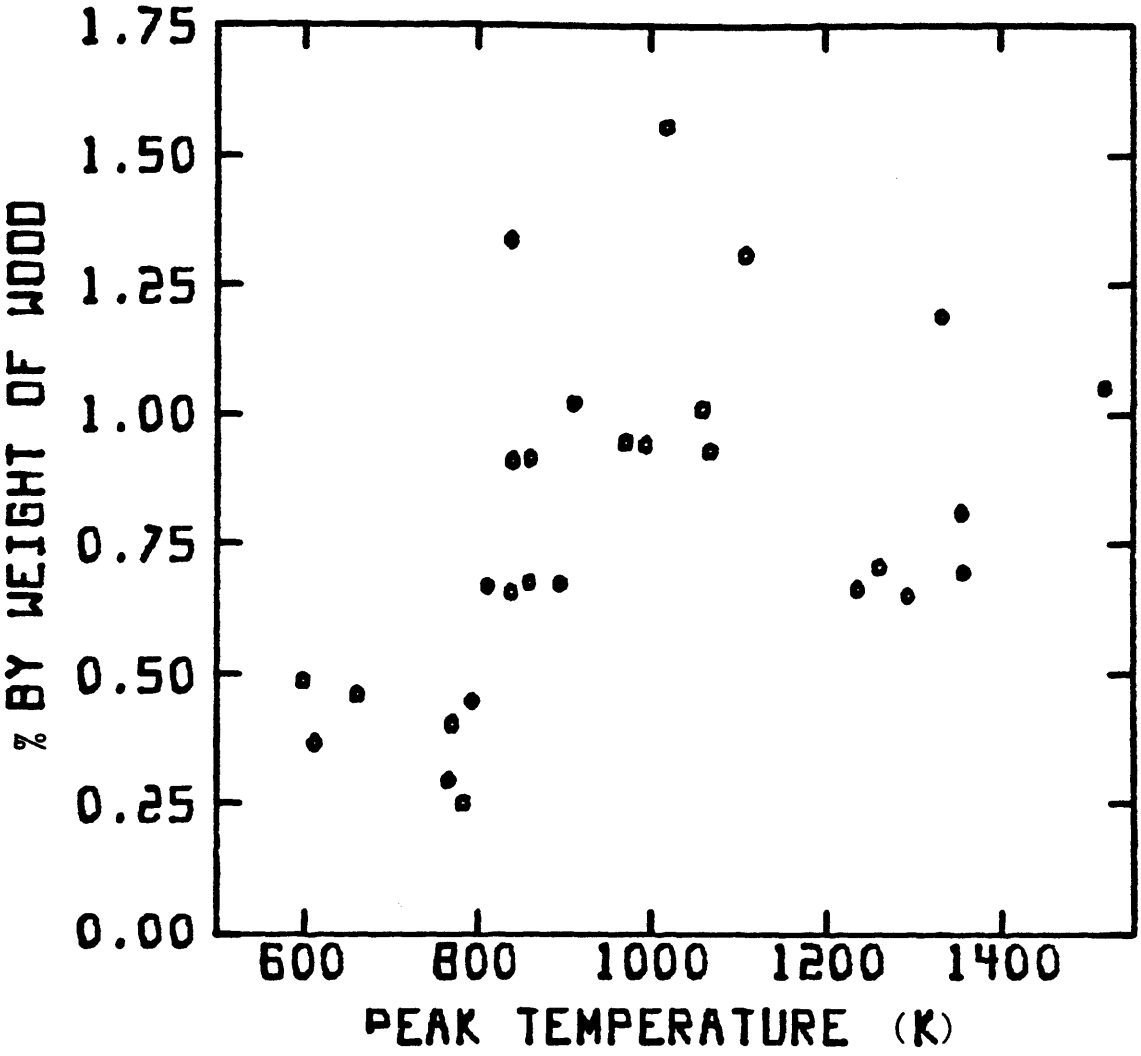

Figure 4.1-14 Acetone + Furan Yield From Sweet Gum Wood Pyrolysis.

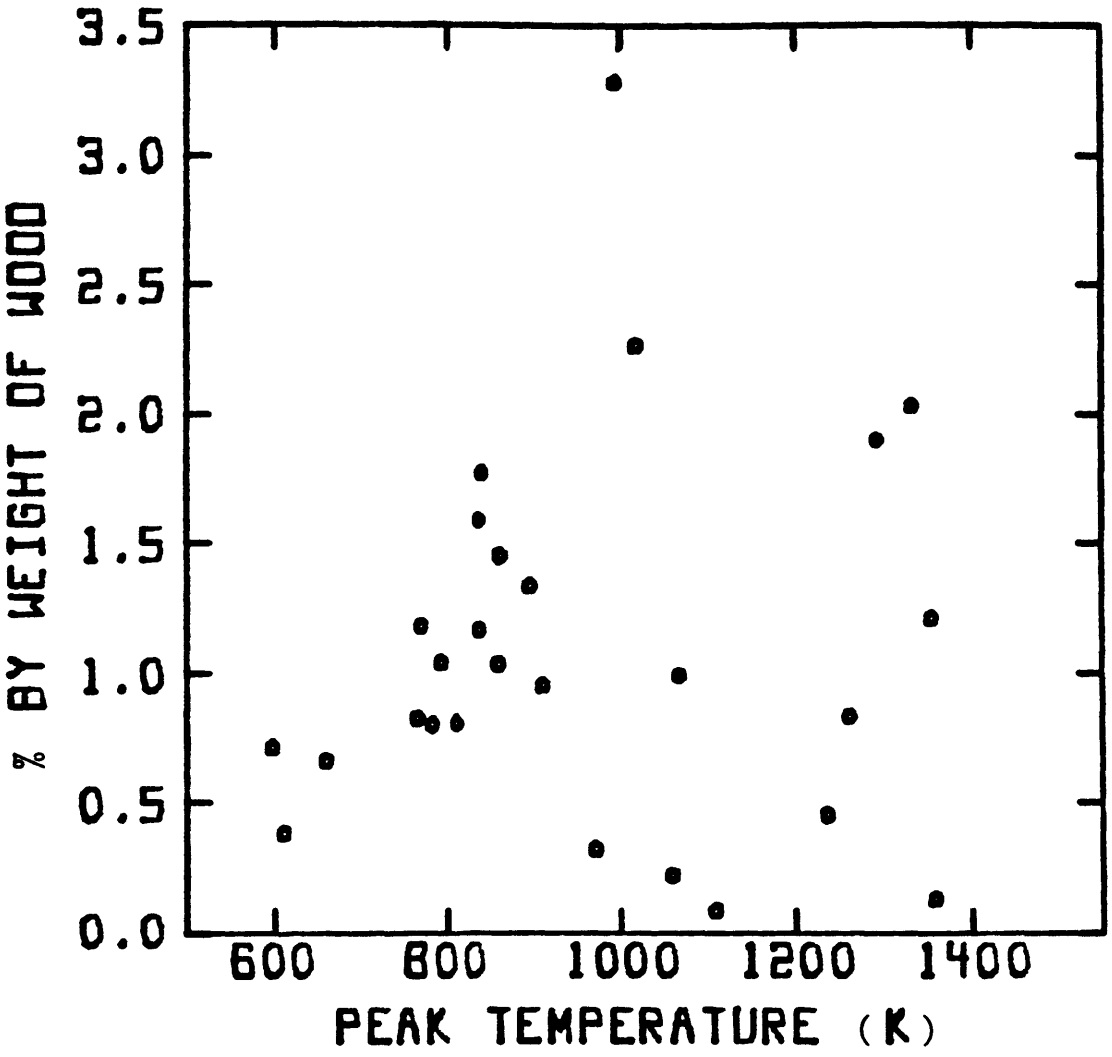

Figure 4.1-15 Acetic Acid Yield From Sweet Gum Wood Pyrolysis.

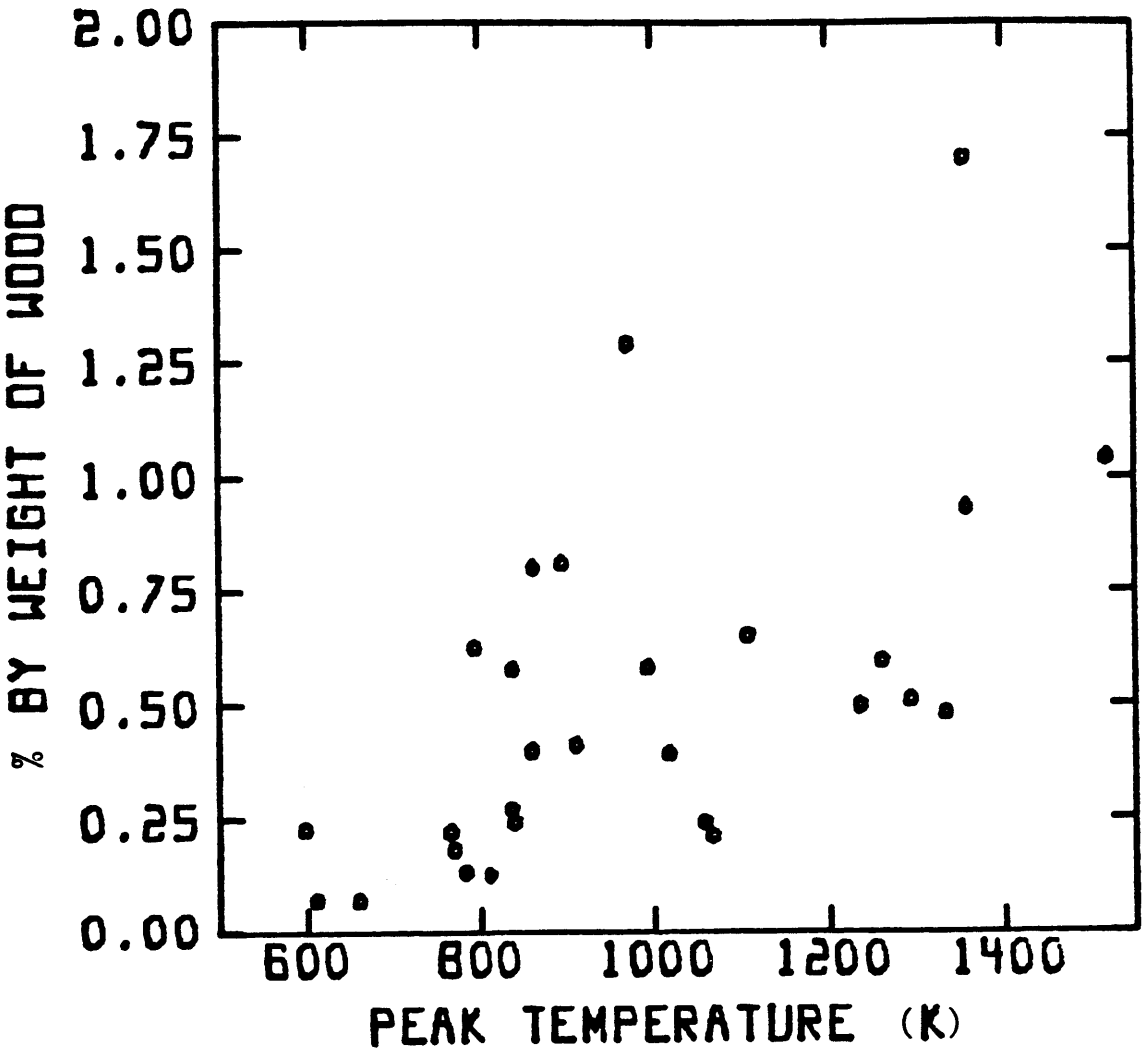

Figure 4.1-16 Miscellaneous Oxygenated Compound Yield From Sweet Gum Wood Pyrolysis.

1.4 wt. % near 900K.

The fact that, unlike many of the light oxygenated compounds, most of the acetaldehyde produced (up to 85 percent) is collected in the downstream lipophilic trap, and is thus relatively shielded from the water tailing GC phenomenon, gives further credence to the explanation given above for the good precision of the propylene data.

A brief investigation of the effects of peak temperature on the yield of hydrogen from wood pyrolysis ran into several problems, mainly with the gas chromatograph. The ultimate yield of hydrogen is believed to be not more than 1.0 wt. %, but this value could be somewhat lower.

4.2 Milled Wood Lignin

Data on the effect of peak temperature on the yields of individual components from milled wood lignin flakes are presented in this section. The data were obtained under conditions similar to those for sweet gum hardwood pyrolysis presented in the previous section. The lignin pyrolysis data are displayed in Figures 4.2-1 through 4.2-15 with all yields being expressed in percent by weight of dry lignin. The curves in these figures were drawn by hand to represent trends in the data.

Figure 4.2-1 presents the effect of peak temperature on the yields of char, tar, and gas (including water), from milled wood lignin pyrolysis. As with wood pyrolysis, decosition of the lignin begins near 600K. The char yield reaches an asymptote of 14 wt. % at about 1000K with most of

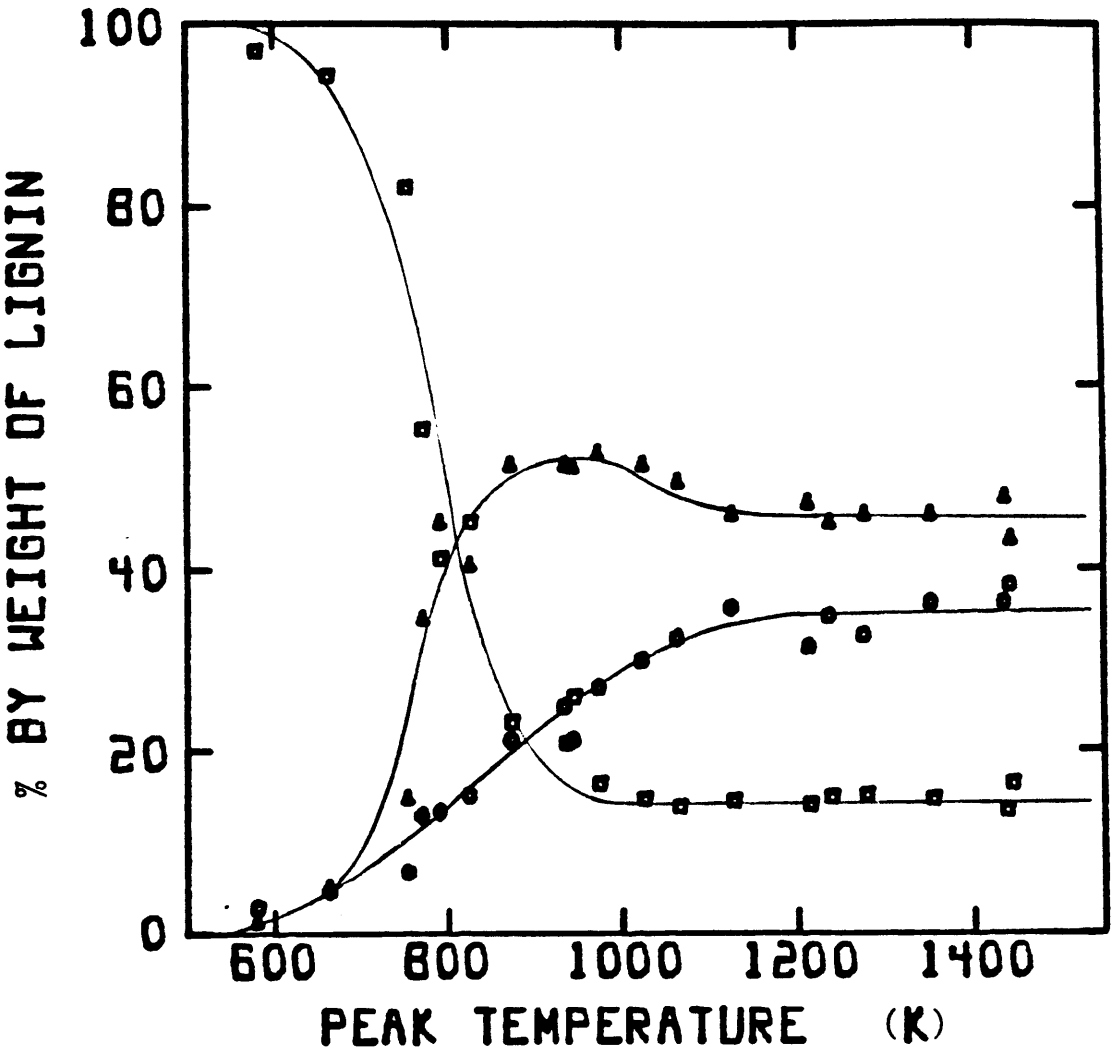

Figure 4.2-1 Char (□), Tar (Δ), and Gas (○) Yields From Milled Wood Lignin Pyrolysis.

the weight loss occurring between 700 and 900K.

Between 600 and 700K, the yields of tar and gaseous products increase with temperature at about the same rate. At peak temperatures greater than 700K, the tar yield becomes increasingly greater than the gas yield until about 950K when the tar yield begins to decrease. As with the wood pyrolysis behavior, this decrease in tar yield at 950K is accompanied by an increase in gas yield without further decrease in char yield, indicating that the lignin pyrolysis tars are cracked to light volatile compounds.

The lignin tar maximum yield is approximately 53 wt. % and occurs over the peak temperature range of 850-950K. The lignin tar asymptotic yield is achieved near 1150K and is about 47 wt. %. When comparing the tar maxima of the wood, cellulose, and lignin pyrolysis experiments, the lignin tar maximum appears to be somewhat broader and flatter than either the wood or cellulose maxima. This may be indicative of the fact that lignin is a more thermally stable compound than either wood or cellulose (Pearl, 1967), and that lignin tars may be more resistant to secondary cracking reactions. However, scatter in the tar data makes it difficult to formulate any rigid statements concerning the relative thermal degradation behavior of tars from the pyrolysis of wood and wood constituents.

The lignin pyrolysis gas yield reaches a plateau near 1150K at a value of approximately 36 wt. %. The gas yield increases smoothly with temperature to this plateau without the abrupt increase in yield corresponding to secondary tar

cracking that was witnessed for both the wood and the cellulose pyrolysis gas yields. This may be further indication of the relative thermal stability of lignin pyrolysis tars.

The individual gas product yields obtained from the pyrolysis of lignin flakes at peak temperatures ranging from 600K to 1450K are included in Figures 4.2-2 through 4.2-15. Table 4.2-1 contains the ultimate yields of the individual gas components along with the approximate peak temperatures at which these yields are achieved.

Figure 4.2-2 presents the effect of peak temperature on the yield of carbon monoxide from lignin pyrolysis. Carbon monoxide is first produced at about 750K and its yield increases rapidly with peak temperature to 16 wt. % at about 1100K. Above this peak temperature, the CO yield rises more slowly with increasing temperature, attaining a yield of about 19 wt. %, but no plateau, at 1440K. Since total weight loss from lignin seems to be constant above 1100K, these observations suggest that CO is evolved from both the primary decomposition of lignin and from secondary cracking of its pyrolysis tars. The CO formed from 950 to 1100K, the temperature range over which most of the tar decrease occurs, amounts to about 7 wt. %. The decrease in tar over this range is approximately 8 wt. %, which is consistent with the picture that much of the decomposing tar goes into CO.

The pyrolysis yield data for methane production are included in Figure 4.2-3. The shape of the methane yield curve is almost identical to the CO yield curve, although on a somewhat smaller scale. Methane production begins near 750K,

Table 4.2-1 Yields of Individual Gaseous Products From Milled Wood Lignin Pyrolysis

Product	Estimated Ultimate Yield (wt.% of dry lignin)	Approximate Peak Temperature (K)†
Carbon Monoxide	19.0*	1440*
Methane	3.2*	1440*
Carbon Dioxide	4.1*	1440*
Ethylene	0.9*	1440*
Ethane	0.29	1100
Water	3.8	900
Formaldehyde	1.4	900
Propylene	0.27	1100
Methanol	1.7	900
Acetaldehyde	0.85	900
Butene + Ethanol	0.3-0.8	**
Acetone + Furan	0.2-0.4	**
Acetic Acid	0.1-0.3	**
Misc. Oxygenates	0.1-0.3	**

† Approximate temperature at which the product yield becomes constant.

* Yield still increasing as temperature increases.

** Insufficient data to determine.

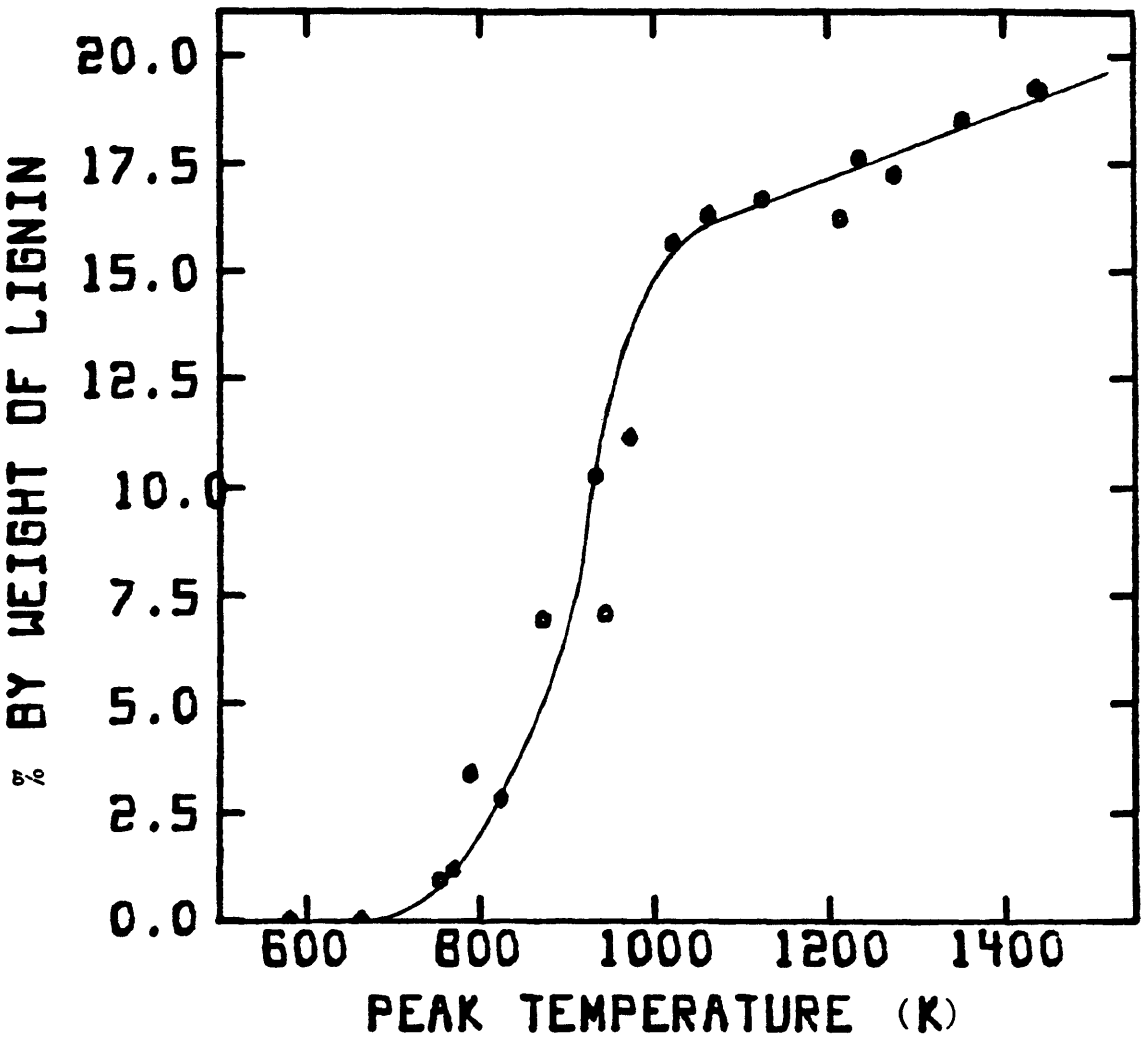

Figure 4.2-2 Carbon Monoxide Yield From Milled Wood Lignin Pyrolysis.

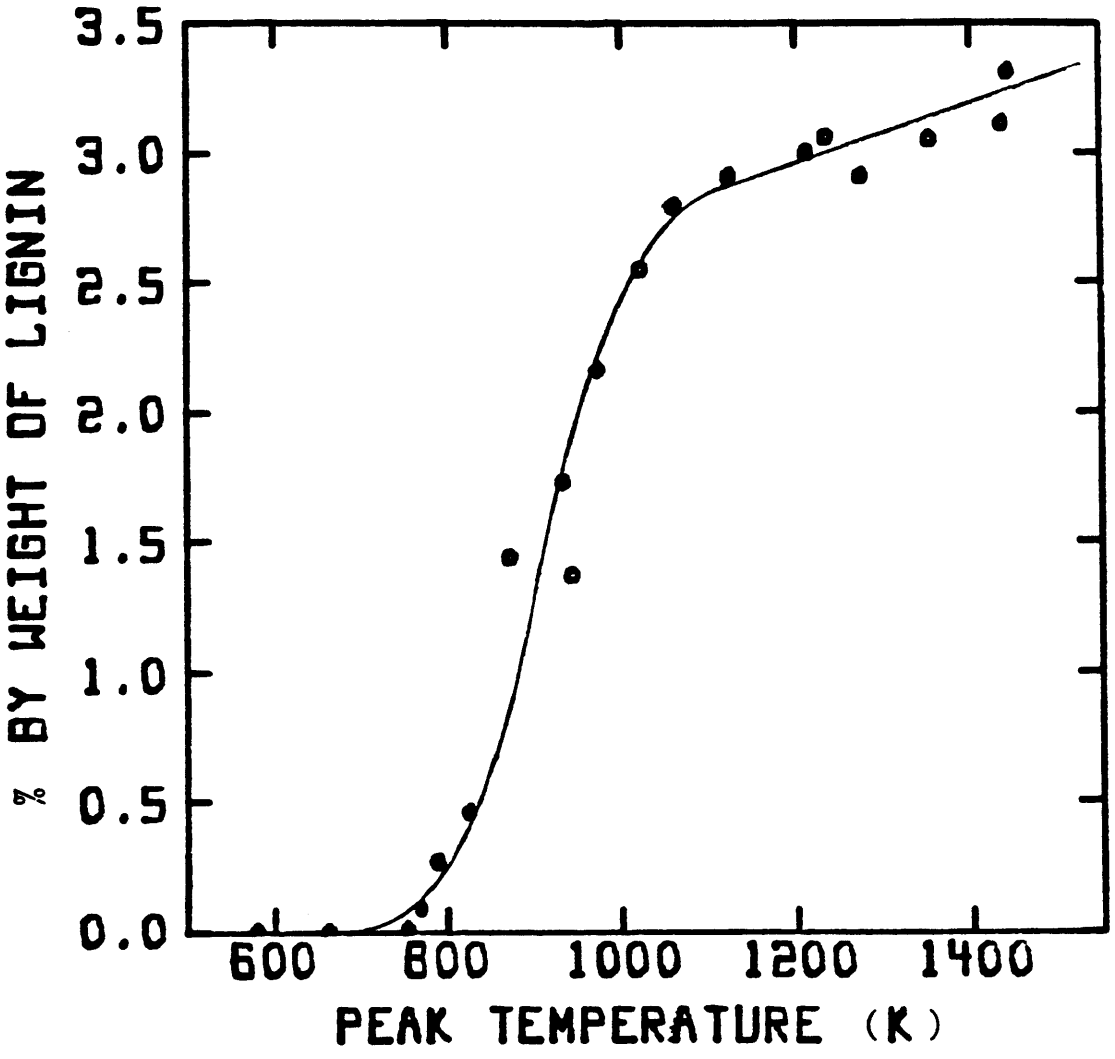

Figure 4.2-3 Methane Yield From Milled Wood Lignin Pyrolysis.

increases steadily to 1000K, and begins to level off but does not reach a constant value. The methane yield at 1000K is about 2.7 wt. % while at 1440K is close to 3.2 wt. %. This 0.5 percent by weight of lignin increase in yield from 1000K to 1440K is approximately a 19 wt. % increase based on the methane yield, almost exactly the same weight percentage increase as for CO over the same temperature range. On a molar basis, the increase corresponds to approximately two (1.7) moles of methane per mole of CO.

The effect of peak temperature on the yield of carbon dioxide is shown in Figure 4.2-4. As with wood, carbon dioxide elution from lignin pyrolysis occurs at temperatures much lower than for either methane or carbon monoxide. However, unlike wood pyrolysis, where the yield of carbon dioxide becomes asymptotic when there is no further weight loss, the behavior of the carbon dioxide yield from lignin pyrolysis above 1000K is very similar to that of methane and CO. Carbon dioxide yield increases from 3.6 wt. % at 1000K to 4.1 wt. % at 1440K, an increase of 17% by weight of carbon dioxide (0.3 percent on a molar basis). This corresponds roughly to half a mole of incremental carbon dioxide formed for each incremental mole of CO formed over this temperature range.

Figure 4.2-5 presents the data for ethylene production from lignin pyrolysis. These data are similar in behavior to those of CO and methane in that ethylene is first detected near 750K and increases steadily with increasing temperature while exhibiting a noticable change in rate at about 1000K. Although the ethylene data are somewhat scattered due to the

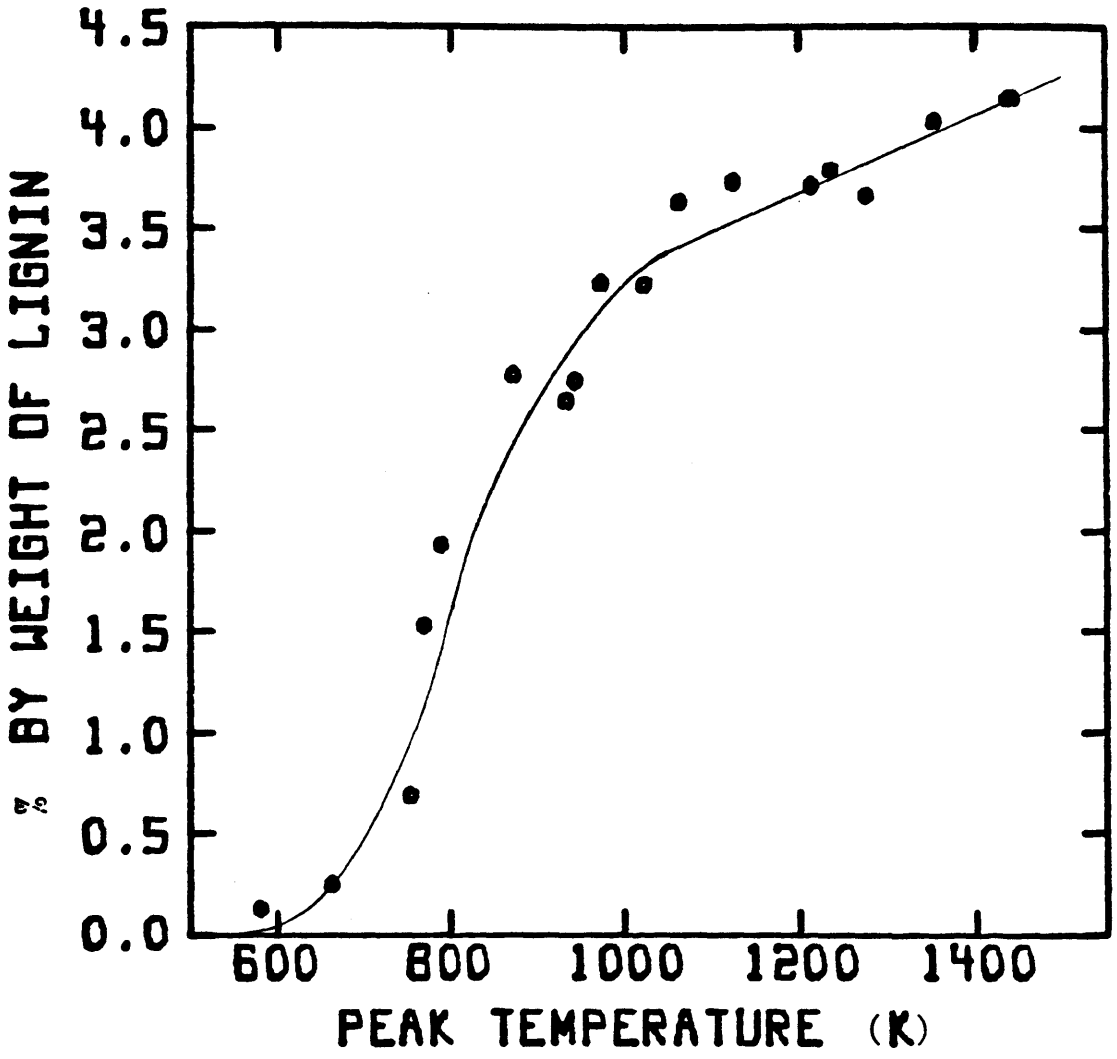

Figure 4.2-4 Carbon Dioxide Yield From Milled Wood Lignin Pyrolysis.

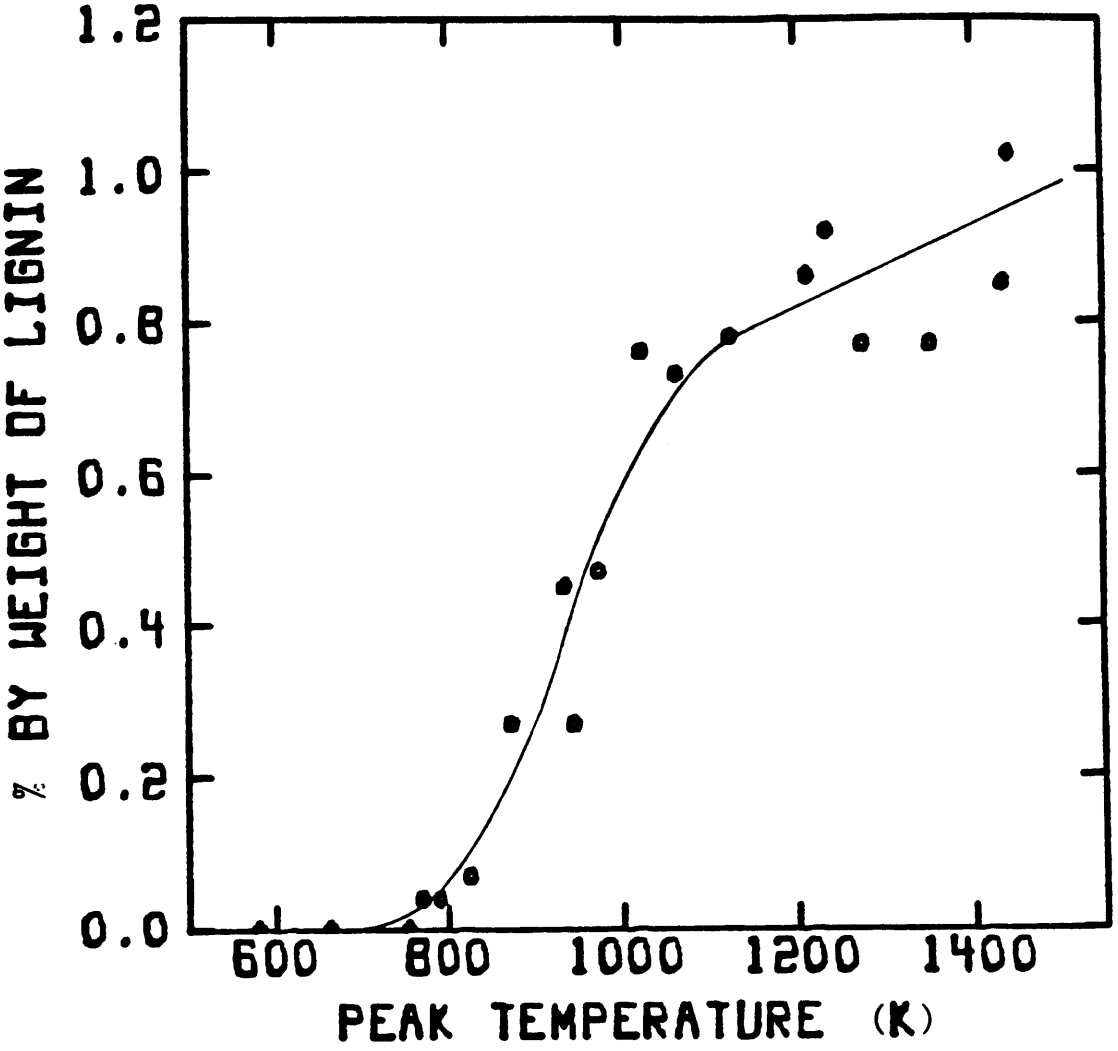

Figure 4.2-5 Ethylene Yield From Milled Wood Lignin Pyrolysis.

small absolute quantities produced, there still appears to be an increase in ethylene yield from 1000K to 1440K on the order of 20 percent based on ethylene yield; from 0.75 wt. % at 1000K to 0.9 wt. % at 1440K.

Ethane yield from lignin pyrolysis as a function of peak temperature is displayed in Figure 4.2-6. This yield curve is similar in behavior to the curve for ethane production from wood pyrolysis in the sense that measurable amounts of ethane are first detected at 750-800K and an apparent asymptote is reached near 1000K. The approximate asymtotic yield of 0.29 wt. % for ethane from lignin pyrolysis is somewhat greater than that from wood pyrolysis, which was 0.17 wt. %.

Figure 4.2-7 presents the yields of chemical water. As with the water data from wood pyrolysis, there is a large amount of experimental scatter; approximately 25 percent based on water yield. Lack of data at temperatures below 600K precludes identification of the threshold temperature for water production from lignin under the present reaction conditions. The water yield plateau of 3.8 wt. % is reached by around 900K, which is well below the temperature where secondary reactions influence tar production. This suggests that water is formed mainly as a primary product of lignin thermal degradation. Klein and Virk (1981) have predicted an ultimate water yield of 6 wt. % from lignin pyrolysis based on model compound studies. The differences may be attributed to the fact that their studies were carried out under different reaction conditions than those of this work.

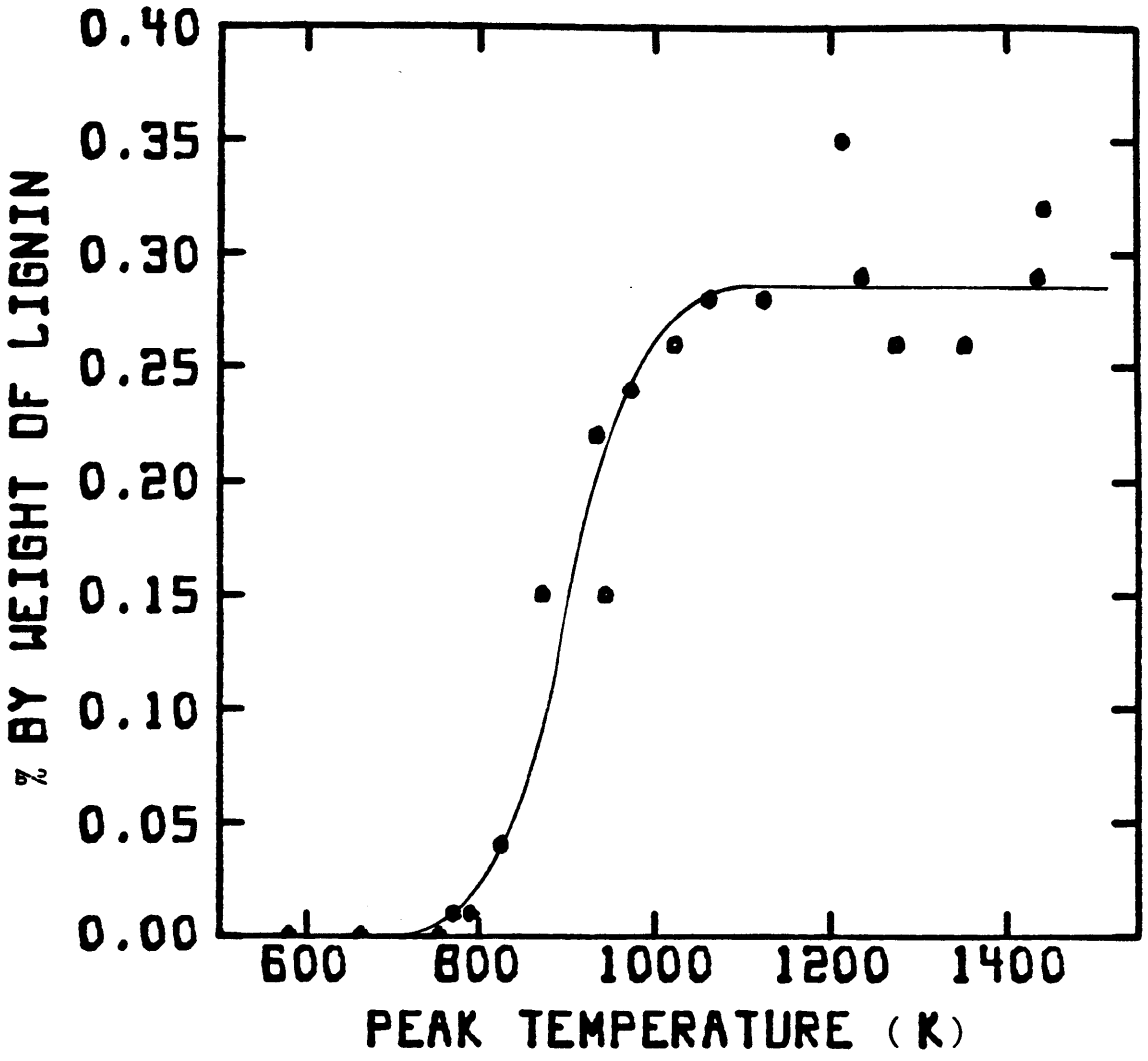

Figure 4.2-6 Ethane Yield From Milled Wood Lignin Pyrolysis.

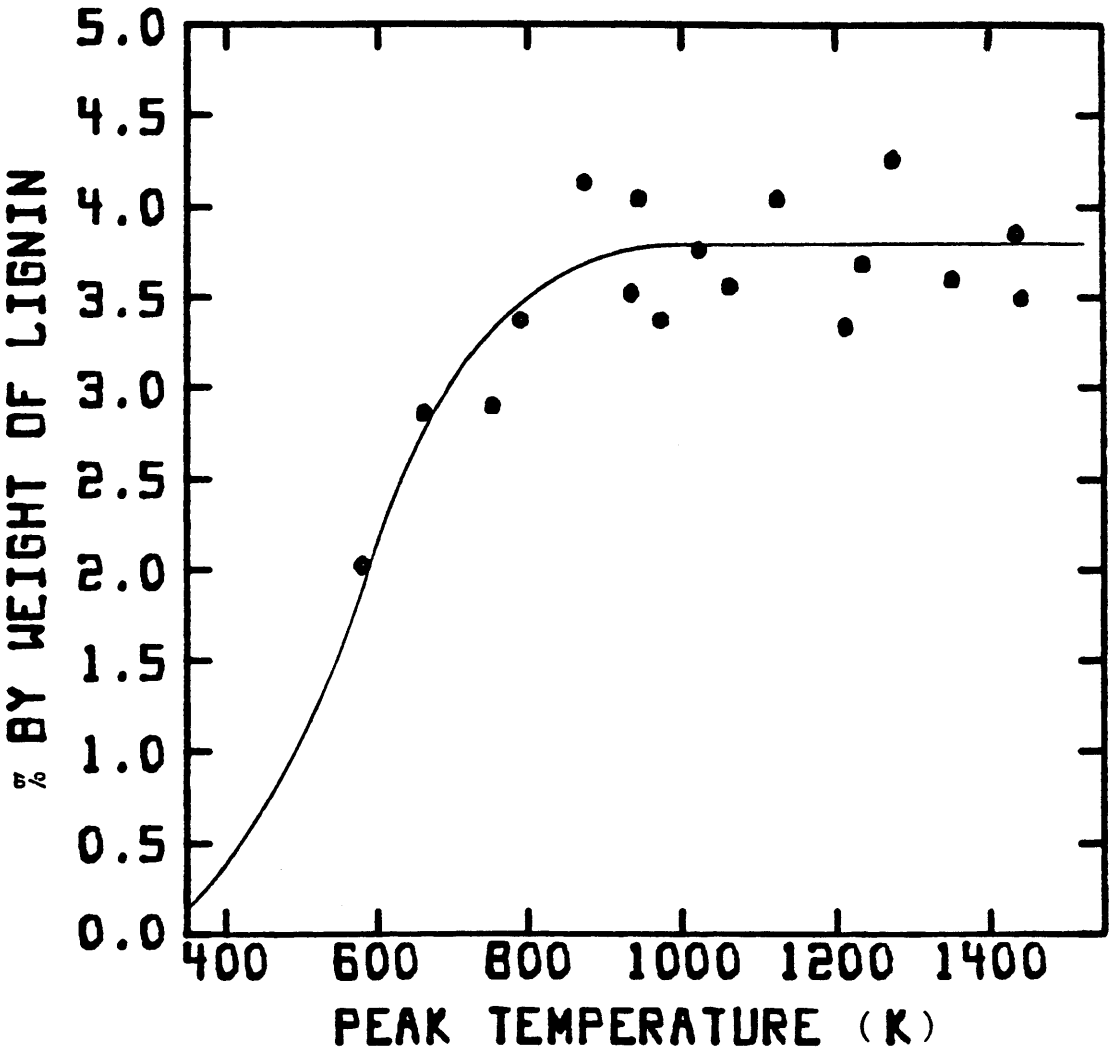

Figure 4.2-7 Water Yield From Milled Wood Lignin Pyrolysis.

Figure 4.2-8 shows the yield of formaldehyde from lignin pyrolysis. The yield behavior with increasing temperature is similar to that of formaldehyde from wood pyrolysis. Formaldehyde is evolved below 600K and reaches an asymptotic yield of 1.4 wt. % by 900K.

The lignin pyrolysis yield of propylene is shown in Figure 4.2-9. Propylene production begins at a peak temperature near 800K and exhibits a rapid increase in the temperature range between 850 and 950K. The ultimate yield of propylene is approximately 0.27 wt. %, and is achieved by 1100K.

The highly scattered yield data for the oxygenated compounds from wood pyrolysis illustrated the need for improvements in the experimental procedure. As was pointed out previously, residual amounts of methanol/acetone solvent in the system could cause major experimental uncertainties in the yield data of these two compounds. With this in mind, extreme care was taken to clean the reactor vessel and gas phase product traps to a higher degree than obtained previously. One modification to the cleaning procedure between runs was to place the gas traps in an oil bath maintained at 425K rather than using a boiling water bath at 373K. Purified helium was then passed through the traps at a flow rate of 15 cc/min for up to 3 hours.

The above alteration in the trap cleaning procedure appears to have been successful. This is evidenced by the methanol yield data presented in Figure 4.2-10. While some degree of scatter is observed, the data behave much more uniformly than the methanol data from wood pyrolysis (Figure

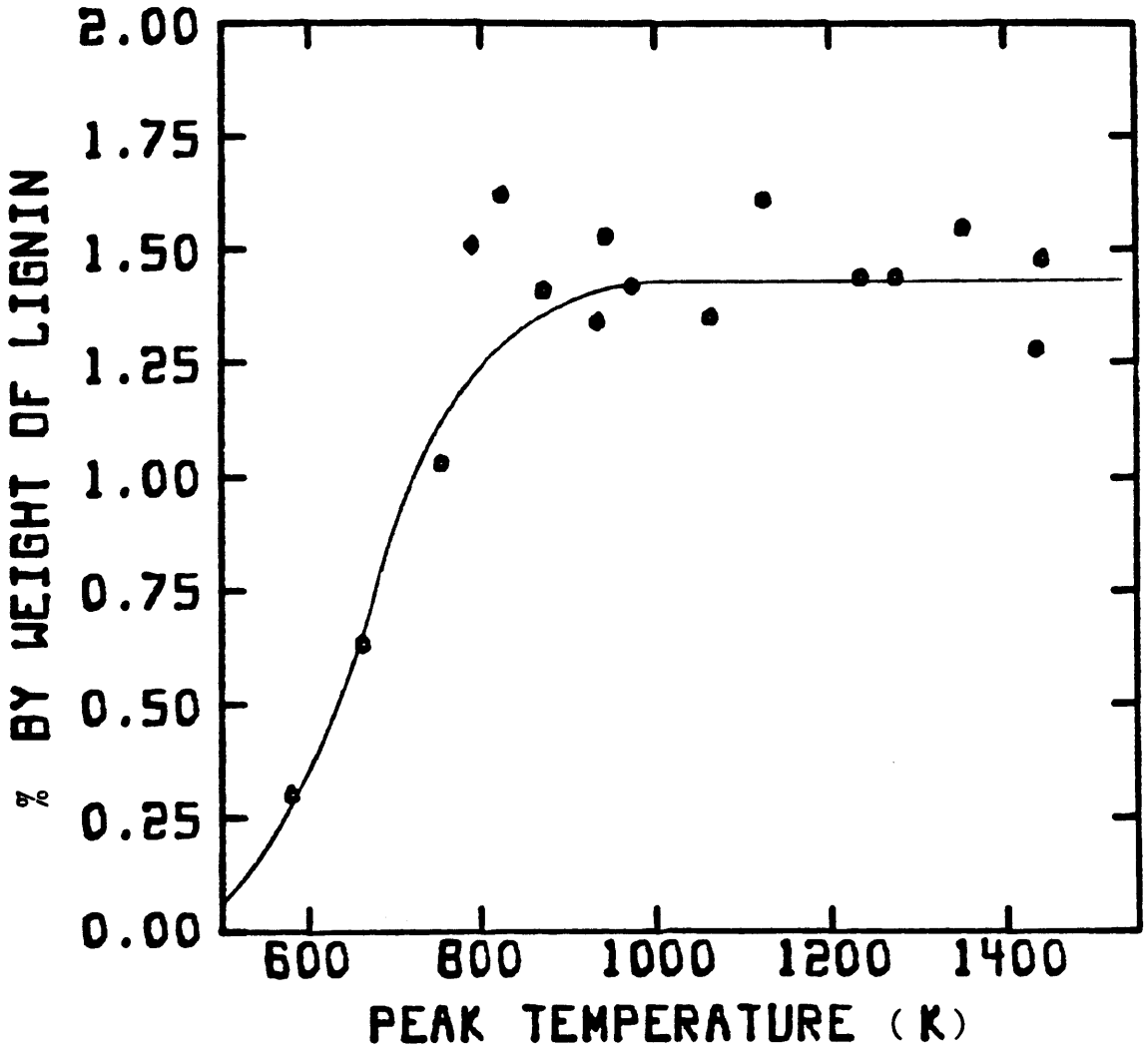

Figure 4.2-8 Formaldehyde Yield From Milled Wood Lignin Pyrolysis.

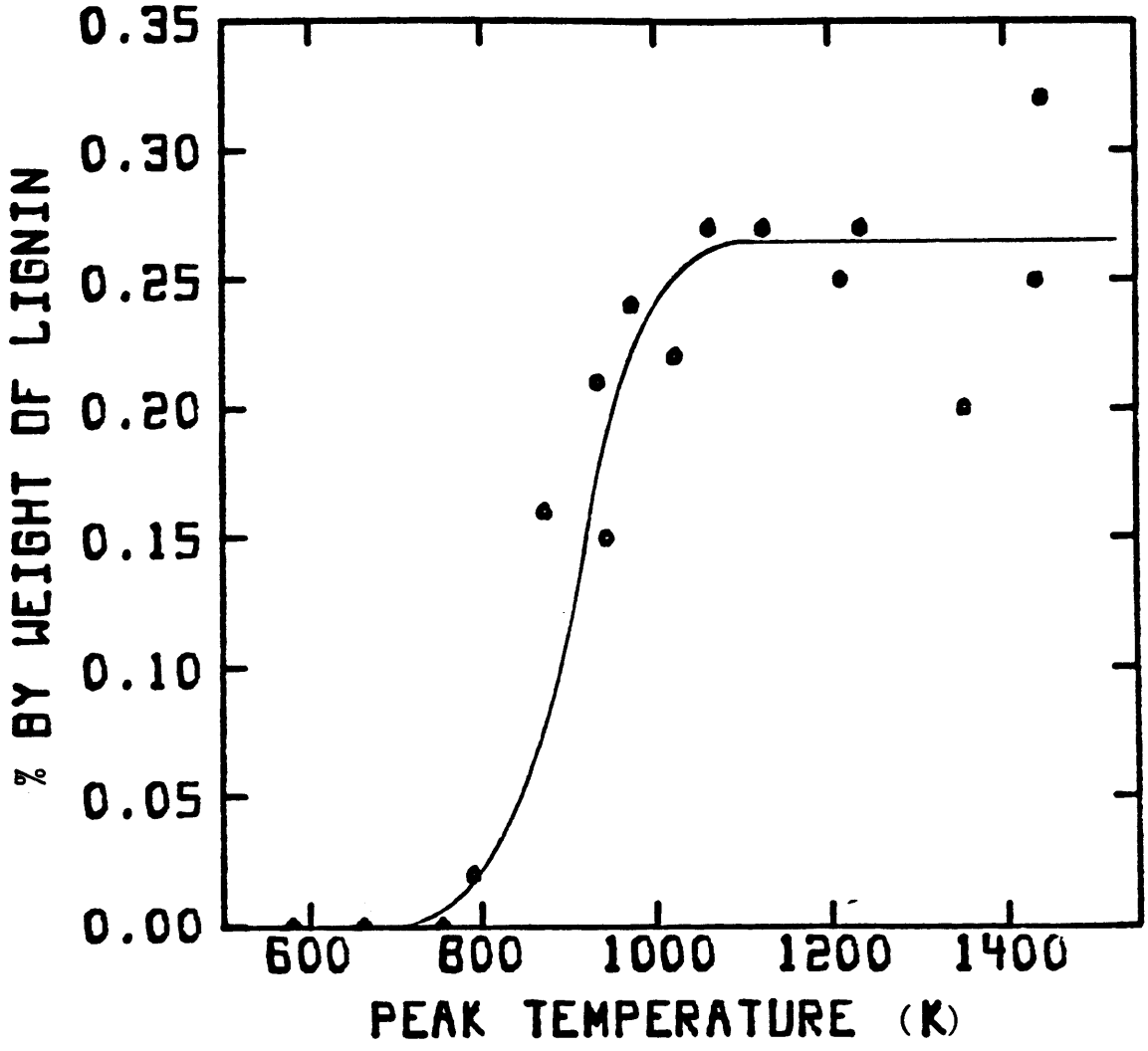

Figure 4.2-9 Propylene Yield From Milled Wood Lignin Pyrolysis.

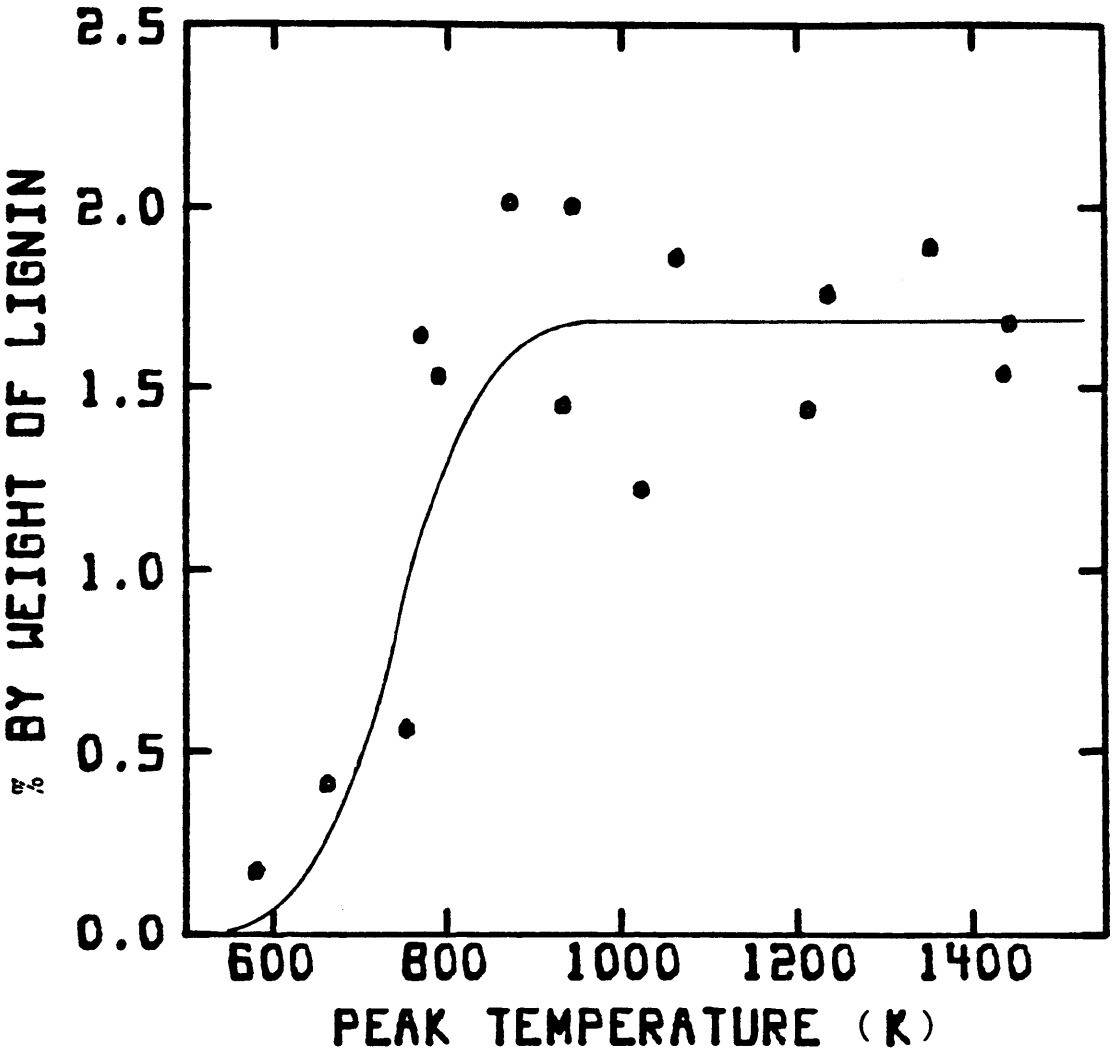

Figure 4.2-10 Methanol Yield From Milled Wood Lignin Pyrolysis.

4.1-11). The data trend is very similar to that of formaldehyde, with methanol production starting below 600K and reaching a plateau of 1.7 wt. % near 900K. Iatridis and Gavalas (1979) obtained an ultimate methanol yield of 2 wt. % from their studies of Kraft lignin pyrolysis in a reactor of similar configuration to the present one. The close correlation with these results is encouraging. The differences are probably within the combined experimental uncertainties of the two studies although they could also be attributed to the fact that Iatridis and Gavalas pyrolyzed Kraft lignin rather than milled wood lignin.

Figure 4.2-11 presents the data on acetaldehyde yields from lignin pyrolysis. Acetaldehyde production begins at about 700K and levels off at 0.85 wt. % near 900K. This behavior is characteristic of both formaldehyde and methanol as well as acetaldehyde which may indicate that these oxygenated compounds are formed in lignin pyrolysis via similar chemical pathways.

The data presented in Figures 4.2-12 through 4.2-15 for butene plus ethanol, acetone plus furan, acetic acid, and miscellaneous light oxygenated compounds, respectively, exhibit scatter on the order of the scatter observed in the wood pyrolysis data for these same components. Even with the great care taken to remove residual methanol/acetone solvent from the system, the acetone and furan data in Figure 4.2-13 exhibit sufficient scatter to make the discernment of any definitive data trend very difficult. Still, the sum of the ultimate yields of these components is at most 2 wt. % and with this fact in mind, coupled with the water tailing CG phenomenon,

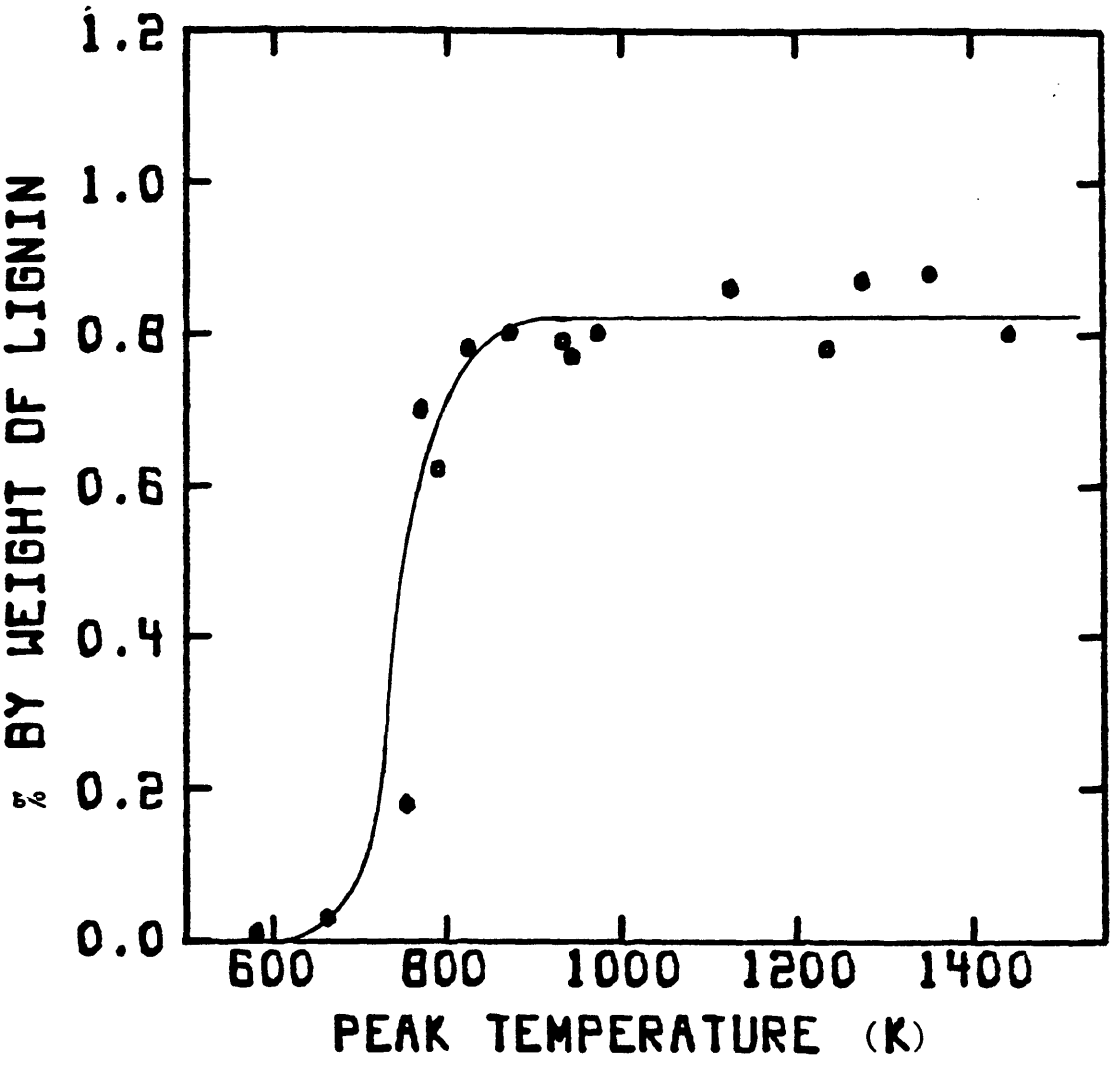

Figure 4.2-11 Acetaldehyde Yield From Milled Wood Lignin Pyrolysis.

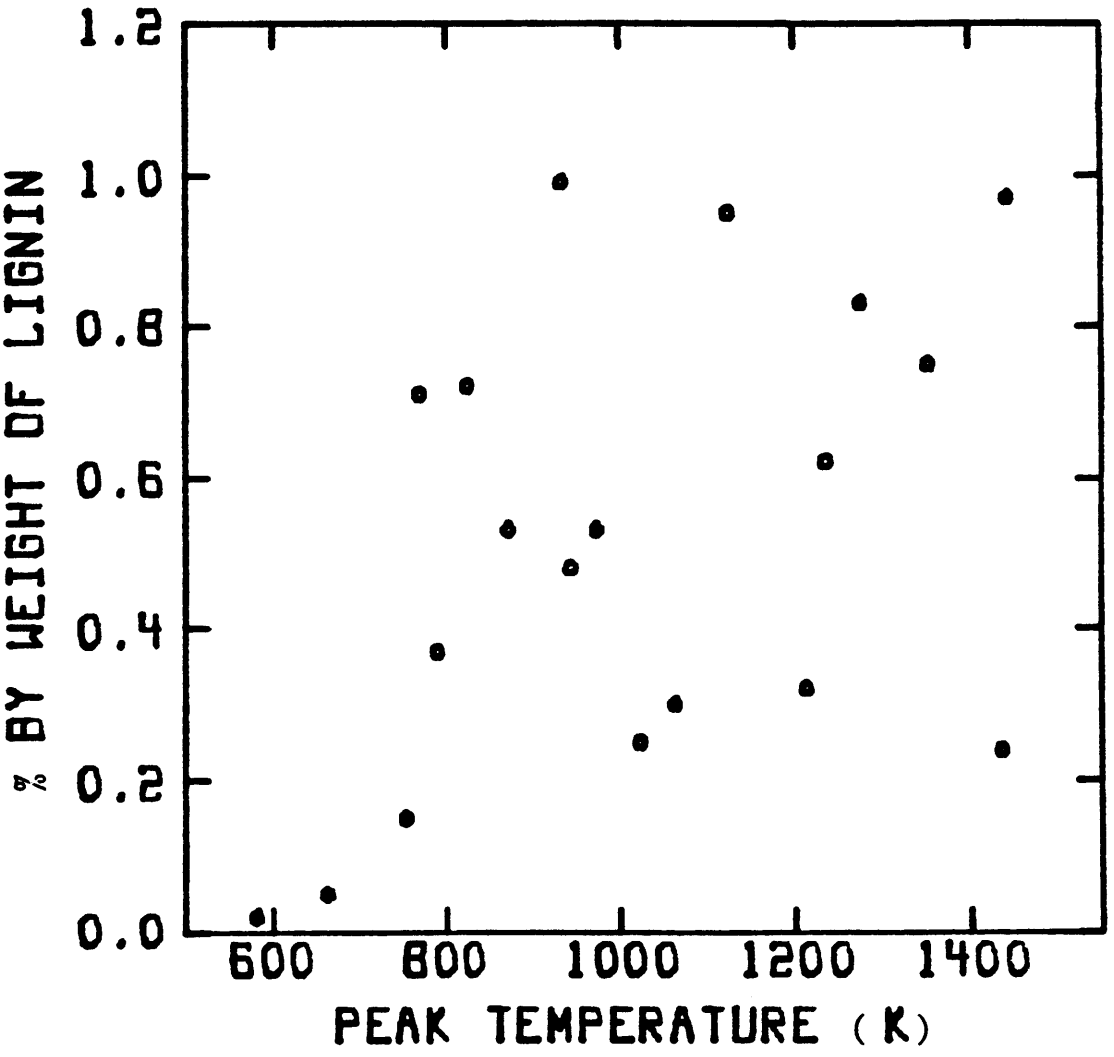

Figure 4.2-12 Butene + Ethanol Yield From Milled Wood Lignin Pyrolysis.

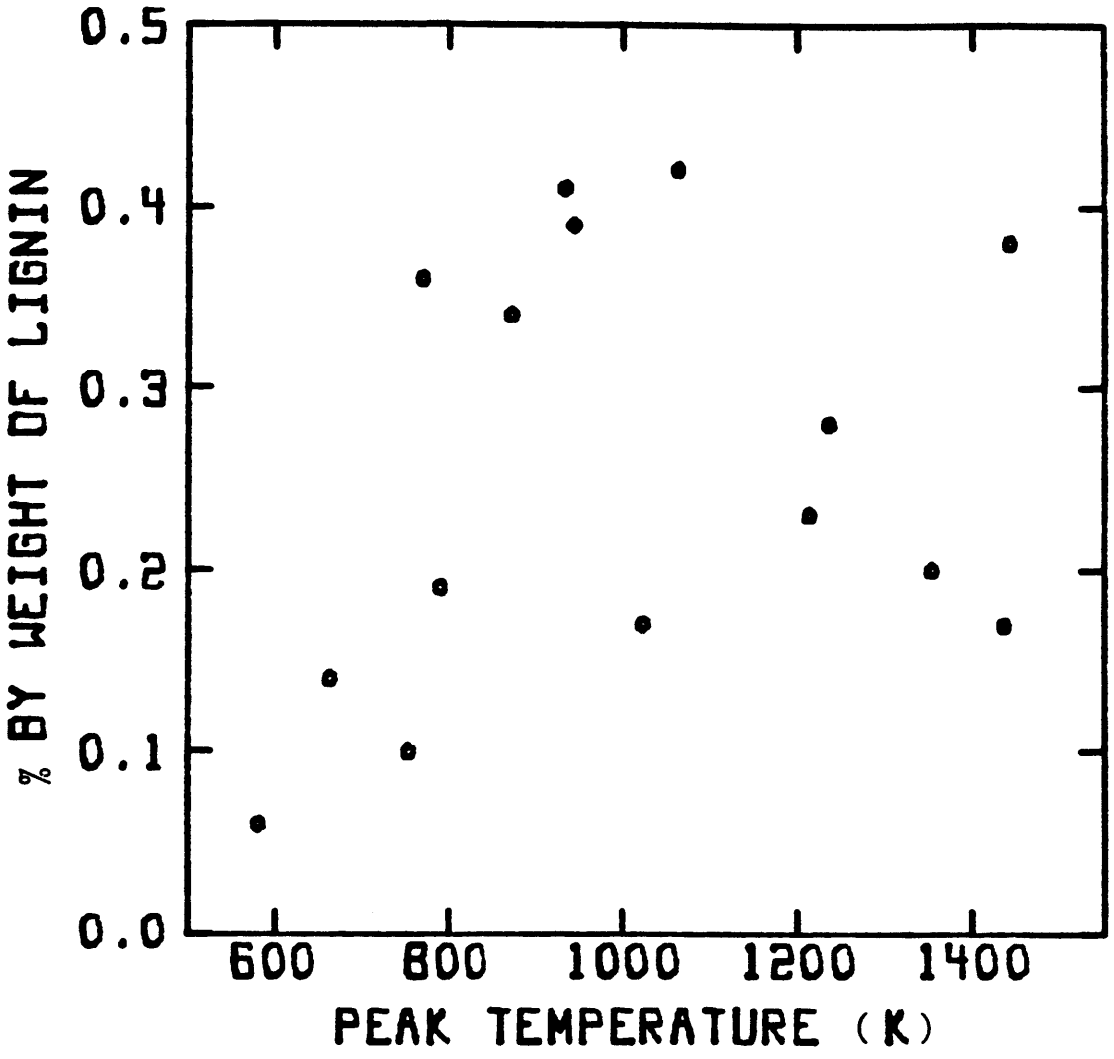

Figure 4.2-13 Acetone + Furan Yield From Milled Wood Lignin Pyrolysis.

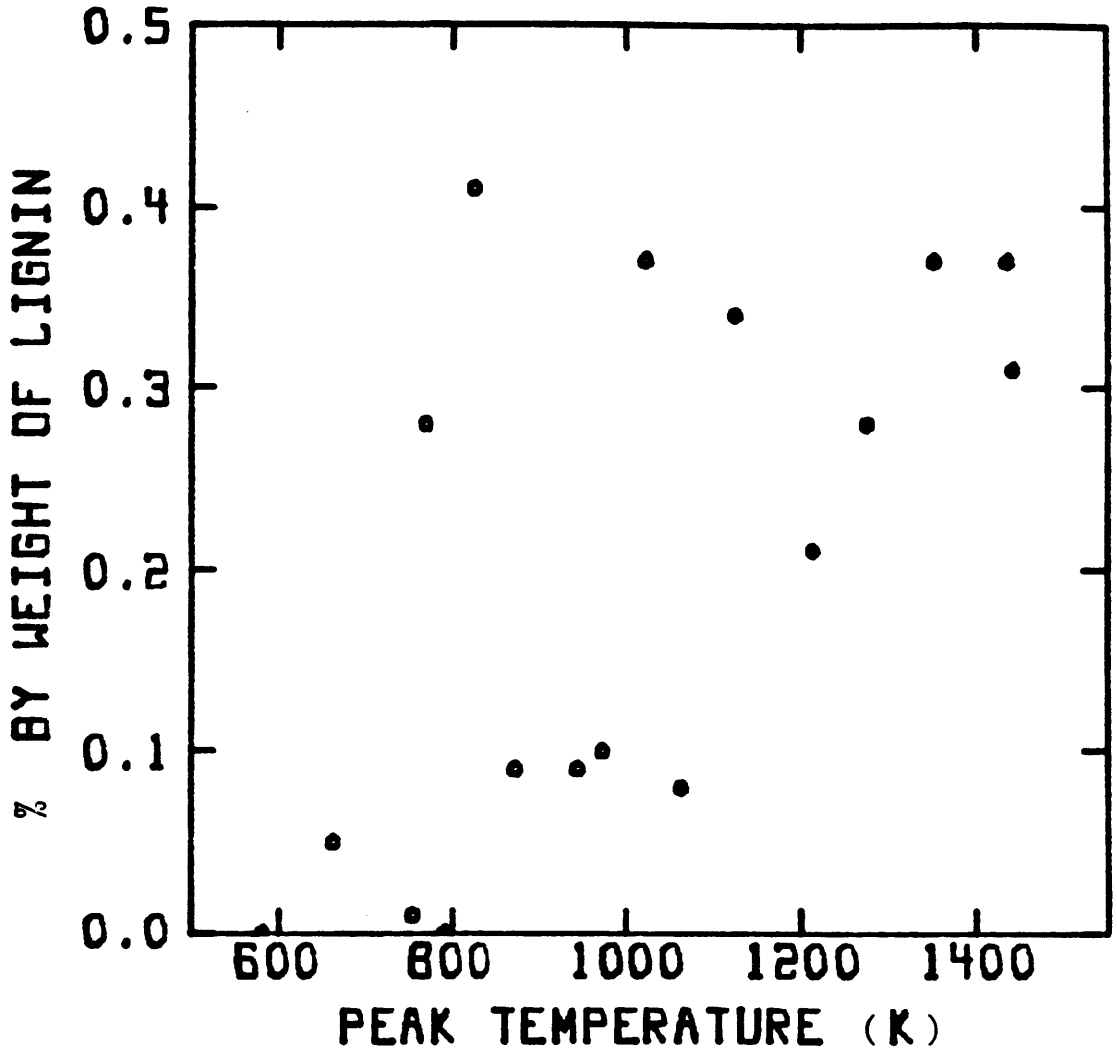

Figure 4.2-14 Acetic Acid Yield From Milled Wood Lignin Pyrolysis.

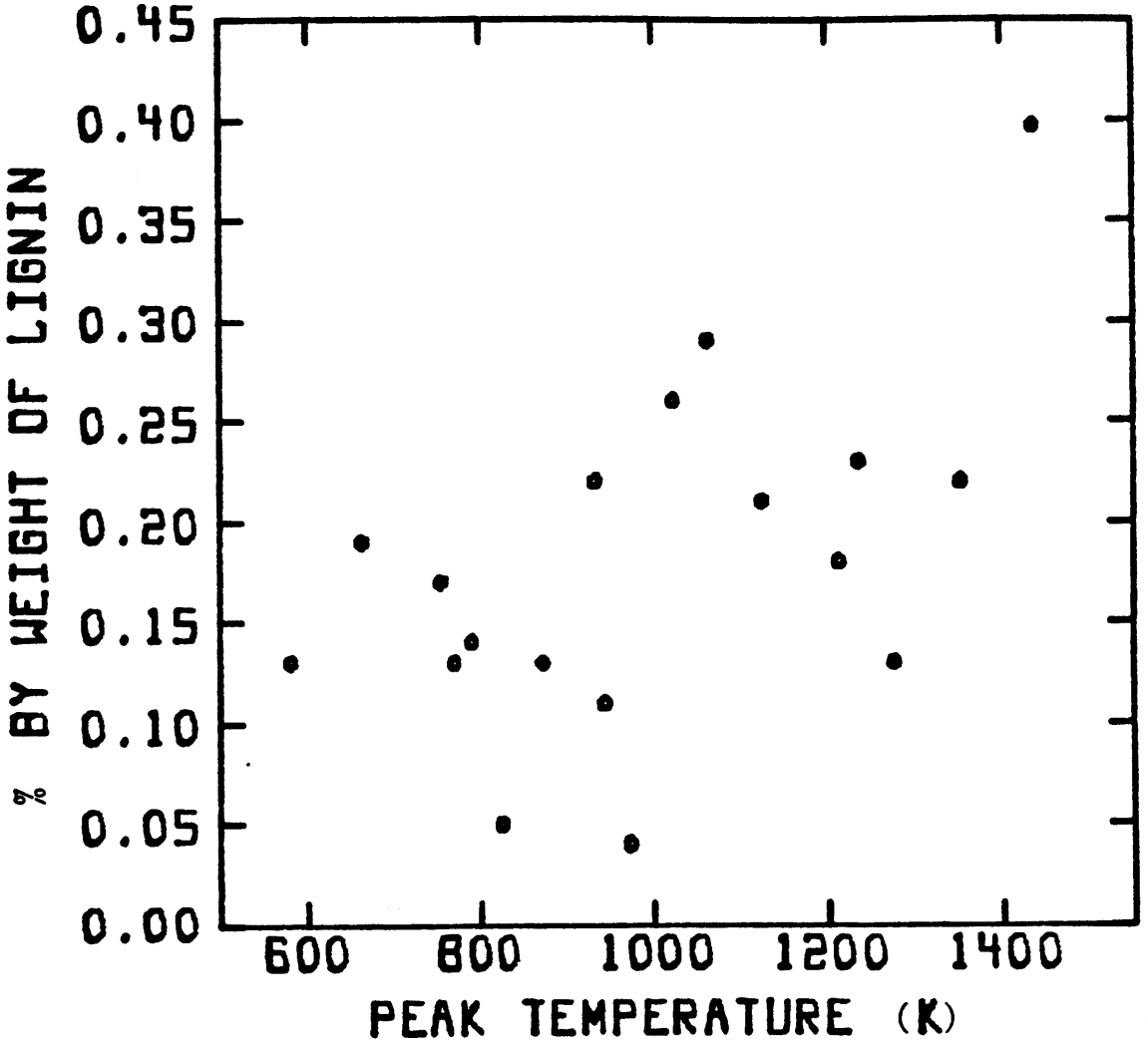

Figure 4.2-15 Miscellaneous Oxygenated Compound Yield From Milled Wood Lignin Pyrolysis.

the level of data scatter is not surprising.

4.3 Material and Energy Balances

The results from the elemental analyses performed by Huffman Laboratories, Inc. are shown in Table 4.3-1. High temperature char elemental analyses were not obtained because not enough material could be scraped off of the captive sample screens. The personnel at Huffman Labs attempted to analyze the char elemental content by inserting a complete screen into their apparatus, but analytical difficulties were encountered and little information was obtained.

The results in Table 4.3-1 are expressed graphically in Figures 4.3-1 through 4.3-4 as the percent of element present in wood or lignin retained in the tar or char. The elemental retention behavior for char is similar for both the wood and lignin; about 50% of the carbon in wood (Figure 4.3-2), and lignin (Figure 4.3-4) is volatilized by 800K. The tar elemental retention curves show maxima for both wood (Figure 4.3-1) and lignin (Figure 4.3-3) which reflect the maxima in tar yields for these two materials.

Table 4.3-2 presents an elemental, total mass, and energy balance for sweet gum wood pyrolysis. Since some of the light volatile data are highly scattered, this analysis was performed by considering the asymptotic yield data rather than the data from a specific experimental run. For the purposes of this rough analysis the butene and ethanol, acetone and furan, and miscellaneous oxygenated compound fractions were

Table 4.3-1 Elemental Compositions of Sweet Gum Wood, Milled Wood Lignin and Selected Pyrolysis Tars and Chars

	Run #	Temp (K)	Yield (wt.%)	C	H	O*
Sweet Gum Wood	-	-	-	49.5	6.1	44.6
Tar	32	770	22.9	52.6	6.1	32.3
Tar	78	895	52.5	53.9	5.9	37.1
Tar	64	1355	50.2	55.0	6.2	32.3
Char	36	610	91.0	50.1	6.2	42.2
Char	73	810	53.2	51.5	6.1	39.7
Milled Wood Lignin	-	-	-	59.1	6.0	32.0
Tar	97	770	34.4	54.2	5.4	30.5
Tar	99	970	52.6	59.9	5.5	-
Tar	85	1020	51.4	62.0	5.2	21.9
Tar	100	1440	43.1	62.1	5.4	24.0
Char	88	580	96.9	59.8	5.8	29.4
Char	93+97	800	50	62.1	5.5	29.0
Char	84	1350	14.5	91.3	-	-

* Oxygen elemental analysis obtained from a Coulometrics carbon dioxide coulometer (Raines,1981).

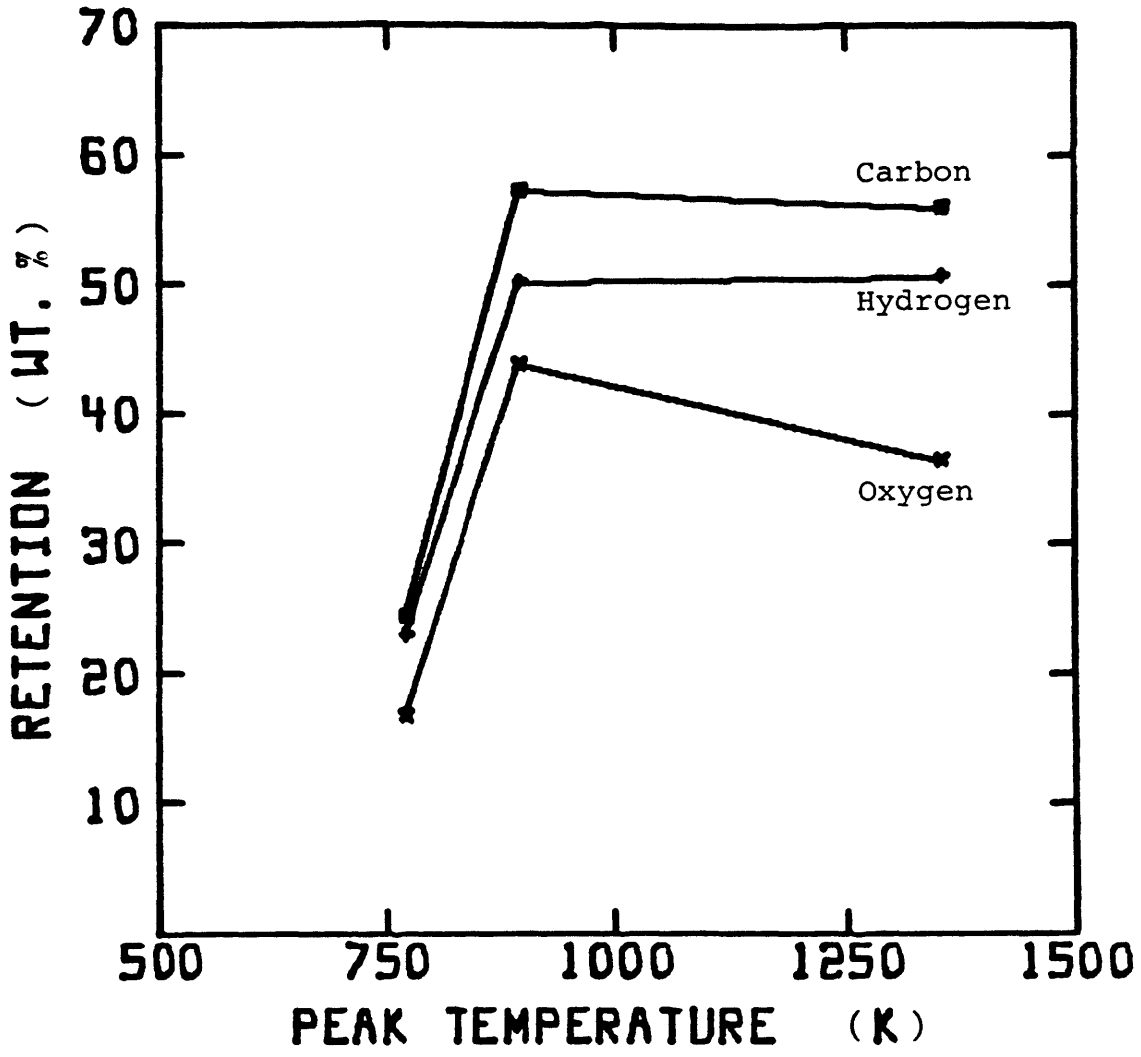

Figure 4.3-1 Percentage of Elements in Sweet Gum Wood that Remain in Tars From Pyrolysis.

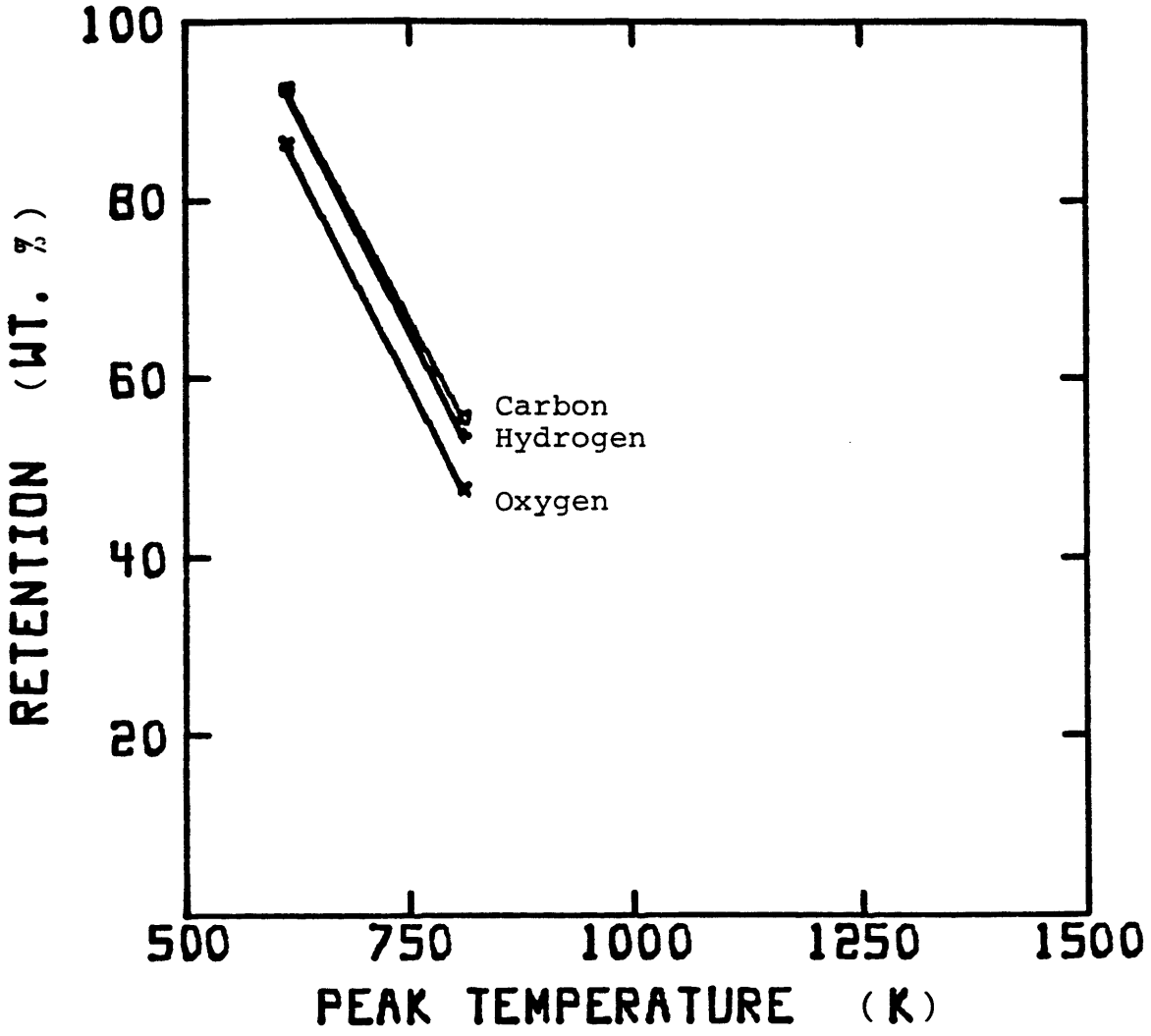

Figure 4.3-2 Percentage of Elements in Sweet Gum Wood that Remains in Chars From Pyrolysis.

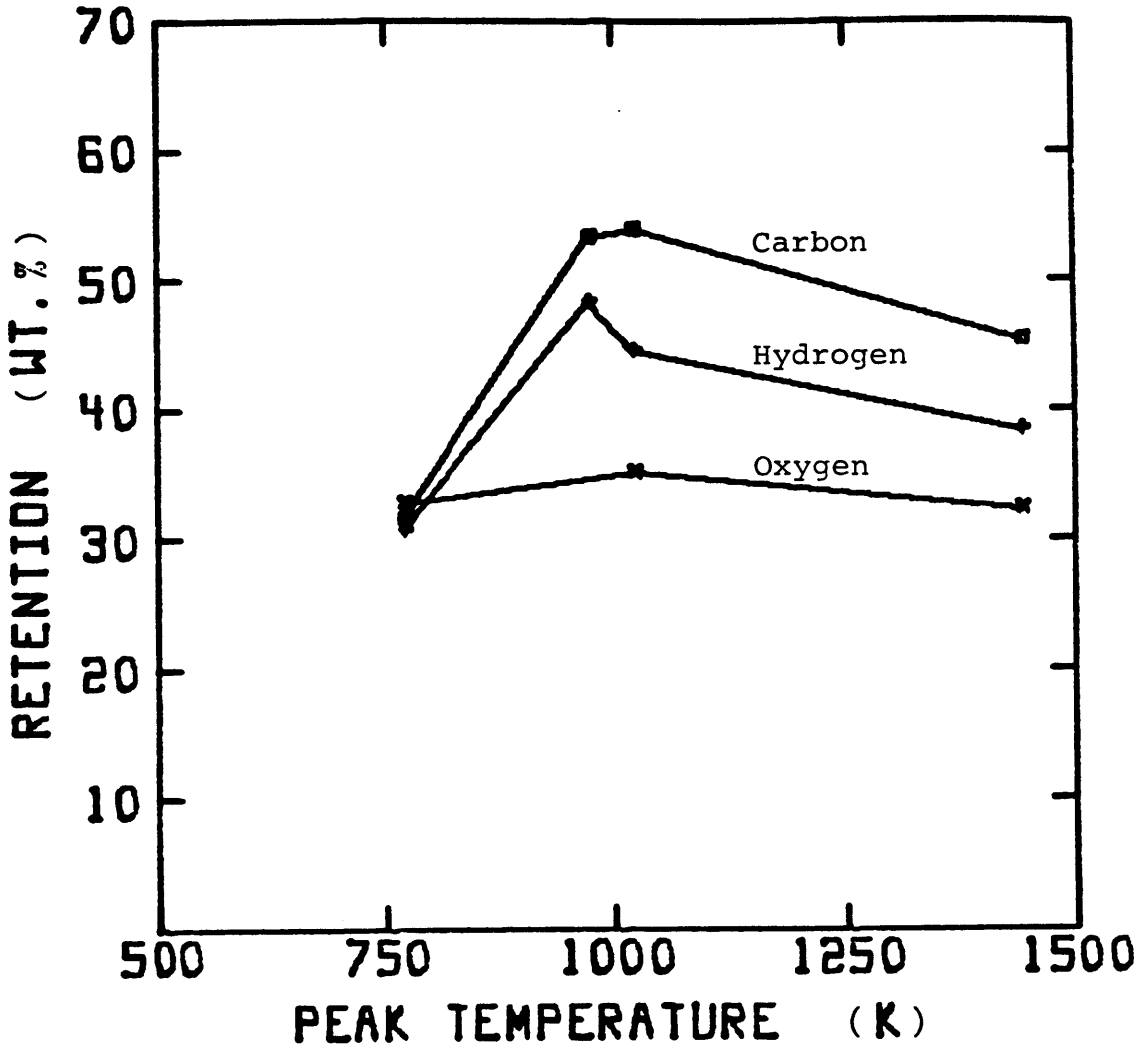

Figure 4.3-3 Percentage of Elements in Milled Wood Lignin that Remain in Tars From Pyrolysis.

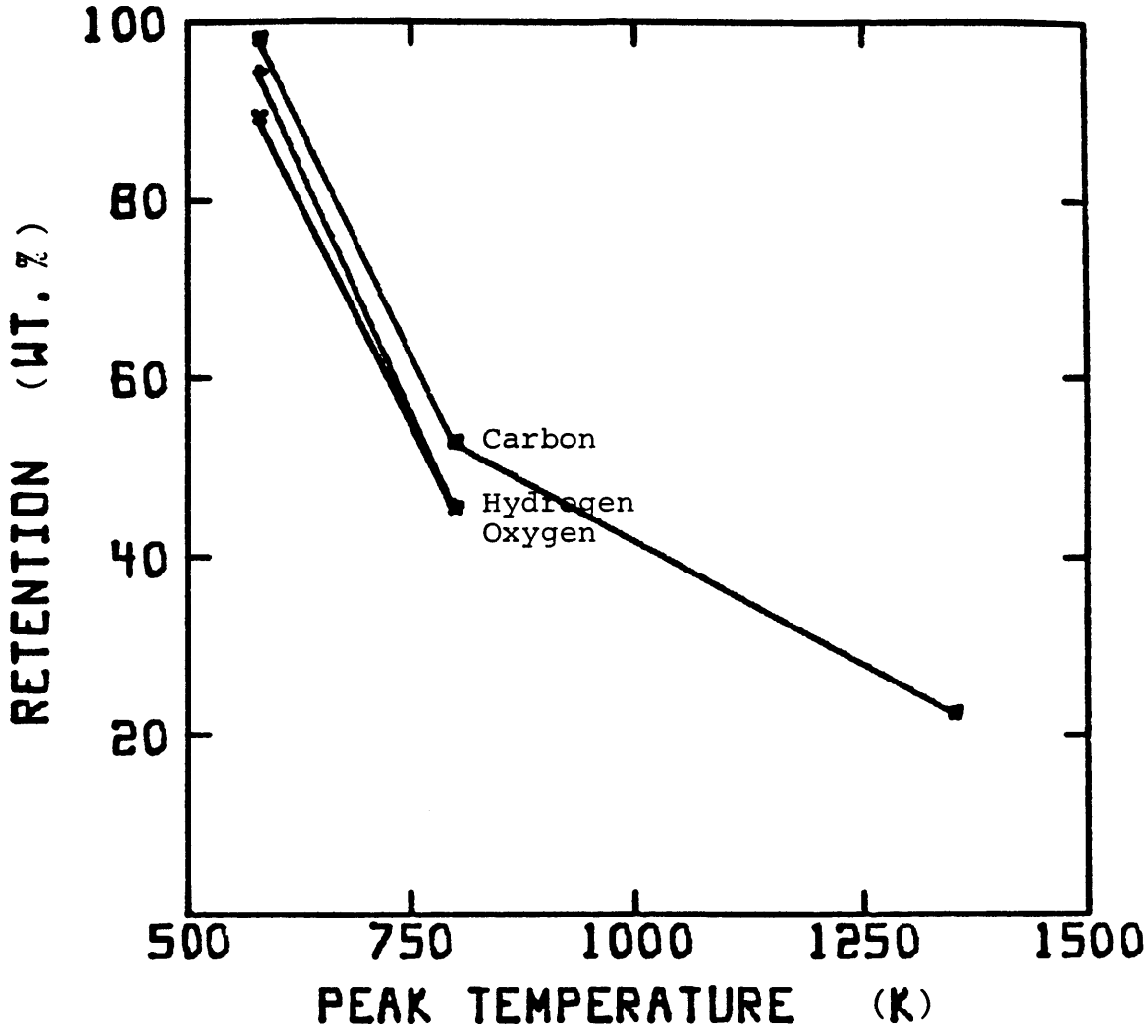

Figure 4.3-4 Percentage of Elements in Milled Wood Lignin that Remains in Chars From Pyrolysis.

Table 4.3-2 Elemental, Total Mass, and Energy Balances For Sweet Gum Wood Pyrolysis

Component	Approx. Ultimate Yield (wt. %)	C	H	O	Heat of Combustion (Btu/lb)*	% of Wood Energy in Component
Wood	-	49.5	6.1	44.6	8450	100.0
Char	7.0	7.0	-	-	14660	12.1
Tar	46.0	26.0	3.7	16.3	11470	62.4
CO	17.0	7.3	-	9.7	4340	8.7
CH_4	2.3	1.7	0.6	-	23860	6.5
CO_2	6.1	1.7	-	4.4	-	-
C_2H_4	1.3	1.1	0.2	-	21630	3.3
C_2H_6	0.2	0.16	0.04	-	22300	0.5
H_2O	5.1	-	0.6	4.5	-	-
HCHO	2.0	0.8	0.1	1.1	8190	1.9
C_3H_6	0.4	0.3	0.1	-	21000	1.0
CH_3OH	1.5	0.6	0.2	0.7	9770	1.7
CH_3CHO	1.4	0.8	0.1	0.5	11400	1.9
Butene+ Ethanol	0.6	0.3	0.1	0.2	12780	0.9
Acetone +Furan	0.9	0.6	0.1	0.2	13280	1.4
Acetic Acid	1.5	0.6	0.1	0.8	6270	1.1
Misc. C.H.O.	0.7	0.6	0.1	-	18020	1.4
Total	94.0	49.5	5.9	38.6		104.8
Closure	94%	100%	97%	86%		105%

* All heats of combustion are from the "Handbook of Chemistry and Physics" (1976), except for wood, char, and tar which are calculated from equation 4.3-1.

assumed to be ethanol, acetone, and benzene, respectively. Also, since no high temperature char analysis was available, the char was assumed to be 100% carbon. Heats of combustion for the individual gas products were extracted from the "CRC Handbook of Chemistry and Physics" (1976) and the values for wood, char, and tar were calculated from (Mason and Gandhi, 1980),

$$Q = 146.58(C) + 568.78(H) - 51.53(O) \qquad (4.3\text{-}1)$$

where Q is the gross heating value in Btu/lb on a dry basis and (C), (H), and (O) are the respective contents of carbon, hydrogen, and oxygen in weight present.

The balances for total mass, carbon, and hydrogen from wood pyrolysis are excellent while the oxygen balance is somewhat low. The low oxygen balance may be due to the assumptions that the char and miscellaneous oxygenated compounds contain no oxygen, or may be a result of errors in the elemental analysis of char, tar, and wood.

The asymptotic yield energy balance is quite revealing in that only 12.1% of the wood energy content is retained in the char, while tar accounts for over 62% of the wood energy content. The product gases account for another 30%. Carbon monoxide and methane together contain more than half of the gaseous heating value. Although the asymptotic CO yield is over seven times greater than that of methane, methane accounts for almost as much of the energy of the wood as does CO.

The fact that the energy content of the individual products accounts for more energy than was present in the original wood is not surprising given the experimental errors and

assumptions made in this analysis. However, it should be noted that the energy content of the products could be either greater or lower than that of the wood depending on whether the pyrolysis reaction is endothermic or exothermic. In any case, the heat of pyrolysis is thought to contribute very little to the energy balance, and the results reported in Table 4.3-2 support this postulate.

Similar elemental, total mass, and energy balances were applied to milled wood lignin pyrolysis, and the results are shown in Table 4.3-3. The heating values for lignin, tar, and char were calculated from Equation 4.3-1. The total mass, carbon, hydrogen, and oxygen balances are excellent. In lignin pyrolysis, it is seen that about 20% of the lignin energy content remains in the char, which reflects the lower degree of lignin volatilization. About 57% of the lignin energy is contained in the pyrolysis tars and 23% is contained in the gases. As with the wood, carbon monoxide and methane account for about 15% of the lignin energy. The methane fraction again accounts for almost as much energy as does CO, even though the CO yield is almost six times greater than the methane yield.

4.4 Modelling of Pyrolysis Kinetics

An important tool used for describing the behavior of organic material under pyrolysis conditions is the kinetic model. Modelling efforts in coal and biomass pyrolysis studies have produced schemes that vary in sophistication from simple models for overall material weightloss to models which incor-

Table 4.3-3 Elemental, Total Mass, and Energy Balances For Milled Wood Lignin Pyrolysis

Component	Approx. Ultimate Yield (wt. %)	C	H	O	Heat of Combustion (Btu/lb)	% of Lignin Energy in Component
Lignin	-	59.1	6.0	32.0	10430	100.0
Char	14.0	13.3	0.3	0.4	15000	20.1
Tar	47.0	31.1	3.5	12.4	12580	56.7
CO	19.0	8.1	-	10.9	4340	7.9
CH_4	3.2	2.4	0.8	-	23860	7.3
CO_2	4.1	1.1	-	3.0	-	-
C_2H_4	0.9	0.8	0.1	-	21630	1.9
C_2H_6	0.3	0.2	0.1	-	22300	0.6
H_2O	3.8	-	0.4	3.4	-	-
HCHO	1.4	0.8	0.1	0.5	8190	1.1
C_3H_6	0.3	0.26	0.04	-	21000	0.6
CH_3OH	1.7	0.6	0.2	0.9	9770	1.6
CH_3CHO	0.9	0.5	0.1	0.3	11400	1.0
Butene+ Ethanol	0.6	0.3	0.1	0.2	12780	0.7
Acetone +Furan	0.3	0.2	-	0.1	13280	0.4
Acetic Acid	0.2	0.1	-	0.1	6270	0.1
Misc. C.H.O.	0.2	0.18	0.02	-	18020	0.3
Total	97.9	60.0	5.8	32.2		100.3
Closure	98%	101%	96%	101%		100%

* All heats of combustion are from the "Handbook of Chemistry and Physics" (1976), except for lignin, char, and tar which are calculated from equation 4.3-1.

porate complex physical and chemical mechanisms.

The data obtained in this study were correlated using a single-step, first order reaction model for the yield of each individual product. This model was chosen for its simplicity, its usefulness in engineering calculations, and its history of successful utilization in other studies of this nature (Hajaligol, 1980; Franklin, 1980; Suuberg, 1977; Thurner and Mann, 1981). A non-linear least squares program was used to fit the parameters to the experimental data. For the ith component,

$$\frac{dVi}{dt} = (V_i^* - V_i)\, k_{oi} \exp\left(-\frac{Ei}{RT}\right) \qquad (4.4\text{-}1)$$

where k_{oi} is the pre-exponential factor and Ei is the apparent activation energy for component i. In integrated form, the model becomes

$$\ln \frac{V_i^* - V_i}{V_i^*} = -\int_o^t k_{oi} \exp\left(-\frac{Ei}{RT}\right) dt \qquad (4.4\text{-}2)$$

Data for the yield, V_i, and the time-temperature history, $T = f(t)$, are fed to the computer which then integrates the data over each time-temperature history using initial guesses for the three unknown parameters k_{oi}, E_i, and V_i^*. Optimum parameters (i.e. those that minimize the sum of squared errors between calculated and observed yields) are then obtained by a non-linear least squares regression procedure.

The parameters obtained from the first order reaction model for the wood and lignin pyrolysis data are included in

Tables 4.4-1 and 4.4-2 along with a statistical parameter known as the standard error of the estimate in the fitting procedure. Even though it is obvious that some of the pyrolysis products are not formed by simple reactions, the single-step, first order kinetic model provides a good basis for comparison of the different data.

A kinetic analysis as described above was also performed on Hajaligol's (1980) cellulose pyrolysis data taken from the pyrolysis of cellulose filter paper under conditions similar to those of this work, and the results are included in Table 4.4-3. The cellulose pyrolysis kinetic parameters in Table 4.4-3 are somewhat different than those reported by Hajaligol (1980), which may be a result of the different data reduction techniques used by the different investigators. The computer code used to generate kinetic parameters in the current work was a modified version of a non-linear least squares regression program, named POWELL, in the library of the M.I.T. Department of Chemical Engineering computer (Franklin, 1980). This program is an updated version of the program thought to have been used by Hajaligol (1980) on the same computer system. As a criterion for determining the goodness of the fit of the model to the data, the standard error of the estimate indicates that the POWELL data fitting procedure produces a fit to the experimental data which is superior to the fit generated by the program used by Hajaligol for all but one component analyzed (see Appendix A-4). The kinetic parameters in Table 4.4-3 were used in the present work because of the improved fit to the data and for the sake of being consistent within the context

Table 4.4-1
Kinetic Parameters for Sweet Gum Wood Pyrolysis

Product	E_i (kcal/mole)	$\log_{10} k_{oi}$	V* (wt.%)	standard error of estimate *(wt.%)
Weight Loss	16.5	4.53	92.97	7.66
Total Gases	11.8	2.88	41.01	2.54
CO	14.6	3.36	17.05	2.15
CH_4	16.6	3.79	1.91	0.21
CO_2	14.3	3.77	5.97	0.51
C_2H_4	19.2	4.41	1.17	0.12
C_2H_6	23.7	5.87	0.17	0.02
H_2O	11.5	3.35	5.14	0.65
HCHO	12.9	3.51	1.99	0.27
H_2O+HCHO	11.5	3.26	7.13	0.74
C_3H_6	42.8	11.20	0.41	0.06
CH_3CHO	21.3	5.80	1.40	0.34

* defined as $\sqrt{\sum_{j=1}^{n} (V_{j,model} - V_{j,exper.})^2/(n-3)}$

where n is the number of data points

Table 4.4-2
Kinetic Parameters for Milled Wood Lignin Pyrolysis

Product	E_i (kcal/mole)	$\log_{10} k_{oi}$	V* (wt.%)	standard error of estimate (wt.%)
Weight Loss	19.6	5.53	84.35	5.76
Total Gases	9.6	2.17	36.54	1.85
CO	16.0	3.66	18.24	1.00
CH_4	17.8	4.16	3.07	0.18
CO_2	9.7	2.23	4.01	0.26
C_2H_4	20.2	4.64	0.86	0.07
C_2H_6	20.7	5.03	0.29	0.03
H_2O	5.8	1.59	3.74	0.31
HCHO	12.5	3.91	1.46	0.21
H_2O+HCHO	7.1	2.07	5.18	0.39
C_3H_6	20.9	5.21	0.26	0.03

Table 4.4-3

Kinetic Parameters for Filter Paper Cellulose Pyrolysis*

Product	E_i (kcal/mole)	$\log_{10} k_{oi}$	V* (wt.%)	standard error of estimate (wt.%)
Weight Loss	25.0	6.54	95.78	4.91
Total Gases	17.6	3.97	42.22	3.02
CO	27.3	6.07	21.69	1.64
CH_4	24.1	5.06	2.59	0.16
CO_2	11.8	2.35	3.76	0.23
C_2H_4	30.7	6.61	2.10	0.13
C_2H_6	35.2	7.65	0.25	0.03
H_2O+HCHO	11.3	2.90	8.22	1.21
C_3H_6	29.8	7.14	0.70	0.14

of this report.

Some of the pyrolysis products were not analyzed with the single-step first order kinetic model due to the degree of uncertainty in the data. The tar yields were not analyzed because single-reaction first order kinetics cannot predict a maximum in yield.

The kinetic parameters were used to fit curves to the experimental data. The modelled curves for the components listed in Tables 4.4-1, 4.4-2, and 4.4-3 are included in Figures 4.4-1 through 4.4-9 along with the pyrolysis data. The plots are arranged to allow comparison of the kinetic behavior of the three materials studied with respect to generation of each of the products analyzed.

The overall weightloss data for cellulose, lignin, and wood pyrolyses are presented in Figure 4.4-1 along with the curves fitted by the first order kinetic model. Cellulose is seen to be the ultimately most volatile of the three materials, achieving an ultimate weight loss of 96 wt. % with wood and lignin reaching 93 and 84 wt. % respectively.

All three curves fit the corresponding data points extremely well. However, care must be taken in drawing any inferences about the mechanistic meaning of this, such as concluding that the reactions involved in the initial pyrolyses of these biomass materials may be of a simple nature. This is because the values of the activation energies for all three materials (see Tables 4.4-1, 4.4-2, and 4.4-3) are much lower than those generally expected for unimolecular thermal decomposition reactions (typically 30-70 kcal/mole (Suuberg et al.,

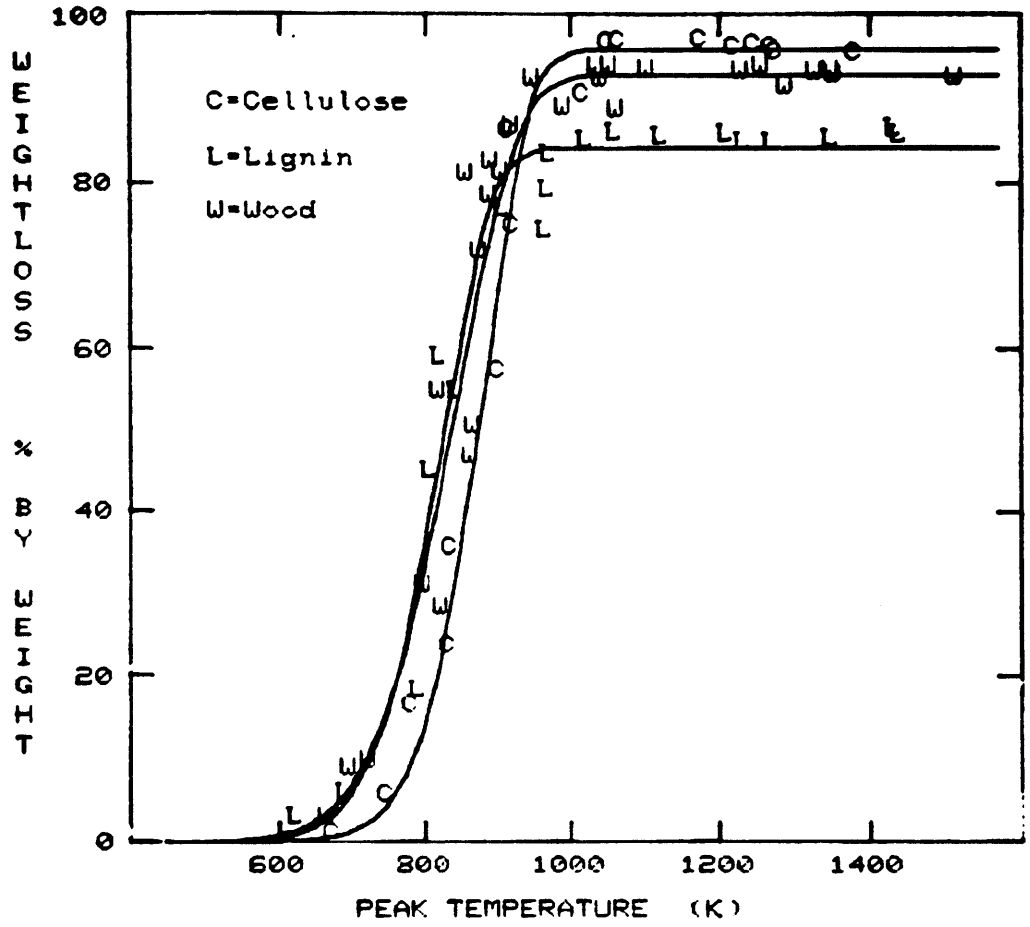

Figure 4.4-1 Experimental Data and Modelled Curves for Overall Weight Loss From Biomass Pyrolyses.

1978).

It is interesting to note that at temperatures below 900K, lignin and wood exhibit similar weight loss reactivity and both exceed cellulose. Above this temperature, the cellulose weight loss curve exceeds wood modestly and both exceed lignin. The former behavior is contrary to the expected order of thermal reactivity for wood components, which would be (Wenzl, 1970; Roberts, 1970)

hemicellulose > cellulose > lignin (reactivity).

The slightly lower reactivity of cellulose, as indicated by its higher activation energy (Table 4.4-3) may be due to the fact that a filter paper cellulose rather than natural cellulose was pyrolyzed. Wenzl (1970) points out that differences in the cellulose structure, characterized by the degree of hydrolyzability of the cellulose, can influence the product distribution in cellulose pyrolysis. It is also known that the degree of polymerization (DP) of cellulose varies from up to 10,000 for natural cellulose fibers to 400 for bond paper. Basch and Lewin (1973) have shown that many of the reported literature differences in the behavior of cellulose in vacuum pyrolysis may be attributed to differences in crystal structure and orientation as well as to variations in the degree of polymerization.

Figure 4.4-2 presents the first order kinetic models for total gas production. Cellulose produces the most total gases, yielding 42 wt. %. Again it is seen that the models fit the corresponding data fairly well, even thought the gas production above 1000K is due solely to secondary tar cracking

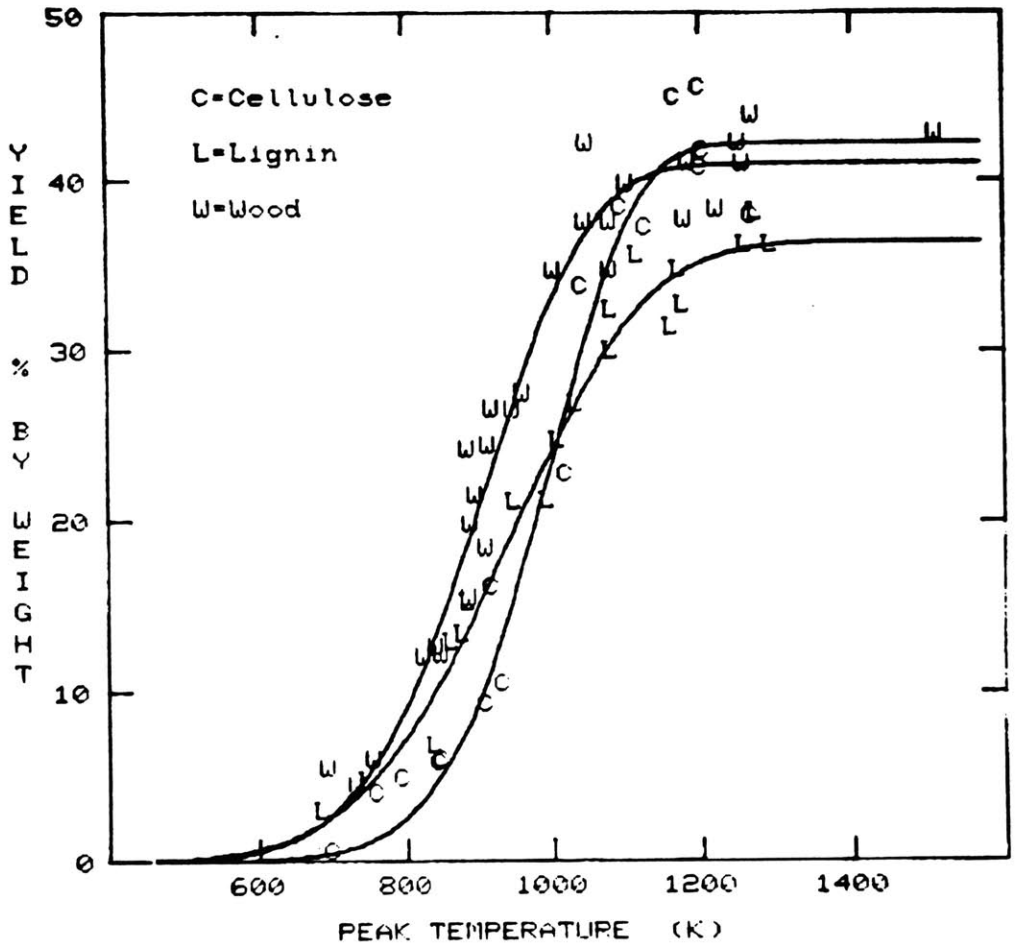

Figure 4.4-2 Experimental Data and Modelled Curves for Total Gas Production From Biomass Pyrolyses.

reactions, and not primary degradation of the biomass (see sections 4.1 and 4.2). It is also apparent that the wood behavior at lower temperatures is somewhat more closely matched by the lignin, although the lignin rises more slowly with increasing temperature. At temperatures above 1000K, the cellulose curve very closely approaches the wood curve. With most of the individual gas components in Figures 4.4-3 through 4.4-9, as well as with weight loss and total gas production, it appears that the low temperature wood pyrolysis behavior can be modelled by the lignin pyrolysis kinetics, while higher temperature behavior resembles the cellulose pyrolysis results. This may be due to the cellulose structural differences explained previously, but it may also be an indication that the wood pyrolysis kinetics change as temperature is increased. The phenomenon of wood pyrolysis kinetics changing with progression of reaction has been observed in other biomass pyrolysis studies (Roberts, 1970).

Shafizadeh and Chin (1977) report that there is no significant interaction among the three major components during the thermal degradation of wood. Therefore, it would not be surprising for the wood pyrolysis behavior to vary as the hemicellulose, lignin and cellulose fractions become active at different temperatures. The low temperature wood pyrolysis could resemble hemicellulose and lignin decomposition and the high temperature wood pyrolysis could resemble cellulose decomposition, with intermediate temperature pyrolysis behavior being controlled by some combination of the three components. An investigation of the hemicellulose pyrolysis behavior under

the conditions of this study would shed light on the validity of this argument.

Figure 4.4-3 shows the modelled and experimental yields of carbon monoxide as a function of peak temperature. The first-order kinetic models do not follow the data as well in this case as for the previous two figures, especially for lignin and cellulose at higher temperatures. Apart from experimental error, this is most probably due to the fact that the single-step, first-order model is trying to fit a set of data that is obviously the result of a more complex kinetic scheme that includes high temperature contributions from secondary cracking of tar. Nevertheless, the data trends are followed fairly well and it is interesting to see that both lignin and cellulose produce more CO than wood at higher temperatures. The ultimate (modelled) CO yields are 18.2, 21.7, and 17.1 wt. %, respectively, for lignin, cellulose, and wood. Using the fact that this sweet gum hardwood contains about 42.5 wt. % cellulose, 30.6 wt. % hemicellulose, and 26.9 wt. % lignin, the limiting yield of CO from hemicellulose would therefore not be expected to exceed 10 wt. % if additivity rules are valid (that is, if the wood pyrolysis behavior can be simulated by the weighted sum of the pyrolysis results of the individual wood constituents).

The modelled curves for the yields of methane from lignin, wood, and cellulose are given in Figure 4.4-4. Again, the model fittings leave something to be desired, for the reasons explained previously for CO. Lignin produced the most methane, yielding about 3.1 wt. % while cellulose and wood produced 2.6 and 1.9 wt %, respectively. Again assuming

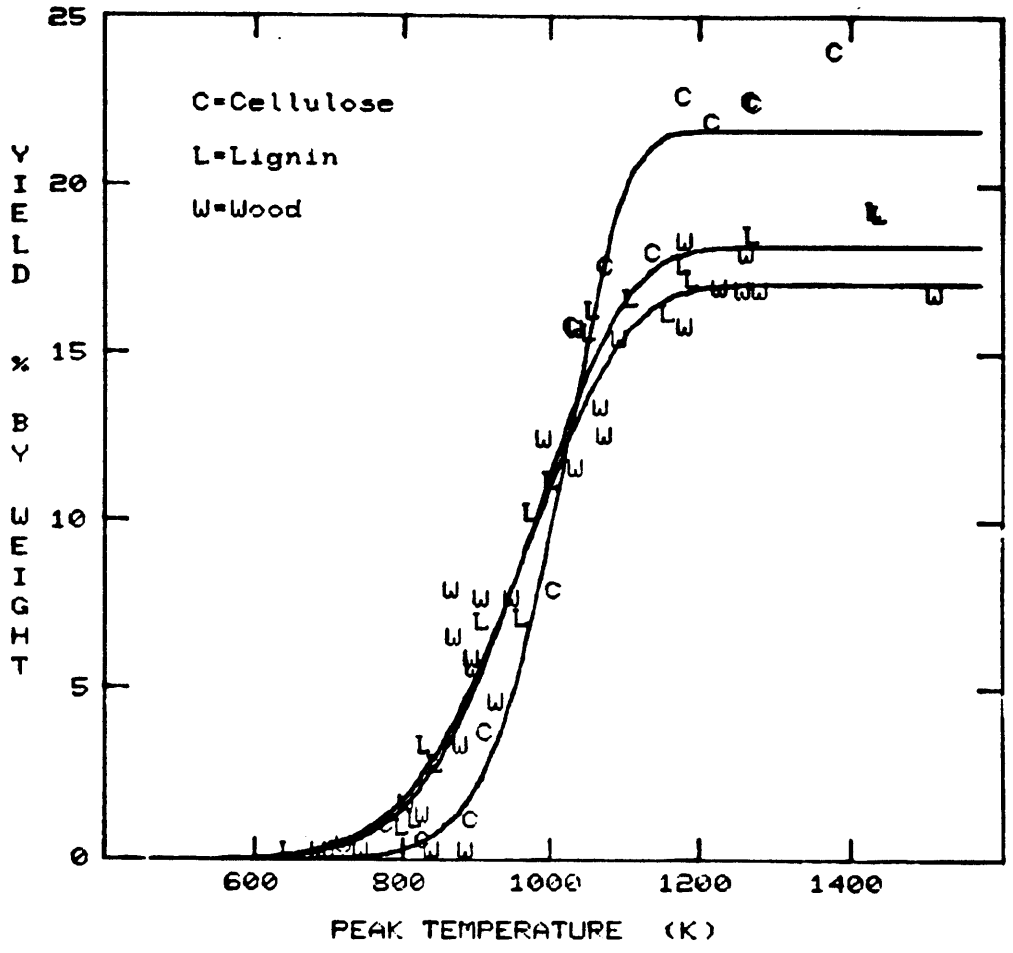

Figure 4.4-3 Experimental Data and Modelled Curves for Carbon Monoxide Yield From Biomass Pyrolyses.

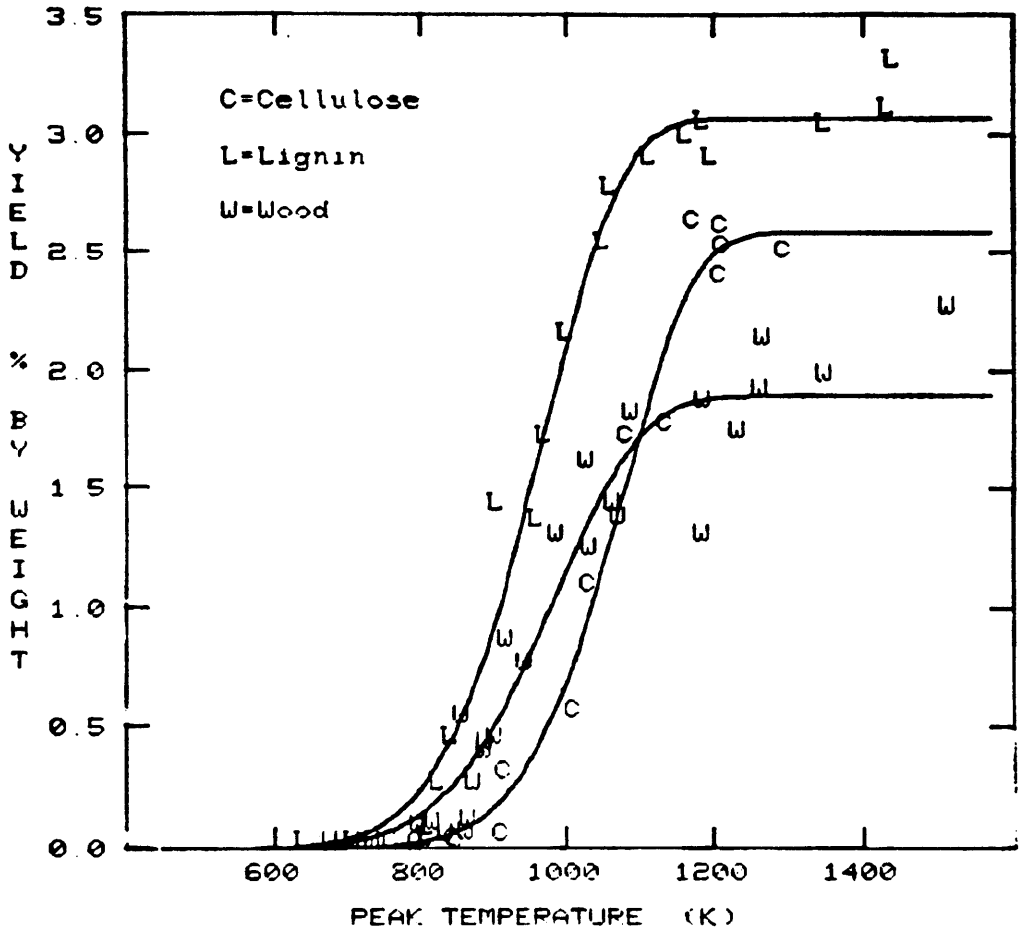

Figure 4.4-4 Experimental Data and Modelled Curves for Methane Yield From Biomass Pyrolyses.

additivity, hemicellulose pyrolysis would be expected to produce negligible amounts of methane.

Figure 4.4-5 presents the results of applying this model to carbon dioxide yield. An interesting point is that much more carbon dioxide is produced from wood than can be accounted for from the weighted lignin and cellulose yields. The yields from cellulose and lignin pyrolysis are about 3.8 and 4.0 wt. %, respectively, and the yield from wood is 6.0 wt. %. Using the weighted fractions from sweet gum hardwood components and assuming additivity, a carbon dioxide yield of over 11 wt. % would be predicted from pyrolysis of hemicellulose. This is an extremely large percentage and it would be informative to determine if such a yield is found experimentally. If this experiment proves negative, and if the structural effects of cellulose pyrolysis turn out to be minor, there may be interactive effects between the wood components that exert a major effect on carbon dioxide production.

Figure 4.4-6 displays the experimental and modelled data for ethylene production. Given the small quantities of ethylene produced for each compound, the theoretical curves fit the data fairly well. Still, especially with the wood pyrolysis data, reactions more complex than the first order reactions are evidenced by the increasing yields of ethylene above 1100K. The ultimate yields of ethylene from pyrolysis of wood, lignin, and cellulose are approximately 1.2, 0.9, and 2.1 wt. %, respectively. The predicted yield of ethylene from hemicellulose pyrolysis would therefore be 0.2 wt. % based on additivity. This would be ten times less than from cellulose and is surpris-

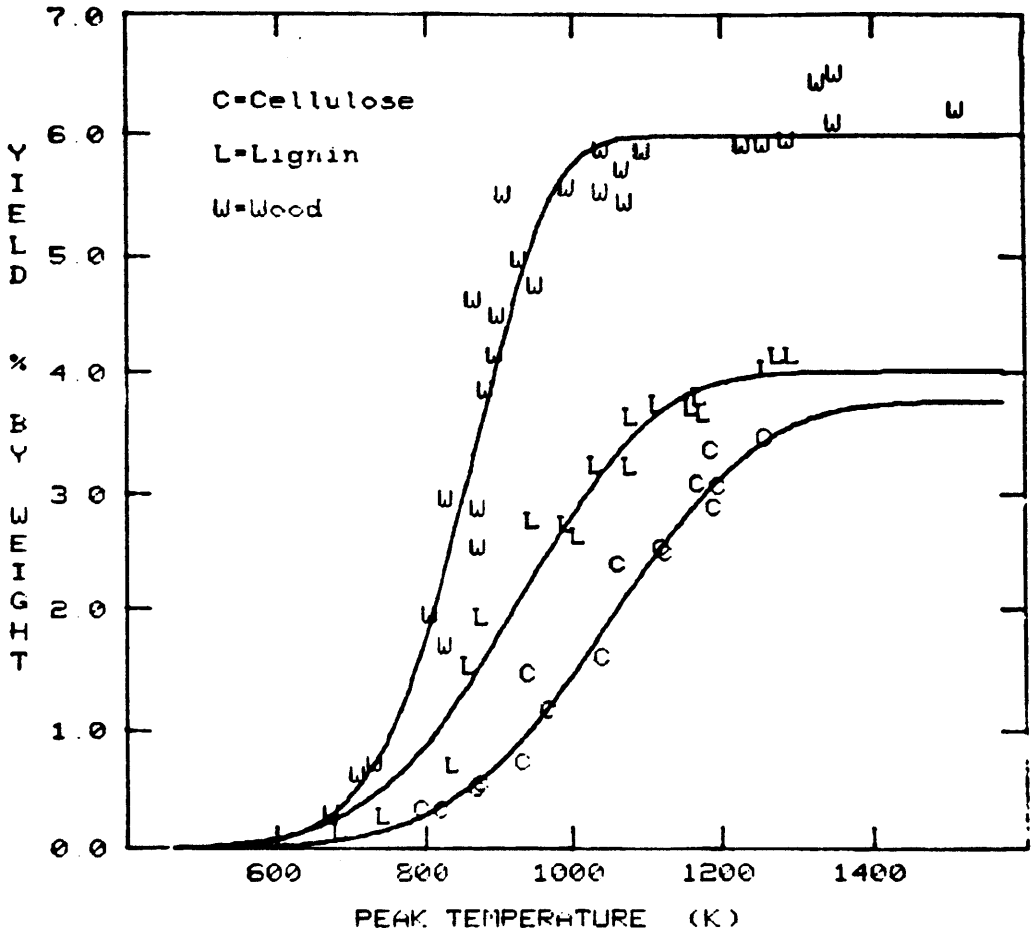

Figure 4.4-5 Experimental Data and Modelled Curves for Carbon Dioxide Yield From Biomass Pyrolyses.

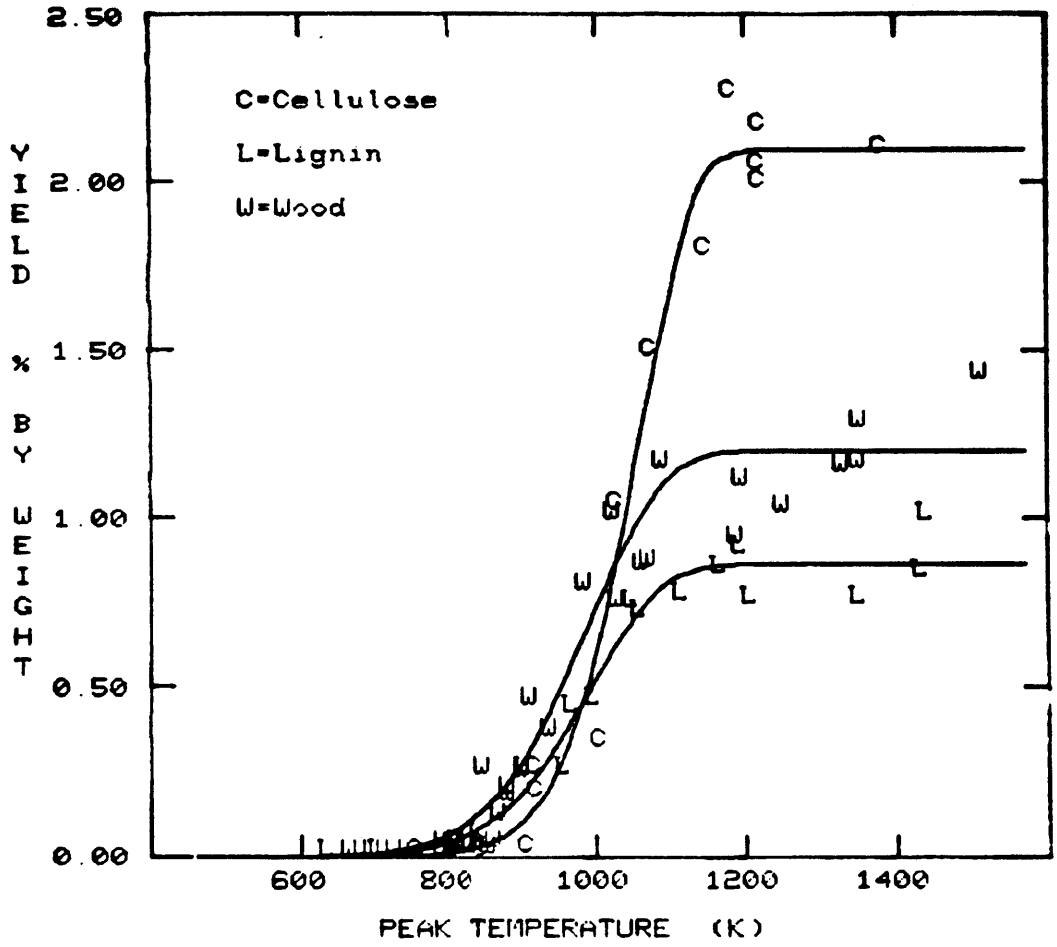

Figure 4.4-6 Experimental Data and Modelled Curves for Ethylene Yield From Biomass Pyrolyses.

ing since these two wood constituents are much more similar in structure than are cellulose and lignin.

The modelled curves for ethane production fit the experimental data much better than would be expected given the small yields of ethane (Figure 4.4-7). The ethane yields from lignin and cellulose pyrolysis (0.29 and 0.25 wt. %, respectively) are both somewhat greater than the yield from wood (0.17 wt. %) leading to a prediction that hemicellulose pyrolysis would produce very little, if any, ethane.

The first-order model curves for water plus formaldehyde in Figure 4.4-8 are all very similar and appear to fit the data well, in spite of the uncertainties due tothe water tailing GC phenomenon (the data reported by Hajaligol [1980] are labelled as water but are actually water plus formaldehyde due to the inability of the GC to resolve the formaldehyde and water peaks in a reproducible manner). The modelled activation energies and frequency factors are all about the same for the three materials pyrolyzed, indicating similar water formation mechanisms. The yield of water and formaldehyde from wood pyrolysis is 7.1 wt. % while the yields from lignin and cellulose pyrolysis are 5.2 and 8.2 wt. %, respectively. Again assuming additivity, a predicted value of 7.2 wt. % is obtained for water and formaldehyde from hemicellulose pyrolysis, which is not unreasonable.

The propylene data are shown in Figure 4.4-9. Cellulose produces the highest ultimate yield, 0.7 wt. %, which is more than twice the ultimate yield of propylene from lignin. From an additivity calculation, the predicted yield of propylene

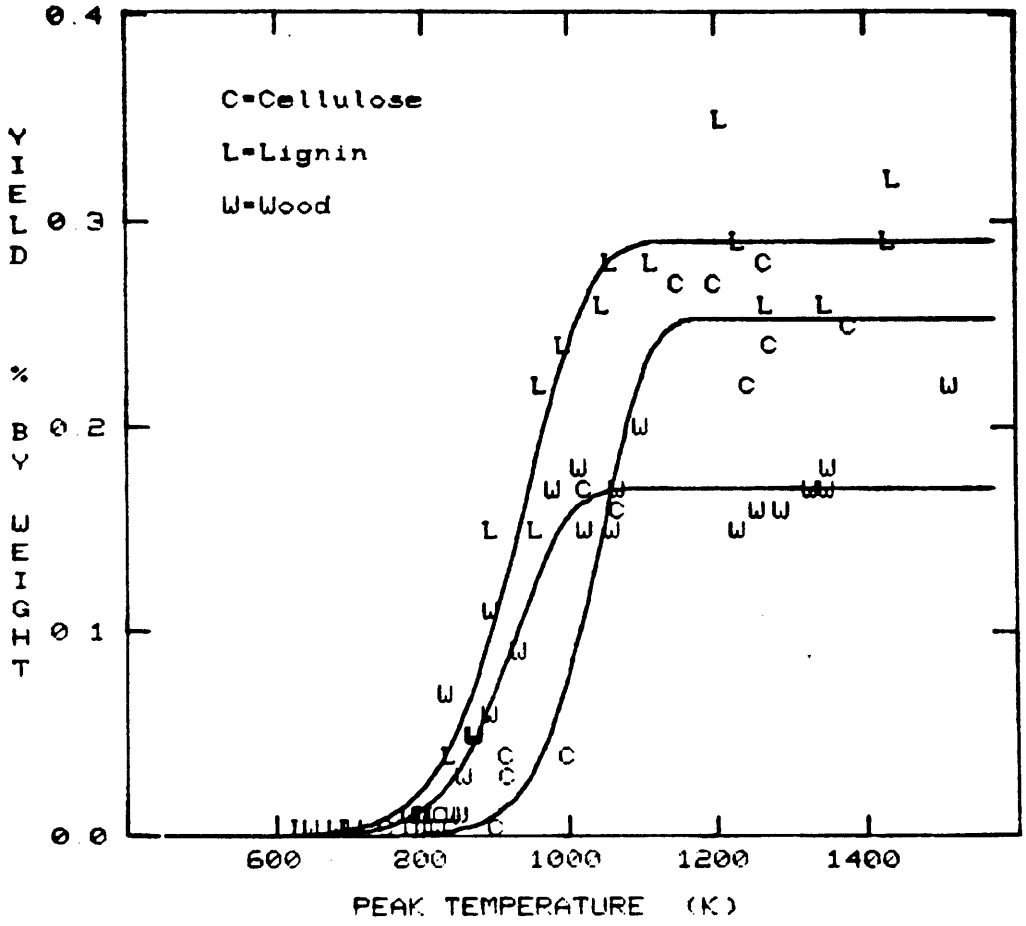

Figure 4.4-7 Experimental Data and Modelled Curves For Ethane Yield From Biomass Pyrolyses.

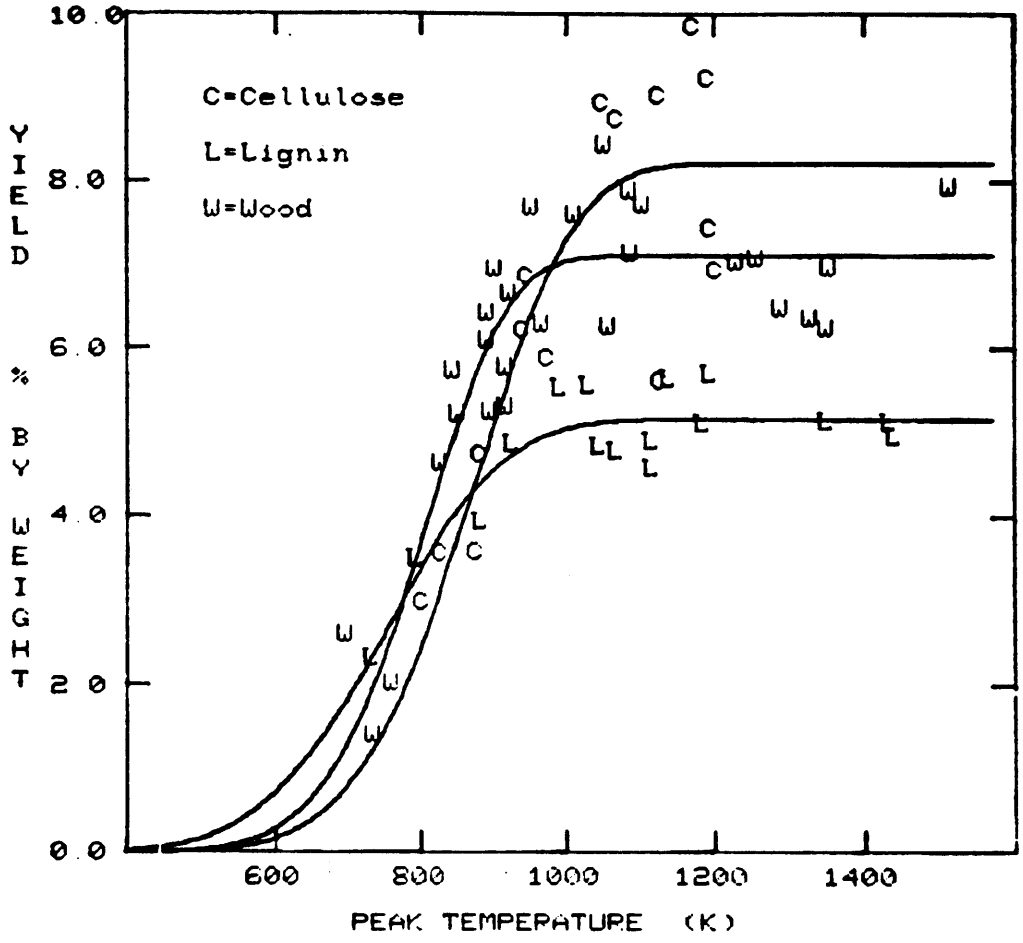

Figure 4.4-8 Experimental Data and Modelled Curves for Water + Formaldehyde Yield From Biomass Pyrolyses.

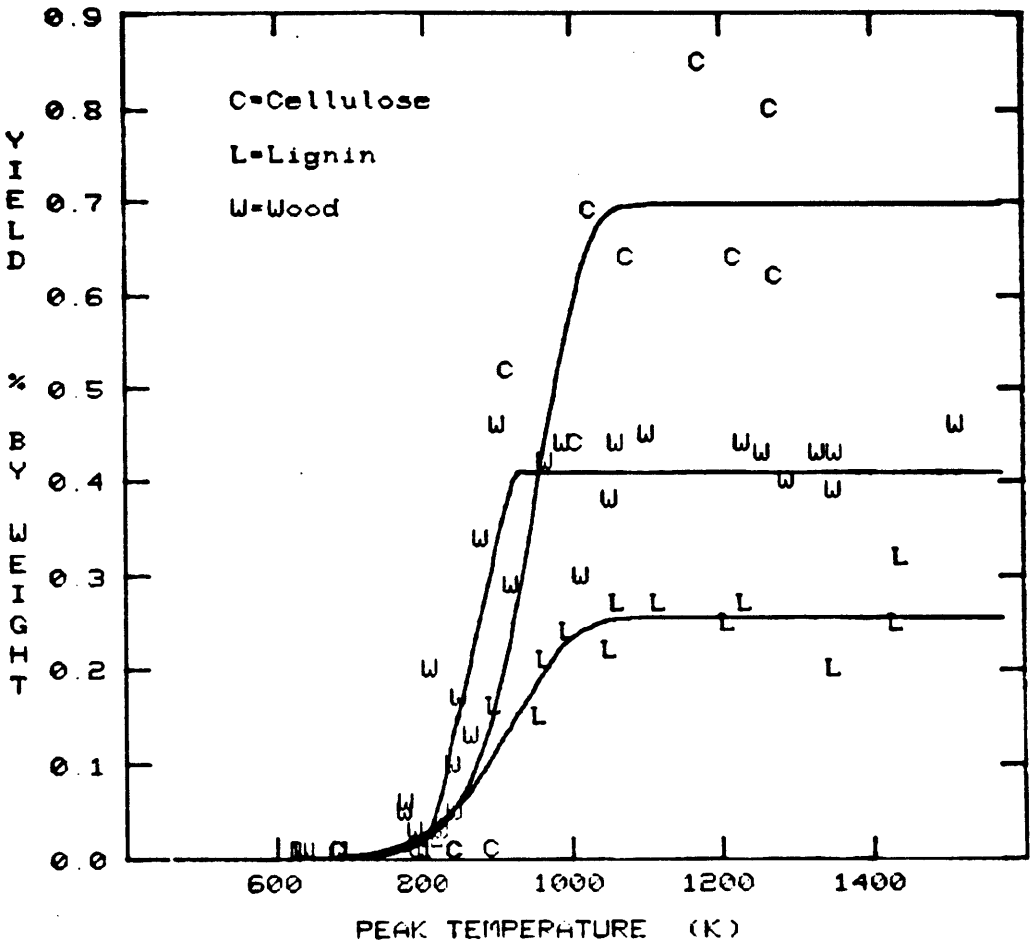

Figure 4.4-9 Experimental Data and Modelled Curves for Propylene Yield From Biomass Pyrolyses.

from lignin. From an additivity calculation, the predicted yield of propylene from hemicellulose would be 0.24, a yield which is closer to that of lignin than that of cellulose. The wood data exhibit a much sharper increase in yield with increasing temperature than do either lignin or cellulose, which may indicate something about the relative reactivities of these compounds, but is difficult to interpret given the amount of scatter in the data.

Most of the values for E_i and $\log_{10}k_{oi}$ in Tables 4.4-1, 4.4-2, and 4.4-3 are much lower than would be expected for organic bond breaking reactions, but are typical of attempts to fit single-step, first-order kinetic models to pyrolysis data on solid organic materials of modestly complex molecular structure. It is quite possible that higher values for each of the parameters could fit the data just as well, as is evidenced by the comparison of the two sets of parameters included in Appendix A-4 for the cellulose pyrolysis models.

The approximate ultimate yields taken at around 1400K for products from wood, lignin, and cellulose pyrolysis are included for comparison in Table 4.4-4. Also included are the predicted yields for sweet gum hemicellulose pyrolysis, which are obtained from the additivity equation

$$V_{i,H} = (V_{i,w} - 0.425\ V_{i,c} - 0.269\ V_{i,L}) \ / \ 0.306 \quad (4.4\text{-}3)$$

where

$V_{i,H}$ = yield of product i from sweet gum hemicellulose pyrolysis;

Table 4.4-4 Approximate Ultimate Yields of Individual Products from Biomass Pyrolysis @1400K (wt.%)

Product	Wood	Lignin	Cellulose*	Hemicellulose (predicted)
Char	7.0	14.0	5.0	4.0
Tar	46.0	47.0	50.0	40.0
Total Gases	42.0	36.0	43.0	46.0
CO	17.0	18.5	21.7	9.2
CH_4	2.3	3.2	2.5	1.2
CO_2	6.1	3.8	3.4	11.9
C_2H_4	1.3	0.9	2.1	0.54
C_2H_6	0.17	0.29	0.26	T**
H_2O	5.1	3.8	-	-
HCHO	2.0	1.4	-	-
H_2O+HCHO	7.1	5.2	8.1	7.4
C_3H_6	0.42	0.27	0.66	0.22
CH_3OH	1.5	1.7	0.92	2.1
CH_3CHO	1.4	0.9	1.5	1.7
Butene+ Ethanol	0.6	0.5	0.3	1.1
Acetone +Furan	0.9	0.3	0.8	1.6
Acetic Acid	1.5	0.2	-	-
Misc. C.H.O.	0.7	0.2	-	-
Acetic Acid + C.H.O.	2.2	0.4	1.2	5.2
H_2	<1.0	T**	1.0	-

* Data from Hajaligol (1980).

** T=trace amounts expected.

$V_{i,w}$ = yield of product i from sweet gum wood pyrolysis;

$V_{i,c}$ = yield of product i from filter paper cellulose pyrolysis;

and $V_{i,L}$ = yield of product i from sweet gum milled wood lignin pyrolysis.

The constants in equation 4.4-3 are the weight fractions of the corresponding components in sweet gum hardwood, normalized to 1.0. Equation 4.4-3 is based on the assumption that the components of wood behave independently under the conditions of wood pyrolysis. Note that the predicted yields for hemicellulose pyrolysis are subject to verification of the validity of using filter paper cellulose pyrolysis product yields in the place of yields from native cellulose pyrolysis.

The interesting points from Table 4.4-4 are the relatively small predicted yields from CO, methane, ethylene, and ethane, and the rather large predicted yields of carbon dioxide and oxygenated compounds from hemicellulose pyrolysis.

The distributed activation energy model is another method of analysis which can be used to correlate the overall pyrolysis weight loss data. This model assumed that the process kinetics are described by a number of independent parallel rate processes which have identical frequency factors but a continuous distribution of activation energies. Anthony and Howard (1976) assumed a Gaussian distribution of activation energies and obtained a good correlation with their experimental weight loss data from the pyrolysis of Montana lignite and Pittsburgh No. 8 bituminous coal.

Suuberg (1978) plotted the cumulative ultimate yields for the individual products from pyrolysis of the same type of lignite as that used by Anthony and Howard against increasing activation energy obtained from the single-step, first-order reaction model for each of the products. The slope of the curve drawn through these points gave a distribution of activation energies which was similar to that obtained by Anthony and Howard (1976).

A preliminary attempt to apply Suuberg's method of analysis to the wood pyrolysis data obtained in the present study showed that a fairly narrow distribution of activation energies for the total weight loss from wood pyrolysis would be derived from the activation energies and yield data for the individual products. Further work on applying this model to biomass pyrolysis could be useful in understanding the underlying phenomena contributing to the distribution of activation energies for total weight loss.

4.5 Simulation of Wood Pyrolysis

In this section, an attempt is made to simulate the wood pyrolysis results by combining the laboratory data from the lignin and cellulose pyrolyses. Since no data are available on the pyrolysis of hemicellulose, it has been assumed for this modelling study that the pyrolysis behavior of hemicellulose would be similar to that of cellulose under the present reaction conditions. This is not an unreasonable assumption given the fact that cellulose and hemicellulose have similar chemical structures, but is somewhat contradictory to the ob-

servation in the previous section that the predicted ultimate yields from hemicellulose pyrolysis based on additivity are, in some cases, drastically different than the yields from cellulose pyrolysis. The chemical composition of the simulated wood would then be 26.9 wt % lignin and 73.1 wt. % cellulose.

The above weight percentages were used as multiplying factors for the lignin and cellulose modelled curves presented in the previous section. These weighted data were added together to generate simulated yield data which were in turn fitted with a single-step, first-order kinetic analysis using idealized time-temperature histories (Franklin, 1980) to obtain the rate parameters shown in Table 4.5-1 and the simulated curves of Figure 4.5-1 through 4.5-9. Also included in Figures 4.5-1 through 4.5-9 are the experimental wood pyrolysis data and the wood pyrolysis modelled curves obtained previously.

Figure 4.5-1 shows the simulated wood weight loss results along with those of the actual wood pyrolysis. The similarity between the two first-order kinetic model curves is remarkable. The simulated curve fits the experimental data almost as well as the curve based on the experimental data itself, and the experimental asymptotic weight loss of 93 wt. % is well matched by the simulation, both in absolute quantity and in the temperature at which the asymptote is reached. The slight differences between simulation and experiment at temperatures below 950K may be attributed to: 1) the assumption that hemicellulose behaves as cellulose and/or 2) differences between native cellulose and filter paper cellulose. However, the

Table 4.5-1 Kinetic Parameters for Simulated Wood Pyrolysis

Product	E_i (kcal/mole)	$\log_{10} k_{oi}$	V_i^* (wt. %)
Weight Loss	21.7	5.77	92.75
Total Gases	15.0	3.39	40.67
CO	23.0	5.15	20.78
CH_4	19.0	4.09	2.72
CO_2	10.2	2.09	3.83
C_2H_4	30.3	6.54	1.17
C_2H_6	24.4	5.45	0.26
H_2O+HCHO	9.5	2.46	7.41
C_3H_6	27.5	6.60	0.58

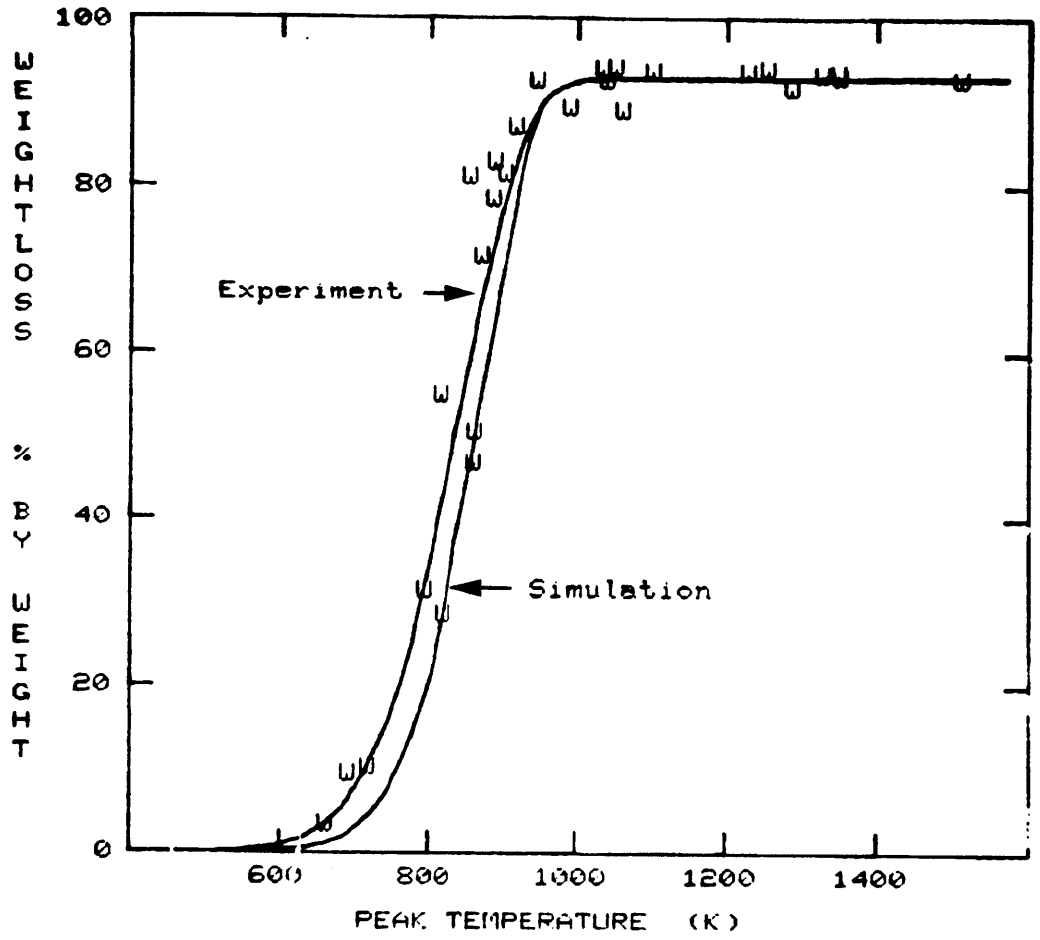

Figure 4.5-1 Modelled Curves Based on Experiment and Simulation for Overall Weight Loss From Wood Pyrolysis. (W's are experimental data)

deviations are minor in the case of total weight loss, indicating that weight loss behavior lends itself well to modelling by this simulation method.

Explanation (1) above would seem quite logical in light of the information reported in the literature on hemicellulose pyrolysis. Stamm (1956) reports that Douglas Fir hemicellulose degrades about four times as fast as the cellulose. This higher degree of reactivity for hemicellulose would have the effect of shifting the simulated curve to the left so that the simulation would more closely agree with the experimental data. The effect that the cellulose structural differences would have on the simulated wood behavior is more difficult to assess. Basch and Lewin (1973) point out that cellulose structures of high crystallinity and low degrees of orientation are more stable towards vacuum pyrolysis. They also conclude that the rate of devolatilization of cellulose bears an inverse relationship to the square root of the cellulosic degree of polymerization (DP). The extent to which these properties - DP, crystallinity, and orientation - affect the pyrolysis of natural and filter paper cellulose under conditions pertinent to the present study is unknown. Pyrolysis of native cellulose in the captive sample apparatus, along with an investigation of the cellulose structural properties, is needed.

Figure 4.5-2 shows the results of the simulation of total gas production from sweet gum wood pyrolysis. Again it is seen that the simulated curve underestimates the wood pyrolysis curve across the entire temperature range of interest, although in this case the differences between the experimental and simu-

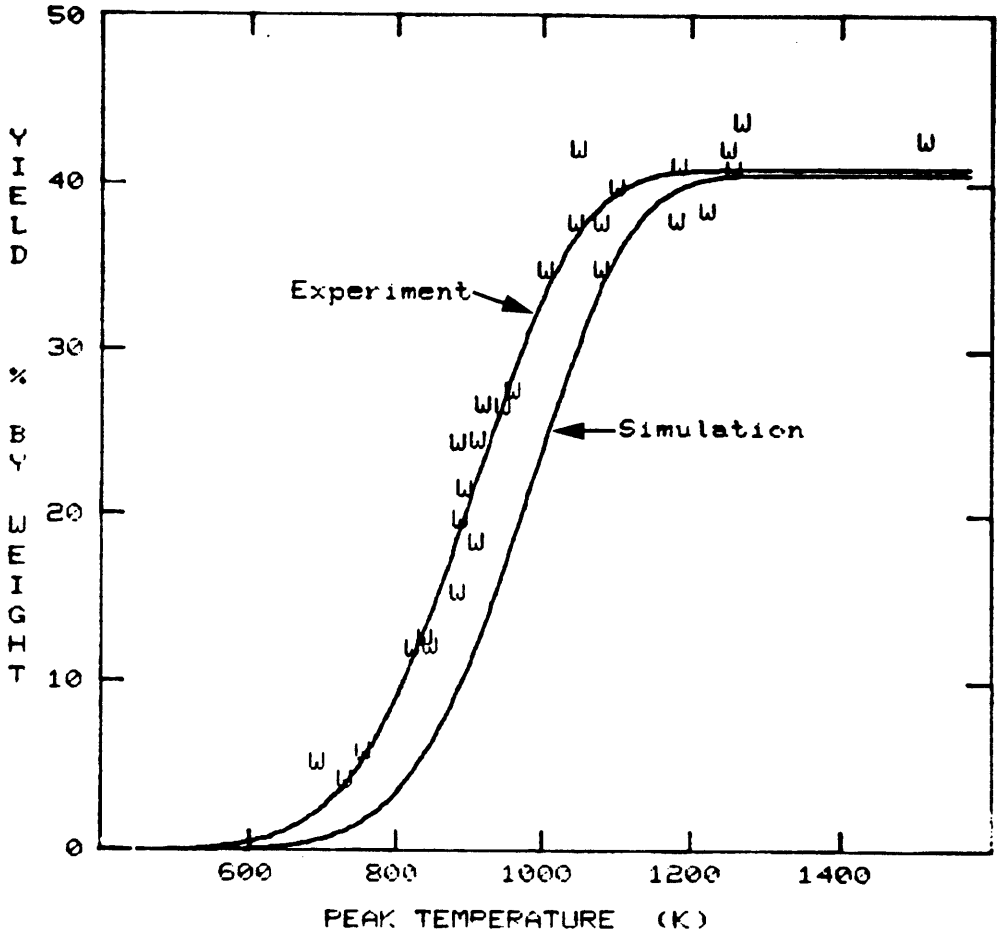

Figure 4.5-2 Modelled Curves Based on Experiment and Simulation for Total Gas Production From Wood Pyrolysis.

lated data are greater than those observed with the total weight loss curves in Figure 4.5-1. The same explanations given above for the deviations between experimental and simulated curves for total weight loss are valid here. The slightly larger discrepancies may be indicative of the fact that gas yields are influenced by secondary tar cracking reactions at higher temperatures. Primary tars from the different wood constituents may be affected differently by the secondary reactions due to suspected structural differences, especially between cellulose and lignin tars, and this effect would not be accounted for in the additivity simulation.

Figures 4.5-3 through 4.5-9 present the simulated wood pyrolysis results for carbon monoxide, methane, carbon dioxide, ethylene, ethane, water plus formaldehyde, and propylene, respectively. Except for the carbon dioxide behavior in Figure 4.5-5, production simulations for the individual components from wood pyrolysis exhibit similar deviations from the experimental data. At peak temperatures below about 1000K, the simulated curves underestimate the product yields. Above 1000K, the simulated curves overestimate the product yields. The relative behavior of the simulated and experimental curves is so simular for these six products that one is led to believe that there is something fundamentally erroneous with one or more of the assumptions made in the simulation of carbon monoxide, methane, ethylene, water plus formaldehyde, and propylene production from wood pyrolysis.

The expected higher reactivity of hemicellulose would have the effect of shifting the simulated curves to the left, yielding a better comparison with the experimental data at low

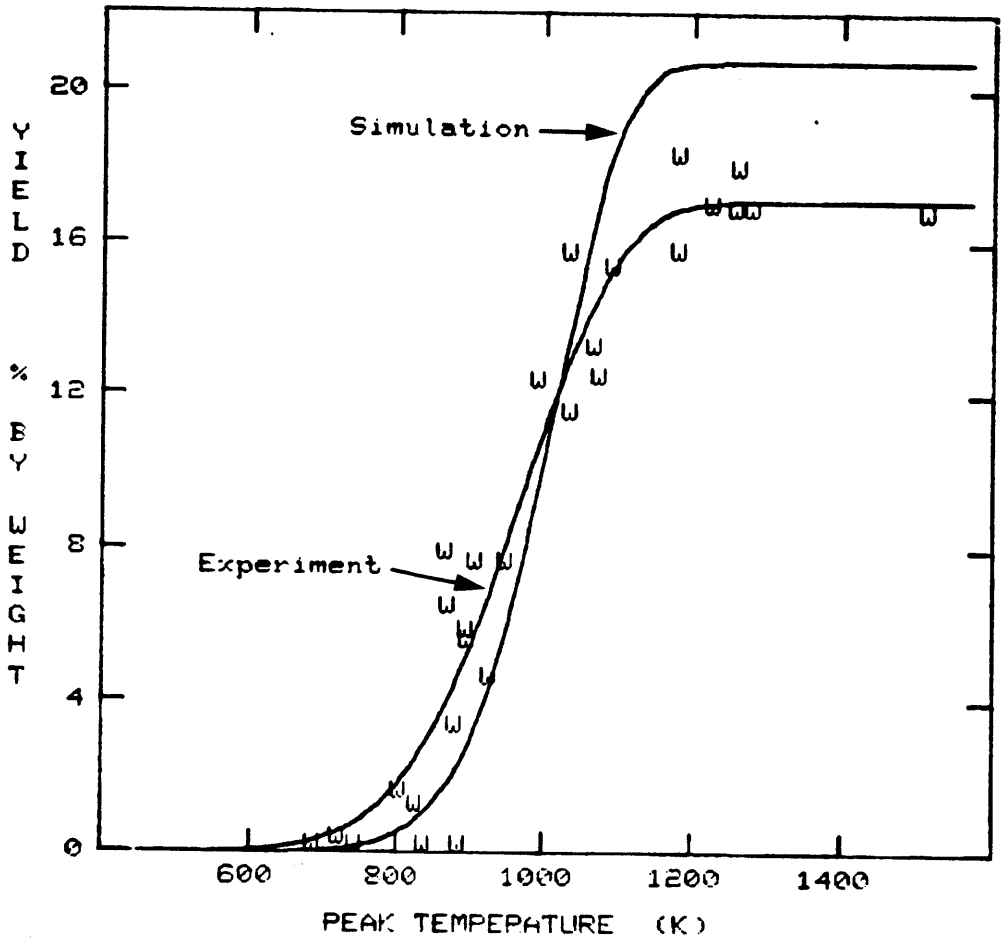

Figure 4.5-3 Modelled Curves Based on Experiment and Simulation for Carbon Monoxide Yield From Wood Pyrolysis.

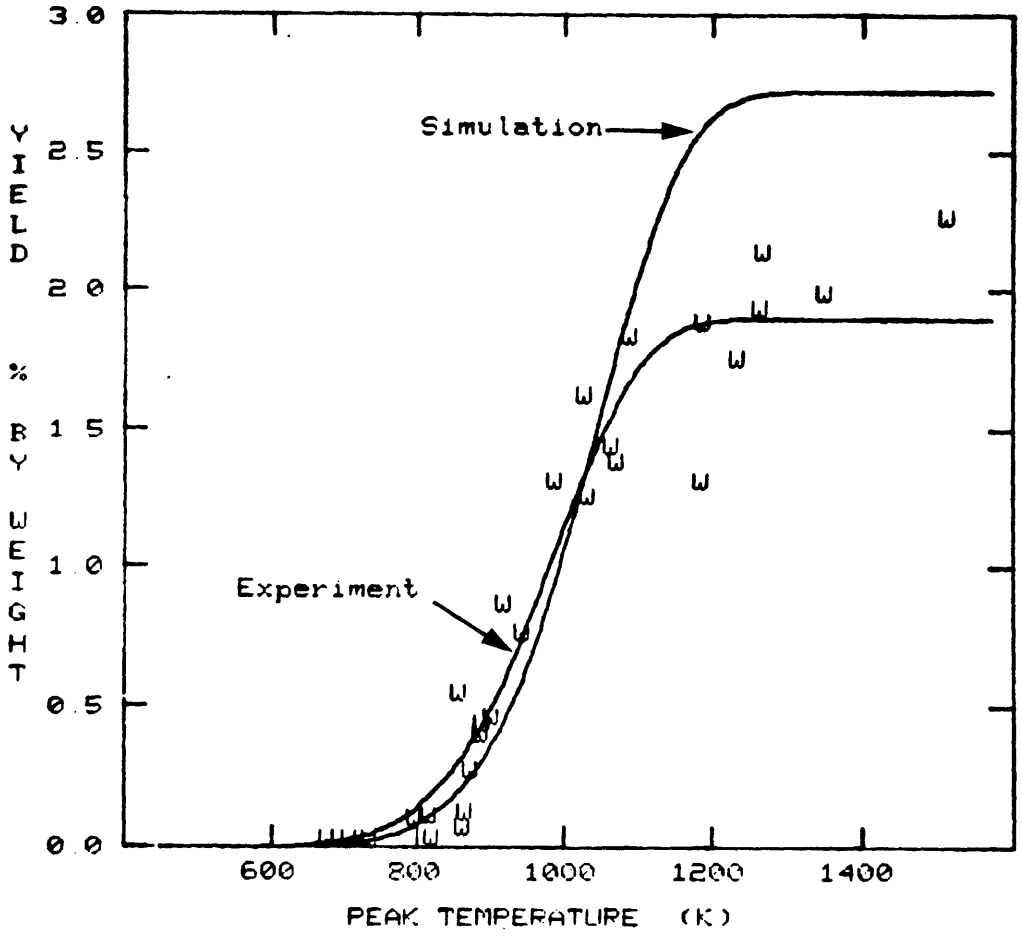

Figure 4.5-4 Modelled Curves Based on Experiment and Simulation for Methane Yield From Wood Pyrolysis.

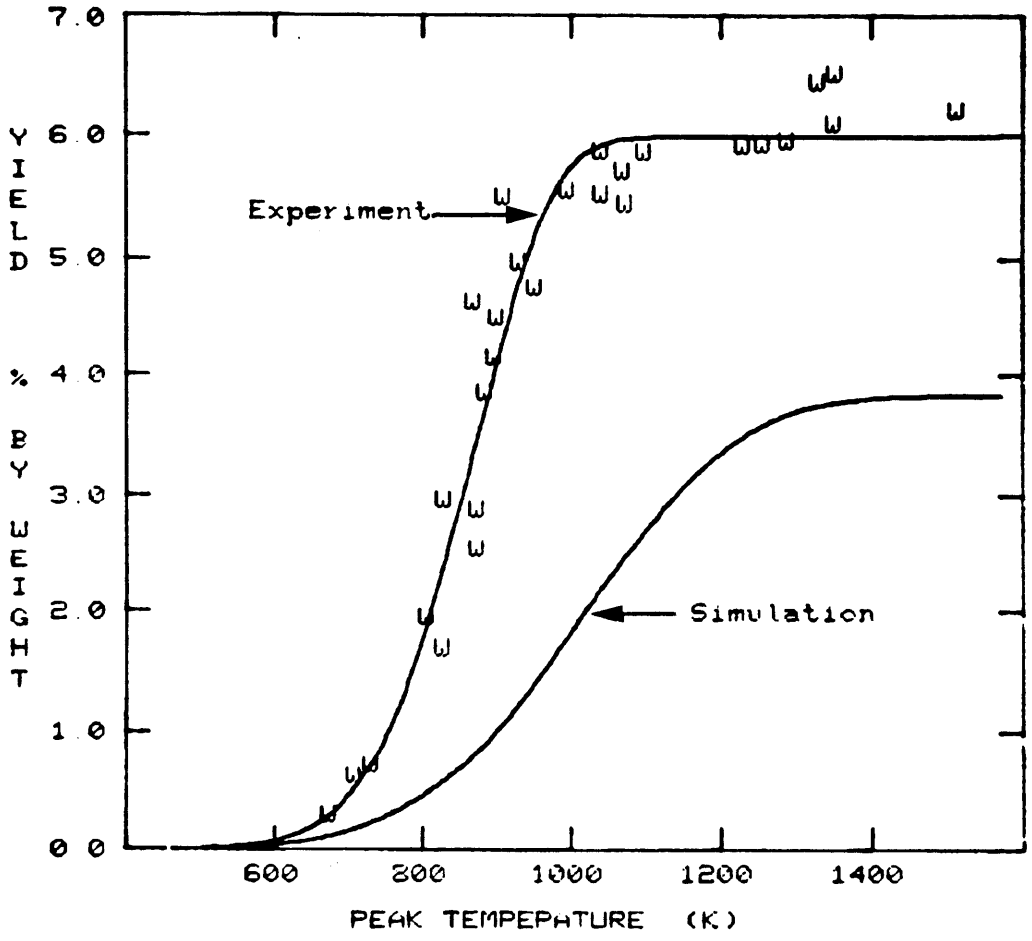

Figure 4.5-5 Modelled Curves Based on Experiment and Simulation for Carbon Dioxide Yield From Wood Pyrolysis.

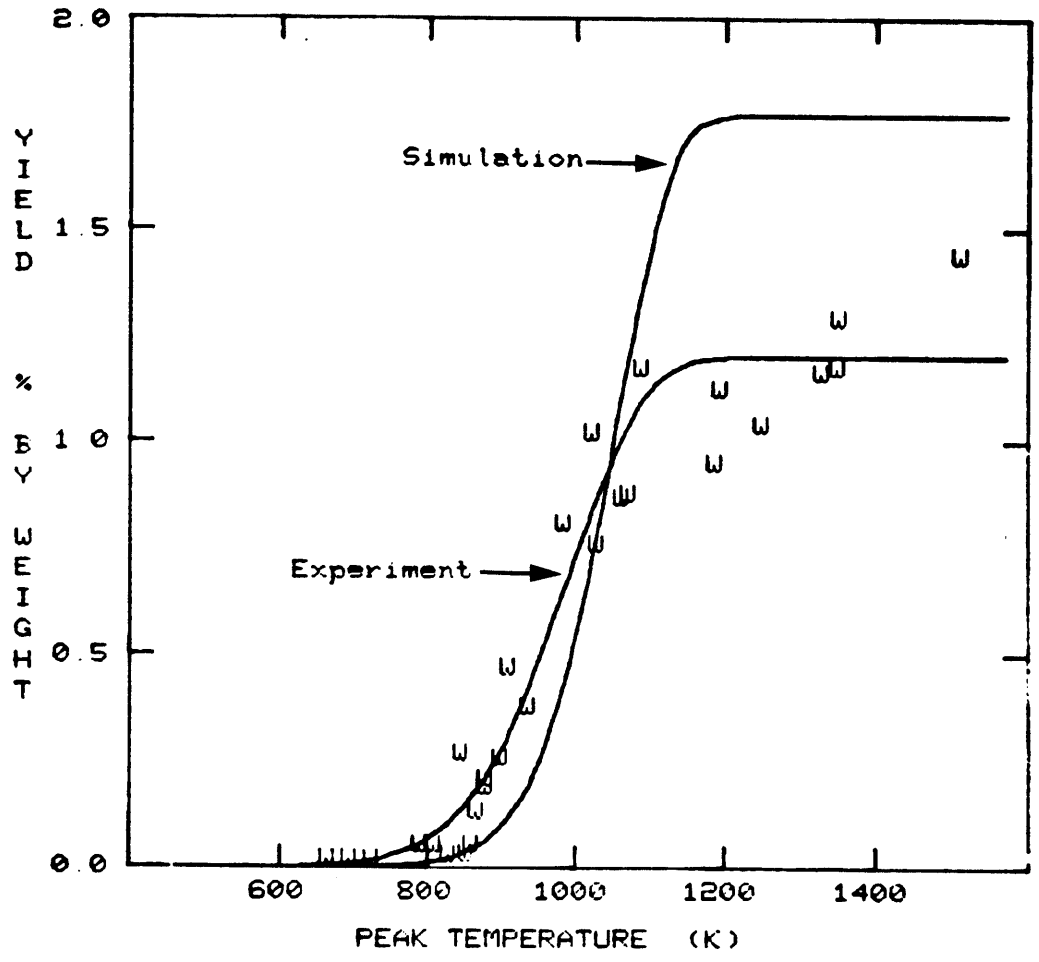

Figure 4.5-6 Modelled Curves Based on Experiment and Simulation for Ethylene Yield From Wood Pyrolysis.

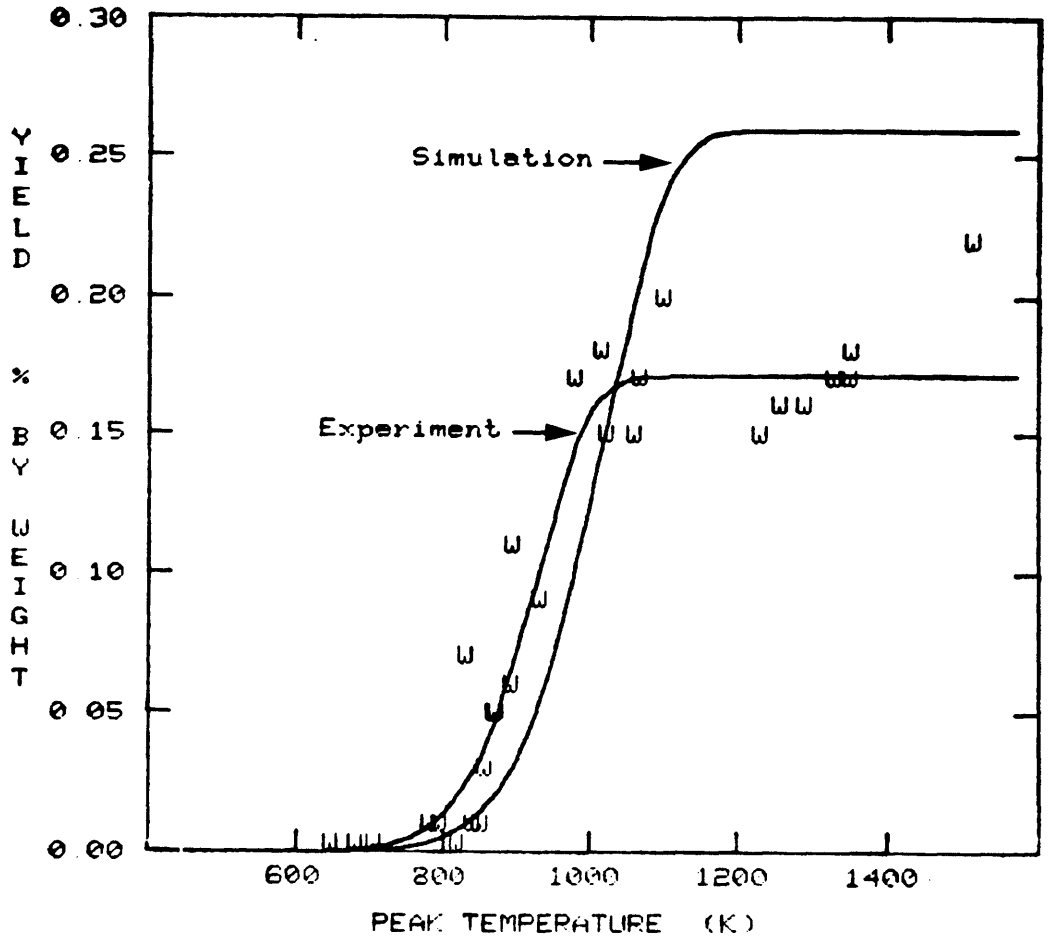

Figure 4.5-7 Modelled Curves Based on Experiment and Simulation for Ethane Yield From Wood Pyrolysis.

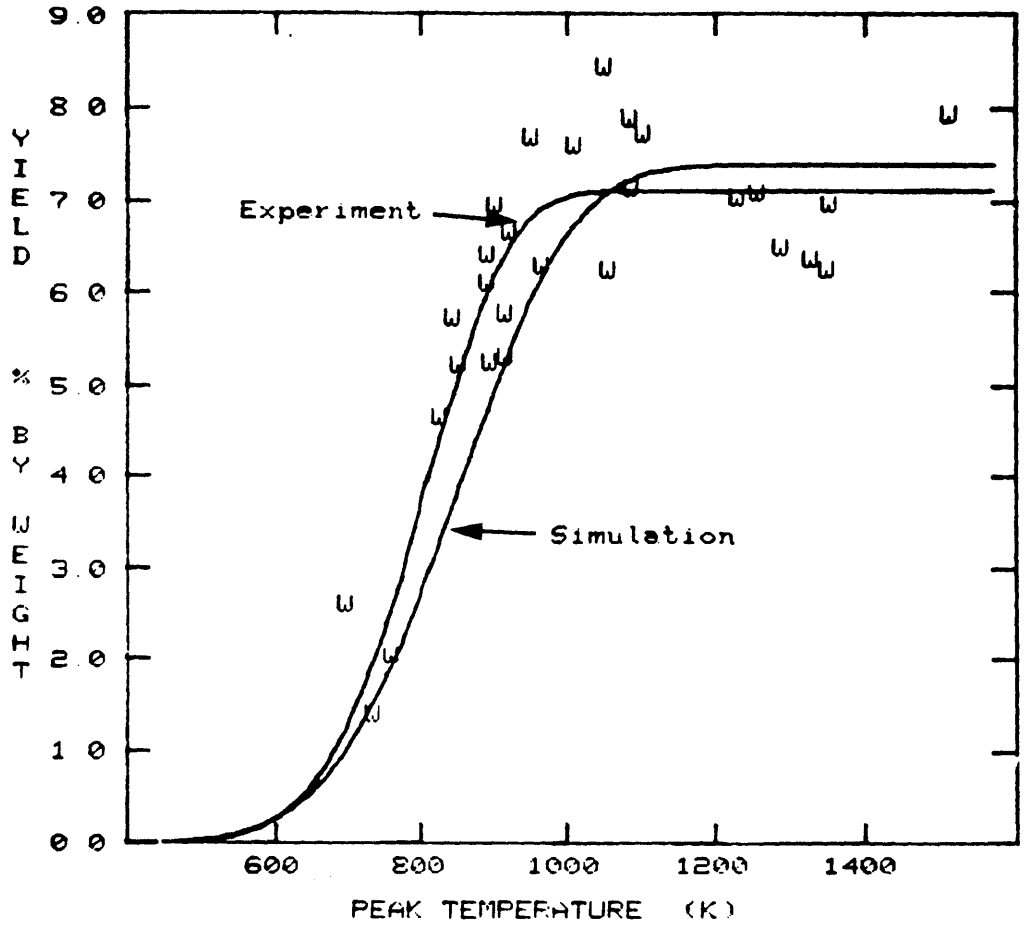

Figure 4.5-8 Modelled Curves Based on Experiment and Simulation for Water + Formaldehyde Yield From Wood Pyrolysis.

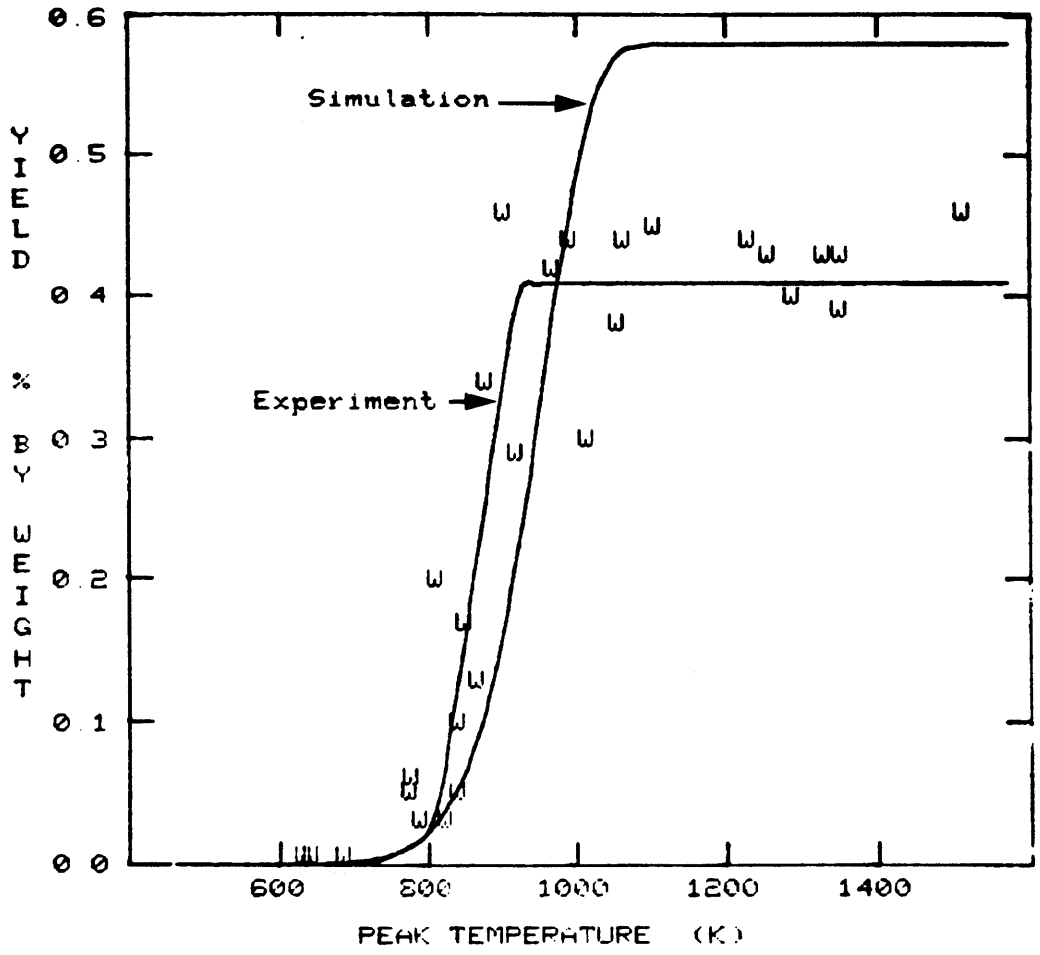

Figure 4.5-9 Modelled Curves Based on Experiment and Simulation for Propylene Yield From Wood Pyrolysis.

temperatures. The high temperature discrepancies could in turn be compensated for by lower ultimate yields of the products in question from hemicellulose pyrolysis. The fact that native cellulose has a higher DP than filter paper cellulose could also lower the high temperature simulation yield. Native cellulose would have fewer end sites available per unit mass and, if cellulose pyrolysis is more active at the ends of the polymer, would therefore be expected to produce fewer light volatiles.

The water plus formaldehyde simulation in Figure 4.5-8, while demonstrating the same general trends as mentioned above, shows a closer correlation with the experimental first-order model than did the other individual gas products. In sections 4.1 and 4.2, water was seen to be one of the products that was least influenced by secondary tar cracking reactions at high temperatures. The relatively close agreement between experiment and simulation in Figure 4.5-8 suggests that the simulations for the other five products (CO, methane, ethane, ethylene, and propylene) are more strongly influenced by the secondary tar cracking reactions and could also explain the high temperature discrepancies between simulation and experiment for these products.

The carbon dioxide modelled curves in Figure 4.5-5 bear little resemblance to the relative trends seen between the experimental and simulated first-order reaction model curves for the other individual gas products. The simulated curve grossly underestimates the experimental wood pyrolysis data in both reactivity and ultimate yield. Hemicellulose pyrolysis

would have to produce much larger quantities of carbon dioxide than cellulose to compensate for the simulated yield discrepancy and, while this is inconsistent with the assumption that hemicellulose and cellulose behave similarly under pyrolysis conditions, this would not be totally unexpected given the structural characteristics of hemicellulose. Some hemicelluloses are known to contain carboxylic acid and methyl-ether groups (SERI, 1979), which could produce substantial quantities of carbon dioxide upon thermal degradation.

An Arrenhius plot for total weight loss from wood pyrolysis is included in Figure 4.5-10. This figure presents the data obtained in this work for both the experimental and simulated single-step, first-order reaction models, as well as some of the data reported in the literature. Table 4.5-2 summarizes the corresponding Arrenhius parameters. The Arrenhius plot again shows the close correlation between the wood pyrolysis weight loss kinetics and the weight loss kinetics predicted by the weighted sums of the lignin and cellulose pyrolyses. The reaction rates from this work are also seen to fall within the range of the literature data although it is apparent that erroneous predictions can be made when attempting to extrapolate the data of one investigation into the range of operating conditions of a different study.

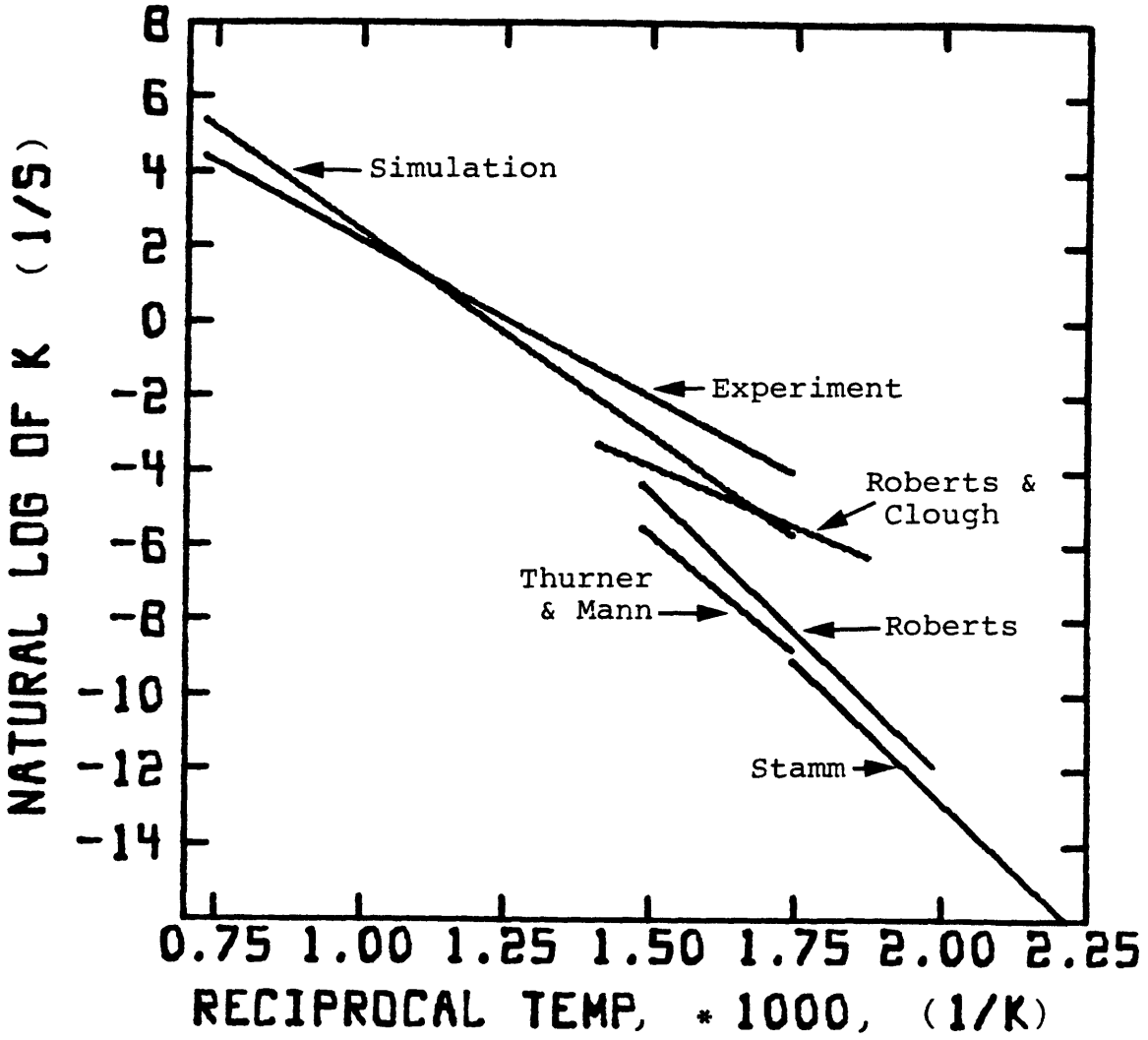

Figure 4.5-10 Modelled Rate Constants Based on Experiment and Simulation From This Work Compared to Those Measured by Various Other Investigators.

Table 4.5-2 Single-Step, First-Order Kinetic Parameters for Wood Pyrolysis Weight Loss

	E (kcal/mole)	$\log_{10} k_o$	V* (wt. %)	Temp (K)
Stamm (1956)	29.8	7.44	12	440-573
Roberts & Clough (1963)	15	3.18	72	553-708
Roberts (1970)	30	7.85	*	503-673
Thurner & Mann (1981)	25.5	5.87	70	573-673
Current Work:				
Experimental	16.5	4.53	93	573-1373
Simulation	21.7	5.77	93	573-1373

* Data not reported.

5.0 Conclusions and Recommendations

The main conclusions of this thesis are:

1) The captive sample apparatus provides excellent data for product distributions from the rapid pyrolysis of sweet gum wood and milled wood lignin for conditions of atmospheric pressure, 1000K/s heating rate, zero holding time at the peak temperature, and peak temperatures ranging 600-1500K.

2) High degrees of devolatilization can be achieved from the pyrolysis of sweet gum wood and milled wood lignin at temperatures above 900K (93% weight loss for wood and 86% weight loss for lignin).

3) Tar is the major product from the pyrolysis of sweet gum wood and milled wood lignin at temperatures above 800K, achieving maximum yields of 55 wt. % and 53 wt. %, respectively. The tar fraction also accounts for most of the heating value of the pyrolysis products (62% for wood pyrolysis and 57% for lignin pyrolysis).

4) Secondary cracking of the pyrolysis tars contributes significantly to the yields of the individual gaseous products at temperatures above 900-950K for both sweet gum wood amd milled wood lignin pyrolysis. Lignin pyrolysis tars are somewhat more resistant to secondary cracking than are wood pyrolysis tars.

5) Carbon dioxide and chemical water are the major gas phase products from sweet gum wood and milled wood lignin pyrolysis below 850K. Above this temperature, carbon monoxide is by far the most abundant gaseous product.

6) Gaseous pyrolysis products account for a substantial

amount of the sample heating value (30% in the case of wood pyrolysis and 24% for lignin pyrolysis). Carbon monoxide and methane account for over 50% of the total gaseous product heating value from both wood and lignin pyrolysis.

7) The kinetics for overall pyrolysis weight loss and for the yields of several individual products from sweet gum wood and milled wood lignin pyrolysis are well fitted by a single-step, first-order reaction model.

8) Total weight loss from pyrolysis of sweet gum hardwood under the above experimental conditions can be predicted from the corresponding weight loss of milled wood lignin and filter paper cellulose weighted, respectively, by the fraction of lignin and of holocellulose (cellulose plus hemicellulose) in the whole wood. Lack of data on the pyrolysis behavior of hemicellulose and other forms of whole biomass under the present conditions prevents one from drawing conclusions on the suitability of this simulation method for predicting the pyrolysis behavior of biomass in general.

Recommendations for further study include:

A) Obtaining pyrolysis data for sweet gum hemicellulose under conditions similar to those used in this study.

B) Obtaining pyrolysis data for sweet gum cellulose under conditions similar to those used in this study and investigating the fine structure chemistry of filter paper cellulose and sweet gum cellulose.

C) Performing a base case pyrolysis study for a different wood species (such as loblolly pine) to check the overall wood pyrolysis simulation developed in this work.

D) Examining the effects of other operating conditions such as pressure, heating rate, and solids residence time, on the product distributions from sweet gum wood and milled wood lignin pyrolysis.

E) Modifying the volatile liquid collection/analysis procedure in order to reduce the amount of data scatter for light oxygenated compounds.

F) Investigating the structural chemistry of the pyrolysis tars, possibly through the use of nuclear magnetic resonance (NMR) spectroscopy.

G) Obtaining higher temperature (greater than 1600K) yield data for sweet gum wood and milled wood lignin pyrolysis by using higher melting point metals for the captive sample screen material.

H) Improving on the pyrolysis modelling efforts to include treatment of secondary reactions and the effects of physical transport within and around the decomposing sample, with the objective of eliminating apparatus effects and obtaining more meaningful empirical parameters.

I) Systematically studying secondary reactions in biomass pyrolysis.

J) Investigating the pyrolysis behavior of other types of lignin (i.e. Kraft lignin) in the captive sample apparatus.

6.0 Literature Cited

Akita, K.,"Studies on the Mechanism of the Ignition of Wood", Rep. Fire Res. Inst. Japan, 9, p 10 (1966).

Allan, G. G., and Matilla, T., in Sarkanen, K. V., and Ludwig, C. H., Lignins-Occurence, Formation, Structure, and Reactions, Wiley Interscience, New York (1971).

Andrews, E. K., "A New Process for the Conversion of Sweet Gum Into Chemical Feedstocks", M. S. Thesis, North Carolina State University (1980).

Anthony, D. B., "Rapid Devolatilization and Hydrogasification of Pulverized Coal", ScD Thesis, MIT, Dept. of Chem. Engr., Cambridge, MA (1974).

Anthony, D. B., and Howard, J. B., "Coal Devolatilization and Hydrogasification", A.I.Ch.E. J., 22, p 625 (1976).

Basch, A., and Lewin, M., "The Influence of Fine Structure on the Pyrolysis of Cellulose - I. Vacuum Pyrolysis", J. Polymer Sci., Polymer Chem. Ed., 11, p 3071 (1973).

Brauns, F. E., Chemistry of Lignin, Academic Press, New York (1952).

Caron, R., "Batch Reactor Manual", a Report in the Dept. of Chem. Engr., MIT, Cambridge, MA (1979).

Carslaw, H. S., and Jaeger, J. C., Conduction of Heat in Solids, 2nd ed., Oxford University Press, Oxford, England (1959).

Chang H.-M., North Carolina State University, Personal Communication, April (1981).

Cosway, R. G., "Ion Effects in Subbituminous Coal Pyrolysis", M. S. Thesis, MIT, Dept. of Chem. Engr., Cambridge, MA (1981).

Domburg, G. E., and Sergeeva, V. N., "Thermal Degradation of Sulphuric Acid Lignins of Hard Wood", J. Thermal Analysis, 1, p 53 (1969).

Franklin, H. D., "Mineral Matter Effects in Coal Pyrolysis and Hydropyrolysis", PhD Thesis, MIT, Dept. of Chem. Engr., Cambridge, MA (1980).

Franklin, H. D., Personal Communication, Aug. (1981).

Freudenburg, K., and Neish, A. C., Constitution and Biosynthesis of Lignin, Springer-Verlag, New York (1968).

Graef, M., Allan, G. G., and Krieger, B. B., in Biomass as a Nonfossil Fuel Source, Klass, D. L., ed., ACS Symp. Series, 144, ACS, Washington (1981).

Hajaligol, M. R., "Rapid Pyrolysis of Cellulose", PhD Thesis, MIT, Dept. of Chem. Engr., Cambridge, MA (1980).

Handbook of Chemistry and Physics, CRC Press, Inc., 57th ed., Weast, R. C., editor (1976).

Iatridis, B., and Gavalas, G. R., "Pyrolysis of a Precipitated Kraft Lignin", Ind. Eng. Chem. Proc. Des. Dev., 18, (2), p 127 (1979).

Klein, M. T., "Model Pathways in Lignin Thermolysis", ScD Thesis, MIT, Dept. of Chem. Engr., Cambridge, MA (1981).

Klein, M. T., and Virk, P. S., "Model Pathways in Lignin Thermolysis", Energy Lab. Report, MIT-EL 81-005, MIT, Cambridge, MA (1981).

Kollmann, F. F. P., and Cote, W. A., "Principles of Wood Science and Technology - I. Solid Wood, Springer-Verlag, Berlin (1968).

Lewellen, P. C., Peters, W. A., and Howard, J. B., "Cellulose Pyrolysis Kinetics and Char Formation Mechanism", Sixteenth Symposium (International) on Combustion, The Combustion Inst., Pittsburgh (1977).

Mason, D. M., and Gandhi, K., "Formulas for Calculating the Heating Value of Coal and Coal Char: Development, Tests, and Uses", ACS Fuel Chem. Div. Preprints, 25, (3), Aug 24-29 (1980).

Molton, P. M., and Demmitt, T. F., "Reaction Mechanisms in Cellulose Pyrolysis - A Literature Review", Batelle Pacific Northwest Laboratories, Richland, WA, Aug (1977).

Pearl, I. A., The Chemistry of Lignin, Marcel Dekker, Inc., New York (1967).

Peters, W. A., "Literature Incentives for the Production of Clean Fuels and Chemicals from Biomass by Thermal Processing", Energy Laboratory, MIT, Cambridge, MA, June (1978).

Probstein, R. F., and Hicks, R. E., Synthetic Fuels, McGraw-Hill, Inc., New York (1981).

Rau, G., 10.91 Research Project Report, Dept. of Chem. Engr., MIT, Cambridge, MA (1981).

Raines, D., Huffman Laboratories, Inc., Personal Communication, October (1981).

Roberts, A. F., "A Review of Kinetics Data for the Pyrolysis of Wood and Related Substances", Combustion and Flame, 14, p 261 (1970).

Roberts, A. F., and Clough, G., "Thermal Decomposition of Wood in an Inert Atmosphere", Ninth Symposium (International) on Combustion, p 158, Academic Press (1963).

Sarkanen, K. V., and Ludwig, C. H., Lignins-Occurence, Formation, Structure, and Reactions, Wiley Interscience, New York (1971).

Satterfield, C. N., Heterogeneous Catalysis in Practice, McGraw-Hill, Inc., New York (1980).

Shafizadeh, F., and Chin, P. P. S., "Thermal Deterioration of Wood" in Wood Technology: Chemical Aspects, Goldstein, I. S., ed., ACS Symp. Series, 43, (1), p 57, ACS, Washington (1977).

Shoemaker, D. P., Garland, C. W., and Steinfeld, J. I., Experiments in Physical Chemistry, 3rd ed., p 53, McGraw-Hill, Inc., New York (1974).

Solar Energy Research Institute (SERI), "A Survey of Biomass Gasification", SERI/TR-33-239 (1979).

Stamm, A. J., "Thermal Degradation of Wood and Cellulose", Ind. Eng. Chem., 48, (3), p 413 (1956).

Stamm, A. J., and Harris, E. E., Chemical Processing of Wood, Chemical Publishing Company, Inc., New York (1953).

Suuberg, E. M., "Rapid Pyrolysis and Hydropyrolysis of Coal", ScD Thesis, Dept. of Chem. Engr., MIT, Cambridge, MA (1977).

Suuberg, E. M., Peters, W. A., and Howard, J.B., "Product Composition and Kinetics of Lignite Pyrolysis", Ind. Eng. Chem. Proc. Des. Dev., 17, (1), p 37 (1978).

Tang, W. K., U. S. Dept. Agr. Forest Serv. Res. Paper, FPL 71 (1967).

Thomas, R. J., "Wood: Structure and Chemical Composition", in Wood Technology: Chemical Aspects, Goldstein, I. S., ed., ACS Symp. Series, 43, (1), ACS, Washington (1977).

Thurner, F., and Mann, U., "Kinetic Investigation of Wood Pyrolysis", Ind. Eng. Chem. Proc. Des. Dev., 20, (3), p 482 (1981)..

Wenzl, H. F. J., The Chemical Technology of Wood, Academic Press, New York (1970).

A.0 Appendices

A.1 Heat Transfer Calculations

In order to analyze the true kinetic behavior in any pyrolysis study, the pyrolysis sample dimensions must be such that heat transfer limitations are insignificant. It would therefore be important to know how small a particle would have to be so that the temperature gradient within the particle is negligible.

The sweet gum wood particles were assumed to be spherical and that all of the resistance to heat transfer was within the sample; i.e. that the Biot number is much greater than unity. The Fourier equation for transient one-dimensional heat conduction in a sphere can then be used in the form

$$\frac{\partial T}{\partial t} = \frac{k}{\rho C_p} \frac{1}{r^2} \frac{\partial}{\partial r} \left(r^2 \frac{\partial T}{\partial r}\right) = \frac{\alpha}{r^2} \frac{\partial}{\partial r} \left(r^2 \frac{\partial T}{\partial r}\right) \qquad \text{(A.1-1)}$$

if it is assumed that k, ρ, and C_p are independent of time and temperature. The appropriate boundary conditions are:

$$T\ (r,O) = T_i$$

$$T\ (R,t) = T_s$$

and $\frac{\partial T}{\partial r}\ (0,t) = 0$ or $T(0,t) = T_c(t) = \text{finite}$

Solutions to this equation are presented graphically by Carslaw and Jaeger (1959) in terms of a non-dimensional parameter, $N_F = \alpha t_h / l^2$, the Fourier number. From their calculations, which assume that α and l are independent of time and temperature, the center temperature of a sphere of diameter 2l will be within 95% of the surface temperature, T_s, when the Fourier number is approximately 0.38.

The thermo-physical properties represented by α must be obtained before a relationship between t_h and 1 can be found given the above value of N_F. The density of sweet gum wood is reported in the literature as 0.54 gm/cc (Kollmann and Cote, 1968). The specific heat of wood, as given by Wenzl (1970), follows the temperature relationship

$$C_p = 0.266 + 0.00116T \quad \frac{cal}{gm\,^oC}$$

with T in degrees centrigrade. Stamm and Harris (1953) provide the thermal conductivity for wood as

$$k = 1.72\ \rho + 0.205 \quad \frac{cal}{cm\ hr\,^oC}.$$

Values of α are then calculated for temperatures of 300 and 1000 deg C, which essentially covers the range of temperatures studied in this program. At 300 deg C,

$\rho = 0.54$ gm/cc

$k = 1.13$ cal/cm hr ^oC

$C_p = 0.614$ cal/gm ^oC or $\alpha = 9.6 \times 10^{-4} \frac{cm^2}{sec}$

and at 1000 deg C,

$\rho = 0.54$ gm/cc

$k = 1.13$ cal/cm hr ^oC

$C_p = 1.43$ cal/gm ^oC or $\alpha = 4.1 \times 10^{-4} \frac{cm^2}{sec}$.

Using these values of α and $N_F = 0.38$, the relationships

$t_h = 99.0\ dp^2$ @ 300^oC

and $t_h = 232.0\ dp^2$ @ 1000^oC

are obtained where t_h is the time in seconds that it would take

for the centerline temperature of a particle of diameter dp (cm) to reach 95% of the surface temperature. These relationships are plotted in Figure A.1-1.

During heat up at 1000K/s, the surface temperature, T_s, would be 1000K/s * t_h degrees ahead of the centerline temperature, T_c. With the specification that T_c be 95 percent of T_s, and with T_s increasing at a rate of 1000K/s, we have

$$T_c = 0.95\ (T_s - 1000t_h) \qquad \text{(A.1-2)}$$

That is, if we allow t_h to be 0.020 sec (20 msec), T_c will be 95% of the value of T_s at a time 0.020 sec earlier. If T_s = 1020 deg C, and t_h = 0.020, then T_c will be 0.95 (1020-20) = 950 deg C. This difference of approximately 7% is deemed reasonable so that, from Figure A.1-1, the maximum allowable particle diameter would be about 95 microns.

Based on these calculations, the upper dimensional limit for the wood particle diameter was set at 88 microns.

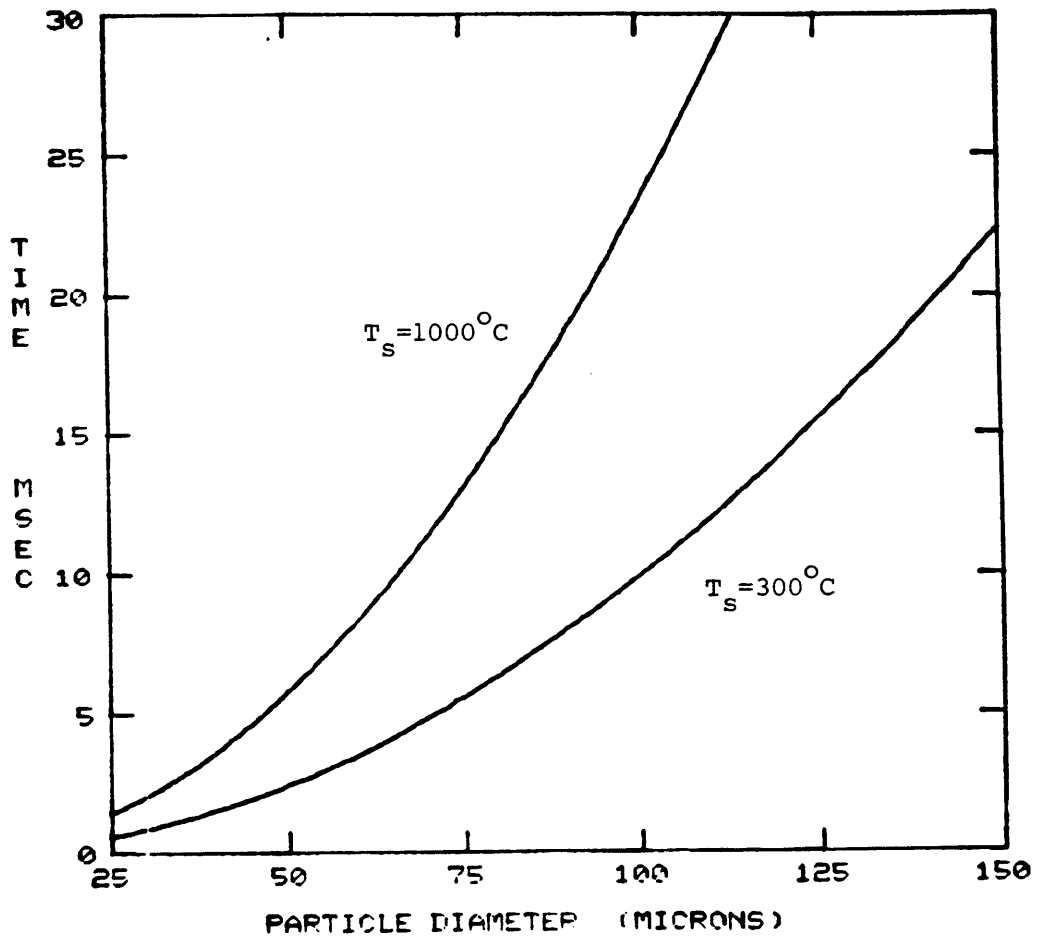

HEAT TRANSFER CALCULATION

Figure A-1.1 Effect of diameter on the time for the increase in the centerline temperature of an initially isothermal spherical particle to reach 95% of an instantaneous increase in its surface temperature.

A.2 Chromatographic Response Factors and Retention Times

Component	Thermal Conductivity Response Factor	Retention Time* (minutes)
N_2	--	6.8
O_2	--	7.4
CO	0.702	7.7
CH_4	0.562	10.7
CO_2	1.000 (ref)	13.6
C_2H_4	0.706	15.7
C_2H_6	0.722	16.7
H_2O	0.695	17.3
HCHO	0.695	18.1 - 19.0
C_3H_6	0.827	19.7
CH_3OH	0.753	20.0
CH_3CHO	0.753	21.2
Butene + Ethanol	0.869	22.1 - 22.6
Acetone + Furan	0.827	24.1 - 24.5
Acetic Acid	1.071	24.7 - 25.0
Misc. Oxygenates	1.200	26.0 - 40.0

*based on oven temperature programmed from 195K to 513K with a two-minute initial hold, a heatup rate of 16K/min and held indefinitely at the final temperature.

The number of milligrams of component i is given by:

$$mg_i = \frac{A_i R_i}{A_{CO_2}} mg_{CO_2} \qquad \text{(A.2-1)}$$

where A_i is the area of the peak produced by component i, R_i is the response factor of i, and A_{CO_2} is the area of the peak produced by mg_{CO_2} milligrams of CO_2.

The response factors, R_i, are found by injecting known

quantities of each component, obtaining the A_i for different mg_i. Rearranging equation (A.2-1) gives

$$\frac{mg_i}{mg_{CO_2}} = \frac{A_i}{A_{CO_2}} R_i \qquad \text{(A.2-2)}$$

A plot of the mass ratios versus the area ratios will yield a straight line of slope R_i going through the origin.

A.3 Error Analysis

The error analysis calculations follow the methods presented by Shoemaker et al. [11].

Let x = weight of sample + screen

y = weight of screen alone

F_1 = weight of sample

$F_1 = x - y$

$\lambda(F_1)$ = error in weight of sample

$\lambda(x) = \lambda(y)$ = error in weight of x or y = 0.1 mg

From Shoemaker et al.

$$\lambda^2(F_1) = \lambda^2(x) + \lambda^2(y) = 2\lambda^2(x) = 0.02$$

Therefore, $\lambda(F_1) = 0.14$ mg

Let z = weight of char + screen

F_2 = weight of char

$F_2 = z - y$

$$\lambda^2(F_2) = \lambda^2(z) + \lambda^2(y) = 0.02 \text{ or } \lambda(F_2) = 0.14$$

Let $F_3 = \frac{F_2}{F_1}$ = fractional yield of char

$$\text{then } \frac{\lambda^2(F_3)}{F_3^2} = \frac{\lambda^2(F_2)}{F_2^2} + \frac{\lambda^2(F_1)}{F_1^2}$$

Let $F_1 = 100$ mg, $F_2 = 10$ mg, $F_3 = 0.10$

then $\lambda(F_3) = 0.0014$

or, on a percentage basis,

$F_3 = 10 \pm 0.14\%$

Similarly, let F_4 = weight of tar on foil

F_5 = weight of tar on filter + nut

F_6 = weight of tar in glasswool trap

then $\lambda(F_4) = \lambda(F_5) = \lambda(F_6) = 0.14$ mg

If F_7 = weight of tar on each tissue, and if the error due to moisture in each tissue weighing is about 2 mg

then $\lambda(F_7) = 2.83$ mg

Let F_8 = total weight of tar collected = $F_4 + F_5 + F_6 + 2F_7$

then $\lambda^2(F_8) = \lambda^2(F_4) + \lambda^2(F_5) + \lambda^2(F_6) + 2\lambda^2(F_7)$

or $\lambda(F_8) = 4.1$ mg = error in total tar weight

Let $F_9 = \frac{F_8}{F_1}$ = fractional yield of tar

then $\frac{\lambda^2(F_9)}{F_9^2} = \frac{\lambda^2(F_8)}{F_8^2} + \frac{\lambda^2(F_1)}{F_1^2}$

Choosing $F_8 = 50$ mg, $F_1 = 100$ mg, and $F_9 = 0.5$

then $\lambda(F_9) = 0.041$

or, on a percentage basis,

$F_9 = 50 \pm 4.1\%$.

A.4 Comparison of Cellulose Kinetic Parameters

The best fit kinetic parameters obtained by Hajaligol (1980) for filter paper pyrolysis are included in Table A.4-1. These parameters are believed to have been produced by a program known as CLFIT in the computer library at the MIT Department of Chemical Engineering. The CLFIT program provided, as an indication of the goodness of the non-linear least squares fit, a quantity called the sum-of-the-squared-errors (SSE). From this quantity, it was possible to determine the standard error of the estimate (SEE) from

$$SEE = \sqrt{SSE/(n-p)} \qquad (A.4\text{-}1)$$

where SSE = sum of the squared errors

$$= \sum_{j=1}^{n} (V_{j,model} - V_{j,exper.})^2$$

n = the number of data points

p = the number of parameters used in the fitting procedure (p=3 in this analysis).

The V_j are the modelled and experimental pyrolysis yields.

The POWELL non-linear least squares program, an updated version of CLFIT, was used to reanalyze the raw cellulose data reported by Hajaligol (1980) and a different set of best fit kinetic parameters was obtained. These parameters are shown in Table A.4-2 along with the standard error of the estimate, which was also provided by POWELL. Hajaligol's time-temperature history format had to be slightly modified in order to be used in POWELL, but the changes were insignificant as far as the fitting procedure was concerned.

Table A.4-1 Best Fit Kinetic Parameters for Cellulose Filter Paper Pyrolysis*(from program CLFIT)

Product	E_i (kcal/mole)	$\log_{10} k_{oi}$	V_i^* (wt.%)	standard error of estimate (wt.%)
Weight Loss	31.8	8.30	94.08	7.05
Total Gases	32.3	7.49	42.17	4.71
CO	52.7	11.75	21.64	1.97
CH_4	60.0	13.00	2.41	0.25
CO_2	23.4	5.39	3.08	0.33
C_2H_4	49.8	10.82	2.07	0.14
C_2H_6	41.6	9.06	0.26	0.027
H_2O(+HCHO)	24.6	6.71	8.04	1.36
C_3H_6	60.7	14.93	0.67	0.12

* Kinetic parameters from Hajaligol (1980).

Table A.4-2 Best Fit Kinetic Parameters for Cellulose Filter Paper Pyrolysis(from program POWELL)

Product	E_i (kcal/mole)	$\log_{10} k_{0i}$	V_i^* (wt.%)	standard error of estimate (wt.%)
Weight Loss	25.0	6.54	95.78	4.91
Total Gases	17.6	3.97	42.22	3.02
CO	27.3	6.07	21.69	1.64
CH_4	24.1	5.06	2.59	0.16
CO_2	11.8	2.35	3.76	0.23
C_2H_4	30.7	6.61	2.10	0.13
C_2H_6	35.2	7.65	0.25	0.026
H_2O(+HCHO)	11.3	2.90	8.22	1.21
C_3H_6	29.8	7.14	0.70	0.14

A comparison between the kinetic parameters in Tables A.4-1 and A.4-2 shows that the parameters obtained from POWELL are somewhat lower than the values produced by CLFIT, extremely so in some cases. This is not altogether suprising given the wide range of activation energies and frequency factors that can be used to fit the data (Franklin, 1981). Satterfield (1980) discusses the problems encountered when trying to fit data such as these and points out that there is a compensation effect by which it is possible for a high activation energy to be countered by a high collision factor, thus producing an apparently adequate fit to the data.

By comparing the standard error of the estimate in Tables A.4-1 and A.4-2, it is seen that the POWELL program provides a better fit to the experimental data than does CLFIT in all cases except propylene.

A.5 Experimental Data Base

Sweet Gum Wood Runs with Zero Holding Time

at 5 psig He and 1000 K/s Heating Rate

Run #	Temp. (K)	Char	Tar	CO	CH_4	CO_2	C_2H_4	C_2H_6	H_2O	HCHO	C_3H_6	CH_3OH	CH_3CHO	Butene+ Ethanol	Acetone + Furan	Acetic Acid	Misc. C.H.O.	Material Balance
81	598	96.82	3.06	0	0	0.27	0	0	2.21	0.40	0	0.97	0.02	0.02	0.49	0.71	0.23	105.2
36	611	91.02	4.23	0.18	0	0.61	0	0	1.10	0.28	0	1.22	0.04	0	0.37	0.38	0.07	99.5
35	660	90.19	7.31	0	0	0.70	0	-	1.69	0.33	-	1.86	0.05	0.01	0.46	0.66	0.07	103.4
74	766	45.02	42.09	-	0.11	2.96	0.05	0.01	4.00	1.22	0.06	1.82	0.50	0.05	0.29	0.83	0.22	99.2
32	770	68.68	22.86	1.65	0.10	1.95	0.05	0.01	3.86	0.79	0.05	1.40	0.24	0.01	0.40	1.18	0.18	103.5
72	783	71.38	19.90	1.28	0.03	1.69	0.01	0	4.42	1.31	0.03	1.36	0.59	0.69	0.25	0.80	0.13	103.9
79	793	18.76	49.57	7.93	0.55	4.62	0.27	0.07	4.65	1.76	0.20	1.14	0.89	0.14	0.45	1.04	0.62	92.6
73	811	53.19	26.29	6.48	0.07	2.53	0.03	0.01	4.18	1.07	0.03	2.36	0.64	0.69	0.67	0.81	0.13	99.2
31	838	28.39	42.06	3.36	0.27	3.84	0.13	0.03	5.15	1.08	0.10	3.32	0.78	0.16	0.66	1.59	0.27	91.9
77	839	17.24	53.47	5.57	0.44	4.49	0.21	0.05	4.26	1.52	0.17	2.68	1.22	0.79	1.34	1.17	0.58	95.2
34	841	49.43	26.41	0	0.12	2.87	0.05	0.01	5.12	0.97	0.05	2.66	0.42	0.20	0.91	1.77	0.24	91.3
75	861	21.47	49.75	5.86	0.40	4.14	0.19	0.05	3.76	1.55	0.13	1.69	1.08	0.77	0.68	1.03	0.40	89.6
80	862	13.06	55.27	4.61	0.87	4.96	0.47	0.11	5.46	2.23	0.34	1.58	1.65	1.11	0.91	1.45	0.80	94.9
78	896	18.50	52.46	7.66	0.46	5.50	0.26	0.06	5.31	1.35	0.46	1.64	1.01	0.13	0.67	1.33	0.81	97.6
71	911	7.57	59.19	7.65	0.77	4.75	0.38	0.09	4.41	1.87	0.29	2.34	1.60	0.97	1.02	0.95	0.41	94.3
30	971	10.81	45.68	12.38	1.31	5.55	0.81	0.17	5.48	2.13	0.42	2.37	1.27	0.29	0.95	0.32	1.29	91.2
68	994	6.18	46.29	15.76	1.62	5.87	1.02	0.18	4.57	1.68	0.44	2.40	1.48	0.52	0.94	3.28	0.58	94.6
28	1018	7.55	44.22	11.53	1.25	5.52	0.76	0.15	6.69	1.73	0.30	4.02	1.18	0.27	1.55	2.26	0.39	89.4
25	1058	6.01	48.75	13.32	1.44	5.71	0.87	0.15	4.97	2.17	0.38	2.78	1.23	0.24	1.01	0.22	0.24	89.5
27	1067	11.19	43.15	12.48	1.38	5.44	0.88	0.17	5.47	2.42	0.44	5.29	1.19	0.29	0.93	0.99	0.21	91.9
24	1108	6.48	43.83	15.41	1.83	5.86	1.17	0.20	5.46	2.27	0.45	2.38	1.82	0.90	1.31	0.08	0.65	90.1
19	1235	6.60	45.10	18.32	1.31	5.91	0.95	0.15	5.23	1.81	0.44	4.06	1.14	0.22	0.66	0.45	0.50	92.8
18	1261	6.14	45.45	15.80	1.88	5.92	1.12	0.16	4.85	2.24	0.43	1.58	1.23	0.26	0.71	0.83	0.60	89.3
66	1293	8.50	44.89	16.96	1.75	5.95	1.04	0.16	4.62	1.86	0.40	1.14	1.10	0.30	0.65	1.90	0.51	91.8
67	1333	6.87	46.07	16.87	1.93	6.45	1.16	0.17	4.63	1.72	0.43	2.36	1.52	1.02	1.19	2.03	0.48	95.1
64	1355	6.72	50.15	16.87	1.99	6.10	1.17	0.17	4.53	1.71	0.39	1.77	1.45	0.53	0.81	1.21	1.70	100.8
40	1357	7.16	41.88	17.96	2.14	6.52	1.29	0.18	4.77	2.20	0.43	1.73	1.59	0.49	0.70	0.13	0.93	90.0
62	1518	7.44	52.63	16.78	2.27	6.27	1.44	0.22	6.21	1.72	0.46	2.59	1.63	1.11	1.05	-	1.04	102.8

Milled Wood Lignin Runs With Zero Holding Time

at 5 psig and 1000 K/s Heating Rate

Run #	Temp. (K)	Char	Tar	CO	CH_4	CO_2	C_2H_4	C_2H_6	H_2O	HCHO	C_3H_6	CH_3OH	CH_3CHO	Butene+ Ethanol	Acetone + Furan	Acetic Acid	Misc. C.H.O.	Material Balance
88	581	96.86	1.73	0	0	0.13	0	0	2.02	0.30	0	0.17	0.01	0.02	0.06	0	0.13	101.4
96	663	94.00	4.94	0	0	0.25	0	0	2.86	0.63	0	0.41	0.03	0.05	0.14	0.05	0.19	103.6
89	754	81.85	14.84	0.92	0.01	0.69	0	0	2.90	1.03	0	0.56	0.18	0.15	0.10	0.01	0.17	103.4
97	770	55.08	34.36	1.16	0.09	1.53	0.04	0.01	(4.27)	(1.95)	(0.03)	1.64	0.70	0.71	0.36	0.28	0.13	102.3
87	790	40.92	45.10	3.37	0.27	1.93	0.04	0.01	3.37	1.51	0.02	1.53	0.62	0.37	0.19	0	0.14	99.4
93	826	45.00	40.37	2.80	0.46	(4.02)*	0.07	0.04	(4.24)	1.62	-	-	0.78	0.72	-	0.41	0.05	100.6
95	873	22.98	51.33	6.94	1.44	2.77	0.27	0.15	4.13	1.41	0.16	2.01	0.80	0.53	0.34	0.09	0.13	95.5
86	934	20.62	51.37	10.24	1.73	2.64	0.45	0.22	3.52	1.34	0.21	1.45	0.79	0.99	0.41	0.63	0.22	96.8
90	944	25.71	51.10	7.07	1.37	2.74	0.27	0.15	4.04	1.53	0.15	2.00	0.77	0.48	0.39	0.09	0.11	98.0
99	973	16.35	52.62	11.14	2.16	3.23	0.47	0.24	3.37	1.42	0.24	2.44	0.80	0.53	0.75	0.10	0.04	95.9
85	1023	14.69	51.39	15.64	2.55	3.22	0.76	0.26	3.76	(0.82)	0.22	1.22	0.41	0.25	0.17	0.37	0.26	96.0
102	1063	13.76	49.48	16.29	2.79	3.63	0.73	0.28	3.56	1.35	0.27	1.86	0.50	0.30	0.42	0.08	0.29	95.6
91	1125	14.31	45.87	16.66	2.91	3.73	0.78	0.28	4.04	1.61	0.27	2.31	0.86	0.95	0.72	0.34	0.21	95.9
101	1213	13.95	47.21	16.21	3.00	3.71	0.86	0.35	3.33	0.79	0.25	1.44	0.49	0.32	0.23	0.21	0.18	92.5
98	1236	14.78	45.05	17.62	3.06	3.79	0.92	0.29	3.68	1.44	0.27	1.76	0.78	0.62	0.28	0.74	0.23	94.6
92	1276	15.03	45.93	17.23	2.91	3.67	0.77	0.26	4.26	1.44	-	-	0.87	0.83	-	0.28	0.13	93.6
84	1353	14.52	45.84	18.49	3.05	4.03	0.77	0.26	3.60	1.55	0.20	1.89	0.88	0.75	0.20	0.37	0.22	96.6
83	1436	13.33	47.69	19.24	3.11	4.14	0.85	0.29	3.85	1.28	0.25	1.54	0.52	0.24	0.17	0.37	0.40	97.3
100	1443	14.15	43.07	19.14	3.31	4.14	1.02	0.32	3.49	1.48	0.32	1.68	0.80	0.97	0.38	0.31	0.86	95.4

(*numbers in parentheses were excluded from the kinetic analysis)